

Master Thesis

Development of an Erosion Function Apparatus for the assessment of the erosion resistance of compacted clay

L. Rook



Master Thesis

Development of an Erosion Function Apparatus for the assessment of the erosion resistance of compacted clay

by

L. Rook

to obtain the degree of Master of Science
at the Delft University of Technology
to be defended publicly on Wednesday March 4, 2020 at 2 PM

Student number: 4359186
Project duration: December 3, 2018 – March 4, 2020
Thesis committee: Prof. C. Jommi Phd MSc, TU Delft, chair committee
R. Lanzafame Phd Msc, TU Delft
A. Dieudonné Phd MSc, TU Delft
R. Sluijsmans MSc, Boskalis

Summary

The erosion resistance of clay is an important aspect when assessing the integrity of a levee. This is because the clay layer of a dike must resist the forces that are imposed in the case of overflow or overtopping.

Currently, the erosion resistance of clay in the Netherlands is being assessed based on the sand content, the liquid limit and the plasticity index. The quality of compaction is assessed by a density requirement. However, the effect of compaction on the erosion resistance of clay is not well understood and although its importance has been widely acknowledged by multiple literature sources, it has never been quantified. Therefore the goal of this thesis is to investigate what the are of compaction on the erosion resistance of clay and how large. To do this first of all a set-up has been designed and built, resembling the Erosion Function Apparatus as suggested by Briaud with some differences.

Then 3 types of clay have been tested with differing initial erosion characteristics: one kind which fully complies with the current Dutch guidelines, 1 which does not quite suffice and 1 which does not suffice in any way. These 3 types of clay have been compacted at various energy levels (Modified Proctor, Proctor and 0.5*Proctor density). Also samples with differing water contents have been produced at each energy level and each clay. These samples were subsequently tested in the Erosion Function Apparatus at several flow-velocities in order to establish an erosion curve from which several erosion parameters were determined.

Having performed the erosion tests and determined the accompanying erosion parameters the results were interpreted in the Proctor curve. Plotting the results in the Proctor curve show that samples compacted at the optimum water content in the Proctor plane perform best, whereas they perform poorer the farther the water content is off from the optimum. Also it shows an increase in the compaction effort will generally result in a lower amount of erosion occurring. This result has been obtained by determining the critical shear stress, critical erosion velocity, the detachment coefficient and the velocity detachment coefficient and plotting these results in the Proctor curve. The first two parameters are measures of the amount of strength the soil has before it starts eroding at all, whereas the latter two are an increment meant to predict how much a soil might erode if the force imposed on the soil is above the erosion threshold. The results consistently showed the detachment coefficients were lowest with the samples compacted at an optimum water content and/or undergone a higher compaction effort (i.e. the soils erode less). On the other hand the critical shear stress/critical erosion velocity was highest at the optimum water content (i.e the soil erodes less), but did not necessarily increase with an increasing compaction effort. This is attributed to the loss of suction. Further, all tested soils showed their optimum erosion characteristics at or close to a degree of saturation of 85 %. Several other methods were tried, but to no avail unfortunately. Also the rates of erosion were compared between the different types of clay. The clay which is in compliance with the Dutch codes showed the least amount of erosion, the one that did not quite suffice showed some more erosion and the clay that did not comply with the erosion guidelines at all showed the most erosion. However, it was also proved that the clay which did not quite suffice the requirements was (if compacted at optimum water content and at a sufficient energy level) only slightly more erodible than the clay which fully complied with the current Dutch regulations. Finally, the results of the tests carried out in this study were also compared to similar tests performed in the United States and the show consistent similar results.

Overall, this study concludes that the use of (currently perceived) unsuitable clay as dike cover can be possible if compacted at or very close to the optimum water content and at a sufficient energy level. Also it can be concluded that compaction at the optimum water content can dramatically reduce the erodibility of a soil or even stop the erosion process. Increasing the compaction effort also reduces erodibility of a soil, although it must be kept in mind that the optimum water content also changes and thus if it is wise to do so.

Finally this thesis leaves some suggestions for further research. These mainly concern the effects of cyclic wetting/drying cycles on the erodibility of the soil as well as trying to better understand the effects of the erosion process happening in the field versus the erosion process that is happening in the laboratory.

Samenvatting

De erosiebestendigheid van klei is een belangrijk aspect in de beoordeling of een klei voldoet aan de wettelijk gestelde eisen. De kleilaag op een dijk moet namelijk bestand zijn tegen de krachten ten gevolge van golfoverloop en golfoverslag.

Momenteel wordt de geschiktheid van de klei voor gebruik op dijken beoordeeld op basis van het zandgehalte, de vloeigrens en de plasticiteitsindex in combinatie met een dichtheidseis. Hoewel aan het positieve effect van verdichting op de erosiebestendigheid niet wordt getwijfeld, wordt de werking ervan slecht begrepen en is het effect niet eerder gekwantificeerd. In dit onderzoek wordt daarom gekeken naar het effect van de verdichting op de erosiebestendigheid en de grootte ervan. Om dit te doen is allereerst een opstelling ontworpen en gebouwd, gebaseerd op de EFA zoals voorgesteld door Briaud al zijn er wel enkele verschillen.

Met deze opstelling zijn drie soorten klei beproefd: de eerste voldoet volgens de huidige normen en regelgeving, de tweede voldoet net niet en de laatste voldoet volstrekt niet. Deze verschillende soorten klei zijn op meerdere energieniveaus verdicht (Verzwaarde Proctor, Proctor en halve Proctor energieniveau's) waarbij tevens per klei per energieniveau ook nog verschillende monsters zijn gemaakt met verschillende vochtgehalten. Vervolgens is van elk monster een schuifspannings/snelheid-erosie curve bepaald, door te variëren in de stroomsnelheid van het water langs het monster. Op basis van deze proeven zijn vervolgens verschillende erosieparameters bepaald.

Nadat de proeven zijn uitgevoerd en de bijbehorende erosieparameters zijn bepaald zijn deze resultaten geïnterpreteerd in context van de Proctor curve. Als deze resultaten in de Proctor curve worden gepresenteerd blijkt namelijk dat de monsters welke op het optimale watergehalte zijn verdicht verreweg het beste presteren. Daar waar de monsters echter een watergehalte hebben welke ver van het optimale gehalte ligt presteren aanzienlijk minder goed. Verder blijkt een toename van de verdichtingsenergie tijdens compactie een beneficiërende invloed te hebben op de prestaties. Deze resultaten zijn verkregen door van elk monster een kritische schuifspanning, kritische erosiesnelheid, onkoppellingscoëfficiënt en snelheidsontkoppellingscoëfficiënt te bepalen. De eerste twee parameters hebben betrekking op de hoeveelheid weerstand op het monster moet worden uitgeoefend voordat de monsters enige erosie beginnen te vertonen, daar waar de andere 2 parameters gebruikt kunnen worden om een voorspelling van de erosie te geven als de kracht die op het monster wordt uitgeoefend boven de grens voor erosie ligt. Deze resultaten tonen consequent aan dat de onkoppellingscoëfficiënten het laagst zijn bij de monsters welke dicht bij het optimum watergehalte liggen (en dus het minst eroderen). Dit zelfde effect wordt gezien wanneer de verdichtingsenergie wordt verhoogd. Aan de andere kant ziet men dat de kritische schuifspanning/erosiesnelheid het hoogst is als het monster op het optimum watergehalte verdicht wordt (in andere woorden de erosie is het minst). Echter, een verhoging van de verdichtingsenergie leidt niet noodzakelijk tot een toename van de kritische schuifspanning/erosiesnelheid. Dit wordt toegeschreven aan het verlies van suctie in het onverzadigde monster. Verder tonen alle monsters hun ideale erosiekenmerken rond de 85 % verzadiging. Enkele andere manieren zijn nog gepoogd om een goed verband tussen de erosiekenmerken en de een andere parameter te vinden, echter zonder succes. Ook is de mate van erosie tussen de verschillende soorten klei vergeleken. Zoals verwacht presteert de klei die volledig voldoet aan de wettelijk gestelde eisen het best, echter de klei die net niet voldoet aan de wettelijk gestelde eisen vertoont nauwelijks meer erosie (indien op optimum watergehalte verdicht en bij voldoende verdichtingsenergie). Als laatste, de klei die volstrekt niet voldoet vertoont heel veel erosie. Tot slot zijn de resultaten die in deze studie zijn behaald vergeleken met resultaten van studies die in de Verenigde Staten zijn uitgevoerd. Deze vertoont consequent gelijkwaardige resultaten.

Concluderend kan gesteld worden dat het gebruik van (momenteel) ongeschikt geachte klei als deklaag van een dijk zeker mogelijk is indien verdicht op het optimum watergehalte en bij een voldoende energieniveau. Verder kan geconcludeerd worden dat verdichting op het optimum watergehalte het erosieproces aanzienlijk kan verminderen tot zelfs stoppen. Tot slot leidt het verhogen van de verdichtingsenergie tot een

vermindering van de erosie indien rekening gehouden wordt met de verschuiving het optimum watergehalte door deze verschuiving.

Tot slot geeft dit onderzoek aanleiding tot verder onderzoek. Deze hebben hoofdzakelijk betrekking op het effect van nat/droog cycli op de erosiebestendigheid van de klei en het beter proberen te begrijpen wat de verschillen zijn tussen de erosie die in het laboratorium optreedt en de erosie die buiten optreedt.

Preface

To begin, it's been one hell of a ride for the last year.....

The thesis before you is testament of the research looking into the effects of compaction on the erosion resistance of soils and has been carried out at Boskalis under the aegis of the TU Delft.

To make this research happen a test set-up has been designed and built, quite akin to the Erosion Function Apparatus of Briaud. Further proof of concept testing and erosion testing of 3 different clays at several different water contents and 3 different energy levels have been conducted.

This means that this research has been quite all-round: A full design cycle has been made from design, to construction and proof of concept testing a testing set-up. Hereby it was also necessary into different areas of expertise to make this set-up work involving not only geotechnical, but also hydraulic , mechanical and electrical engineering. And finally, the set-up could be used to carry out the erosion testing which was what this thesis was all about. Having been able to perform this research was, albeit very tough sometimes, very gratifying.

Now that this research has come to an end, I would like to thank several people in particular.

First of all I would like to thank Robbin Sluijsmans who was my daily supervisor and helped arrange that it was possible to graduate at Boskalis. He was always ready to help and give advice.

Further I would like to thank my university supervisor Cristina Jommi, Robert Lanzafame and Anne-Catherine Dieudonné for their input during my thesis.

The same holds for everybody who helped me at Hydronamic, Boskalis Environmental, Research and Develepoment and E&L.

Finally I would thank my family and friends for their continuing support during the the thesis, and making sure I wouldn't erode away during it!

*L. Rook
Delft, January 1st 2020*

'Overigens blij ik van mening dat de dijken versterkt moeten worden.....'

-Cornelis Lely

Nomenclature

Acronyms

Symbol	Description	Dimensions	Units
<i>CFD</i>	Computation Fluid Dynamics Modelling		
<i>EFA</i>	Erosion Function Apparatus		
RETA	Rotating Erosion Testing Apparatus/Erosion Centrifuge		
SRICOS	Scour Rate in Cohesive soils model		

Soil

Symbol	Description	Dimensions	Units
ϵ	Rate of erosion	$V/A * T$	$\frac{m^3}{m^2 * h}$
λ	Characteristic Length	L	m
ρ_b	Bulk density	M/L^3	$\frac{kN}{m^3}$
τ	Shear stress	F/A	$\frac{N}{m^2}$
τ_c	Critical shear stress	F/A	$\frac{N}{m^2}$
A	Area exposed to erosion	L^2	m^2
a	Activity		%
C_e	Erosion Factor	$M^7 * T/L^7$	$N^2 * s/m^7$
c_u	Undrained shear strength	F/A	kPa
D	Equivalent diameter	L	m
D_{50}	50% particle distribution size	L	m
k	Roughness parameter	L	m
PI	Plasticity Index	M/M	%
s	Detachment coefficient	$\frac{L^3}{F * T}$	$\frac{m^3}{Nh}$
S_i	Initial erodibility	$L/T/F/A$	$mm/hr/N/m^2$
S_{iv}	Velocity detachment coefficient	$(L/T)/(L/T)$	$mm/hr/m/s$
SSA	Specific Surface Area	$\frac{L^2}{m}$	$\frac{m^2}{g}$
v	Fluid flow velocity	L/T	m/s

v_c	Critical erosion velocity	L/T	m/s
w	Water content	$\frac{M}{M}$	%
w_{ll}	Liquid limit water content	M/M	%
w_{pl}	Plastic limit water content	M/M	%
CI	Consistency Index	M/M	%
LI	Liquidity Index	M/M	%
LL	Liquid limit	M/M	%
PL	Plastic limit	M/M	%

Contents

List of Tables	xiii
List of Figures	xv
1 Introduction	1
1.1 Motivation	1
1.2 Problem Description	2
2 Literature Review	5
2.1 General description of erosion and erosion types	6
2.2 Links between soil parameters and erosion	7
2.3 Cyclic loading effects	14
2.4 Effects of Compaction.	14
2.5 Influence of Soil Structure and Salt/Fresh water interaction	16
2.6 Current assessment Standards	18
2.7 Types of Erosion devices	22
3 Erosion Function Apparatus overview	27
4 Soil characterization, clay compaction and erosion testing method	29
4.1 Soil types tested.	29
4.2 Index testing	30
4.3 Discussion on Index Testing tests	31
4.4 Proctor curves	32
4.5 Erosion testing method & Interpretation	35
5 Testing Results erosion testing	41
5.1 Results erosion testing	41
5.2 Erosion analysis in the context of the proctor plane.	45
5.3 Erosion in context with other research	49
5.4 Analysis in different manners	51
5.5 Observations during testing.	51
6 Discussion	53
7 Conclusions	55
8 Recommendations	57
8.1 Recommendations regarding the EFA/sample preparations	57
8.2 Recommendation regarding further testing	58
Bibliography	59
I Appendices	63
A Design Erosion Function Apparatus	65
A.1 General overview	66
A.2 Design Pumping system	67
A.3 Design Flow tube	68
A.4 Sensors	74
A.5 Miscellaneous parts.	75
A.6 Fluid Dynamics Modelling	77

B	Build Erosion Function Apparatus	81
B.1	End result set-up	82
B.2	Unexpected events during the build	82
C	Proof of Concept testing Erosion Function Apparatus	85
C.1	Pumping curve	87
C.2	System accuracy	89
C.3	Differing protrusion.	91
C.4	Diameter effects	92
C.5	Time-effect testing	93
C.6	Repeatability testing	96
C.7	Validation of CFD modelling	97
D	Further Literature review	101
D.1	Proctor compaction procedure	101
D.2	Building Practices Clay cover	101
D.3	Flow through pipes	102
D.4	Hydraulic loads	104
D.5	Additional erosion testing devices	104
E	Overview drawing EFA flow tube	111
F	Calculation flow pump	119
G	Testing method index testing	121
H	Photo's end result EFA	123
I	Testing forms	133
I.1	Proof of concept testing.	133
I.2	Erosion testing	138
J	Working protocol	151
J.1	Protocol soil compaction and extraction	151
J.2	Testing protocol EFA	152

List of Tables

2.1	Specific area of certain clay minerals (Hughes (1981))	8
2.2	Erosion classes according to Kruse	18
2.3	Dutch erosion guidelines	18
2.4	Additional requirements Dutch erosion guidelines	18
2.5	German erosion guidelines	19
3.1	Controlled and measured parameters Erosion Function Apparatus	27
3.2	Capabilities and accuracy EFA	28
4.1	Index testing results tested clays	30
4.2	Clay dry densities, optimum water contents and erosion classes	31
4.3	Testing Programme Boom clay	32
4.4	Testing programme Kampen II clay	32
4.5	Testing programme Kampen III clay	32
5.1	Results erosion testing	42
5.2	Interpretation of erosion testing results	43
5.3	Back-calculated erosion rates at benchmark shear stresses	44
5.4	Ranges erosion parameters different clays	47
A.1	Shear stress development under different flow speeds CFD modelling	78
A.2	Sensitivity analysis w.r.t protrusion	79
A.3	Sensitivity analysis w.r.t diameter	79
C.1	Response Absolute pressure Rosemount	89
C.2	Response Differential pressure Rosemount	89
C.3	Response pitot rosemount	89
E1	Overview pumps	119

List of Figures

1.1	Research set-up	4
2.1	Proposed erosion function	6
2.2	Structure change when subjected to different salt concentration (Hughes (1981))	8
2.3	Shields-curve (Briaud (2001))	9
2.4	Relationship PI and Critical shear stress (Briaud (2001))	10
2.5	Relationship PI and initial erodibility (Briaud (2001))	10
2.6	Relationship PI and Critical shear stress	10
2.7	Relationship PI and initial erodibility	10
2.8	Relationship Liquidity index and Critical shear stress	11
2.9	Relationship Liquidity index and initial erodibility	11
2.10	Relationship consistency index and Critical shear stress	11
2.11	Relationship consistency index and initial erodibility	11
2.12	Erosion class division based on testing by (Kruse (1988))	12
2.13	Relationship undrained shear stress and and critical shear stress	13
2.14	Relationship undrained shear stress and initial erodibility	13
2.15	Example of a proctor curve (Briaud (2013))	14
2.16	detachment coefficient versus water content at a given energy level (United States Federal Bureau of Reclamations (2014))	15
2.17	Detachment coefficient at different energy levels(United States Federal Bureau of Reclamations (2014))	15
2.18	Structural alignment possibilities soil Mitchell and Soga (2005)	16
2.19	Effects of salt/fresh water environment Mitchell and Soga (2005)	17
2.20	Difference German/Dutch guidelines	19
2.21	Proposed erosion function (Briaud (2001))	20
2.22	Possible erosion curves US guidelines (S. Shewbridge (2010a))	20
2.23	erosion class division (J.L Briaud and Shaffi (2017))	21
2.24	Photo of Erosion centrifuge at Deltares (Alkemade and Kruk (2018))	22
2.25	Schematic figure of erosion centrifuge (R. Crowley and Robeck (2012))	22
2.26	Basic functioning of Erosion Function Apparatus	24
2.27	photo of Erosion function apparatus (M.E. Walker III (2013))	24
3.1	End result Erosion Function Apparatus	28
4.1	Erosion class designation tested clays	31
4.2	Proctor curve Boom clay	33
4.3	Proctor curve Kampen II clay	33
4.4	Proctor curve Kampen III clay	34
4.5	Erosion curve sample γ SRICOS model	36
4.6	Shear stress/erosion rate plot in log/log space	37
4.7	Shear stress/erosion rate plot in log/log space	38
5.1	Critical shear stress Kampen III clay	45
5.2	Critical erosion velocity Kampen III clay	45
5.3	Detachment coefficient Kampen III clay	45
5.4	Velocity Detachment coefficient Kampen III clay	45
5.5	Critical shear stress Kampen II clay	46
5.6	Critical erosion velocity Kampen II clay	46
5.7	Detachment coefficient Kampen II clay	46

5.8	Velocity detachment coefficient Kampen II clay	46
5.9	Critical shear stress Boom clay	46
5.10	Critical erosion velocity Boom clay	46
5.11	Detachment coefficient Boom clay	46
5.12	Velocity Detachment coefficient Boom clay	46
5.13	Kampen III shear stress/erosion rate results in Briaud erosion graph	49
5.14	Kampen III velocity/erosion rate results in Briaud erosion graph	49
5.15	Kampen III low plasticity clay ranges	49
5.16	Kampen III low plasticity clay ranges	49
5.17	Kampen II low plasticity clay ranges	50
5.18	Kampen II low plasticity clay ranges	50
5.19	Boom high plasticity clay ranges	50
5.20	Boom high plasticity clay ranges	50
5.21	Progression of failure during testing	51
A.1	Overview drawing Erosion Function Apparatus	66
A.2	Parts of Erosion Function Apparatus	67
A.3	Flow tube erosion function apparatus	68
A.4	Soil feeding mechanism EFA	70
A.5	Soil container EFA	71
A.6	Connection round tube to rectangular tube	72
A.7	Detail pitot tube	73
A.8	Filling cap	74
A.9	Shear stress and pressure drop CFD modelling	78
B.1	End result Erosion Function Apparatus	82
C.1	Velocity in flow tube as a function of the pump operating frequency	87
C.2	Pressure drop over polyflow points	87
C.3	Absolute pressure as a function of pump operating pressure	87
C.4	Accuracy of velocity measurement	90
C.5	Accuracy of shear stress measurement	90
C.6	Accuracy of pressure measurement	90
C.7	Effect of protrusion on velocity	91
C.8	Effect of protrusion on shear stress	91
C.9	Effect of protrusion on the absolute pressure	91
C.10	Normalization with differing protrusions	92
C.11	Diameter effects on the shear stress/velocity relationship	92
C.12	Diameter effects on the shear stress/pump frequency relationship	93
C.13	Normalized shear stress versus operating frequency pump	93
C.14	Normalized shear stress versus velocity	94
C.15	Raw data for producing pumping curve	97
C.16	Comparison of maximum shear stress development CFD and average shear stress test data	98
C.17	Comparison of average shear stress development CFD and average shear stress test data	99
C.18	Comparison of absolute pressure development between CFD and real data	99
C.19	Correlation between average shear stress EFA and shear stress at sample in CFD	99
D.1	Observed clay cover	102
D.2	Fluid flow in conduits	103
D.3	Schematic overview Hole erosion test	105
D.4	Schematic overview Flow pump test	106
D.5	Schematic overview Triaxial erosion test	106
D.6	Hydraulic flume erosion test	107
D.7	Schematic set-up ex-situ erosion device	108
D.8	Schematic set-up in-situ erosion device	108
D.9	Overview Pocket Erodrometer	108
D.10	Overview pluvial erosion simulator	109

D.11 Set-up Jet erosion test	109
E.1 Design drawing Erosion Function Apparatus flowtube	112
E.2 Soil feeding mechanism EFA	113
E.3 Connection round tube to rectangular tube	114
E.4 Filling cap	115
E.5 Pitot tube	116
E.6 Soil container	117
H.1 Overview end result EFA	124
H.2 Result Variable Frequency Drive	125
H.3 Result Opto 22 data box	126
H.4 Result filling cap	127
H.5 Result connection round to rectangular tube	128
H.6 Result transition pieces to gradually change flow	129
H.7 Result connection pitot tube	130
H.8 Result soil feeding mechanism and polyflow connectors	131
H.9 Result soil container	132
I.1 Idealized pumping curve	134
I.2 Output graphs from protrusion differences	136
I.3 Output graphs from diameter differences	137
J.1 Flowchart soil compaction and extraction	151
J.2 Testing protocol EFA	153

Introduction

1.1. Motivation

Erosion resistance of clay is an important topic in many fields: for instance in bed, bank and shore protection, morphology and dike construction. However, the focus of this thesis concerns the erosion resistance of clay used in the clay cover of a dike, being eroded due to overflow or overtopping. It is obvious that this clay cover must be resistant to the forces that are exerted as to protect the hinterland of the levee.

In the past many (laboratory) studies have been performed on the following topics relating to erosion of clay:

- Designing and building devices to measure erosion
- Relating specific soil properties to the erosion resistance
- Quantifying the positive effects of vegetation with respect to the erosion resistance
- Investigating the effects of the soil fabric and salt/fresh water
- Assessing the loads that the clay has to sustain due to overflow or overtopping

This leaves 1 topic that has not been investigated in-depth, but could have a big influence on the erosion properties of the dike: the effect of compaction while processing the clay during dike construction.

To further elaborate on the topic: A limited amount of studies have been done looking into what the effects are of processing the clay. This processing generally means that the clay is compacted on-site. It is generally accepted knowledge that compaction enhances the erosion resistance, but little is known about the quantitative effects of this compaction and at what conditions the clay will behave optimally. When discussing compaction this means compaction in terms of energy level as well as compaction at a proper water content.

Multiple dike revetment projects of Boskalis once again expose the added value of performing research which can contribute to an enhanced understanding of the erosion resistance of clay, the knowledge which can then be used to tailor the design and installation methods.

1.2. Problem Description

1.2.1. Problem Statement

The erosion resistance of clay used in dikes is influenced by many parameters, such as the soil properties, vegetation, soil fabric and fresh/salt water effects. However, also the effect of compaction is of importance, but not yet thoroughly investigated. This is of interest because a varying compaction effort will lead to a varying erosion resistance which could result that some clays which are currently deemed unsuitable to be suitable in fact. The statement above makes clear that it is important to try and better understand effects that contribute to the erosion resistance of clay.

1.2.2. Objective

This research aims to set-up a framework in which the effect of compaction is incorporated. This framework is based on the results of experimental testing. To perform this experimental testing an set-up has been built in the laboratory of Boskalis, as there is no set-up available at the start of the project. In this set-up tests will be done with soil samples that have different levels of compaction energy and water content.

1.2.3. Research Questions

To achieve the objectives stated above, the following main research question has been formulated:

What effect does compaction have on the erosion resistance of unsaturated clay, when used as a dike cover, and how can this be measured and analyzed?

To further break down this research question, it has been divided in the following sub-questions:

1. What is the best type of laboratory set-up that can be built to investigate the erosion resistance of unsaturated clay, when used as a dike cover given the constraints in time and money?
2. What is the quantitative effect of clay compaction on its erosion resistance? Does compaction contribute for example to a lower erosion rate, or to a higher erosion threshold?
3. What loads can be expected to occur induced by the wave over-topping?
4. How can the effects of compaction be incorporated in the current guidelines.

1.2.4. Scope

During this study certain aspects of erosion of clay in dikes will be investigated, however also some aspects will definitely not be handled, therefore here a bullet-point overview is made of what is done, but also what is not done.

What is done:

- Design, Build and Operate an erosion device.
- Look into effects of compaction on erosion resistance of clay, but only surface erosion
- Correlate previous research and guidelines with new findings

What is not done:

- Look into other aspects than surface erosion
- Perform large scale testing
- Perform extensive modelling

1.2.5. Approach

The methodology of this thesis will be as follows:

- Perform Literature Study
- Design Erosion Function Apparatus
- Build Erosion Function Apparatus
- Perform proof of concept tests
- Sampling (at site), sample preparation and Laboratory Testing
- Elaborate on Laboratory Testing
- Write Report

The goal of performing the literature study is to get an overview what the current (Dutch) clay erosion standards are and investigate what other literature and standards are available which are related to the topic. This will cover topics ranging from correlating soil parameters to erosion, the effects of compaction, effects of structure and methods or devices to measure erosion. After having an overview of the available literature a decision has been made what type of clay erosion device will be constructed. This turned out to be a clay erosion device, quite similar to the Erosion Function Apparatus as proposed by (Briaud (2001)) and (J.L. Briaud (2005)). This apparatus is currently not available in the Netherlands and must therefore be built. Why specifically this apparatus will be used is explained in chapter 2. A broad overview of the device is given in chapter 3, whereas the detailed design is cover in chapter A.

When the apparatus is finished testing will commence in 3 phases: index testing of the clays that are tested, proof of concept testing and then the actual erosion testing. The index testing is conducted to fully quantify the clays that are tested, the results which are given in chapter 4. Then the proof of concept testing has been conducted in order to prove and better understand what the capabilities of the Erosion Function Apparatus and how accurate its measurements are, the results which are presented in Appendix C. Finally, the erosion tests have been conducted on the clays which are tested, the results and interpretation which is given in chapter 5.

The approach can be summarized in the scheme given in figure 1.1, correlating each part in the report to the following tasks:

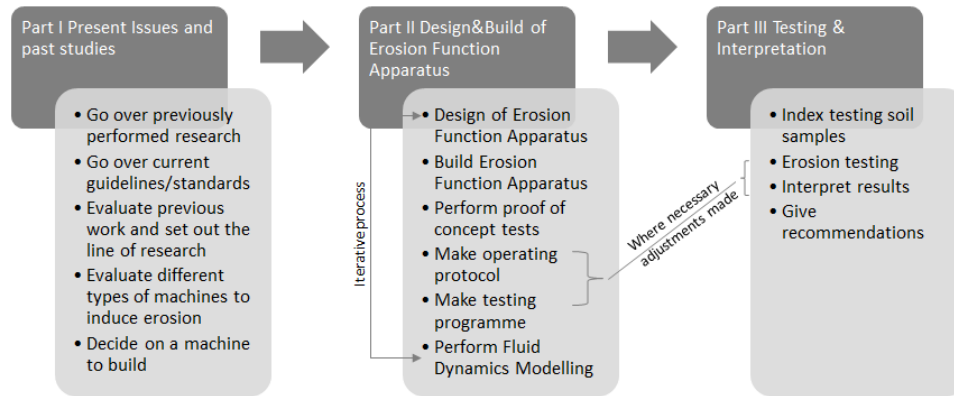


Figure 1.1: Research set-up

By performing the above stated tasks a well-structured research can be conducted with results that can be well analyzed and substantiated.

2

Literature Review

In this chapter a main overview of the research performed will be given, to do this the following topics will be discussed:

- General description of erosion and erosion types
- Links between soil parameters and erosion
- Effects of compaction
- Structure and Salt/fresh water effects
- Current design standards/guidelines
- Types of testing devices
- Cyclic loading effects

At the end of each section a brief conclusion will be drawn.

This does not include the full range of topics looked into. However these topics are not of main importance to the topic and thus are navigated to Appendix D. These topics include:

- Proctor compaction procedure
- Modeling of flow through rectangular pipes
- Clay cover building practices
- Current (compaction) quality control at Boskalis
- Expected loads on the clay
- Additional erosion testing devices not discussed in main report

2.1. General description of erosion and erosion types

Erosion can generally be described as the group of processes that wear away soils and rocks (Haghigi (2013)). It can be described by a loss of Volume per time unit per unit area dependent on the shear stress. This results in such a type of formula:

$$\epsilon = s * (\tau - \tau_c) \quad (2.1)$$

In the equation the symbols represent:

ϵ = rate of erosion, $\frac{m^3}{m^2h}$

s = detachment coefficient, $\frac{m^3}{Nh}$

τ = shear stress, $\frac{N}{m^2}$

τ_c = critical shear stress when erosion starts, $\frac{N}{m^2}$

This can then be represented in an erosion curve of which an example is given in figure 2.1.

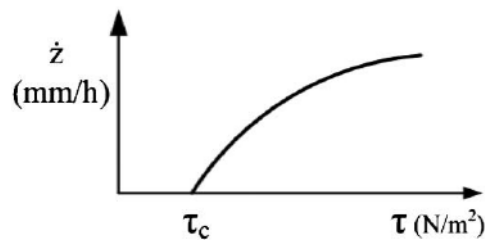


Figure 2.1: Proposed erosion function

\dot{Z} here represents the rate of erosion and is therefore comparable to ϵ .

It is however important to note that erosion is not a single process, but a group of processes. This group of processes can be subdivided in 2 main categories, which are external and internal erosion. These main categories can then be divided in different mechanisms (Haghigi (2013)) (Rice (2019b)) (Rice (2019a)).

Internal Erosion

Internal Erosion involves the erosion of soil when water searches a path through the soil. The following mechanisms can be seen:

- Heave
- Backward erosion
- Contact erosion
- Suffusion

When considering that this thesis mainly focuses on erosion induced by wave over-topping, it is obvious that the internal erosion mechanisms described above are of a limited influence. Therefore, external erosion will be discussed immediately.

External Erosion

External erosion involves the erosion of soil from the superficial layers downward under the influence of different natural agents (water, frost, etc.). Here there are not so much different mechanisms, but different stages in the external erosion process, namely the following:

- Surface Erosion (removal of vegetation and superficial layers)
- Concentrated flow Erosion (Formation of a headcut)
- Erosion progression (Headcut advance)

- Breach formation (Breach formation)

Looking at the difference between external and internal erosion it seems that external erosion is more representative of water flowing over the top of a dike's clay cover. Specifically surface erosion, where only the first part of the soil is being eroded away is important, because the following steps are already considered not acceptable.

Conclusion The main type of erosion that will be looked into concerns external erosion. However, due to limitations in testing the main form of erosion that is measured will be surface erosion. This because in the set-up only samples of a limited size can be tested, making it more difficult to test the progressing stages after surface erosion.

2.2. Links between soil parameters and erosion

A lot of research has been performed to try and correlate the erosion rate to certain types of soil parameters. An overview of this can be found in (Mostafa (2008)), (Briaud (2001)) and (Waterloopkundig Laboratorium (1985)). It states that the erosion resistance of a soil may differ based on the following aspects:

- clay content
- bulk density of the soil ρ_b
- D_{50} of the soil
- liquid limit water content w_{ll}
- plastic limit water content w_{pl}
- undrained shear strength c_u
- Organic content
- Lime content

There has been tried to correlate the erosion resistance of clay to these types of parameters because it is very difficult to calculate the erosion resistance. This because, in contrast to sand not only gravity forces come into play, but also the colloidal forces between all clay particles. It is therefore useful to correlate it to more easy to measure quantities.

2.2.1. Clay content

One of the items mentioned to have an influence on the erosion resistance is the clay content (R. Fell (2013)). This because clay, in contrast to sand, has much more chemical bonds than sand. A method of representing this can be characterized by the specific surface area (SSA) of a soil. This is the amount of surface a soil has per unit weight (Hughes (1981)). If a soil has a relatively high specific surface area, it has more opportunity to create a lot of chemical bonds (possibly resulting in a higher erosion resistance). An overview of how large these surface areas could be is given below in table 2.1.

Table 2.1: Specific area of certain clay minerals (Hughes (1981))

Clay mineral	Specific Area (m ² /g)
Montmorillonite	200-600
Illite	50-100
Kaolinite	5-20
Sand fine	0.02

As can be seen, the differences in specific area between different types of soil is large, and thus intuitively one could deduce that the amount inter-particle forces will vary significantly with the different types of clay minerals. This deduction has not been confirmed by literature however. What is known however, which has been stated by (Kruse (1986)), (Hughes (1981)) and (R. Fell (2013)) is that a higher clay content will result in a higher erosion resistance, regardless of the clay's mineralogy. This is a reason why the clay content is measured, rather than the specific area is. Also it is far more easy to measure the clay content of a soil. Finally, no literature relating the clay mineralogy to the erosion resistance has produced conclusive results.

For instance, (Waterloopkundig Laboratorium (1985)) states that, generally speaking illite clays will tend to be more erosion resistant than montmorillonite clays albeit the latter has a higher SSA. However, it also acknowledges that there is a large spread in results leading to results which are non-conclusive and non-coherent. It tries however to correlate this counter-intuitive result to the fact the montmorillonite clay will tend to take on a very different structure than the illite clays when subjected to the same salt concentration as can be seen in figure 2.2.

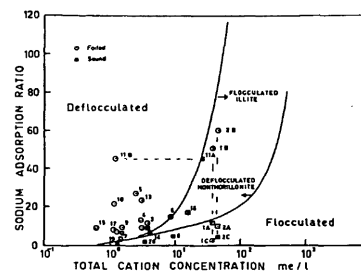


Figure 2.2: Structure change when subjected to different salt concentration (Hughes (1981))

This is also a reason why (Waterloopkundig Laboratorium (1985)) says that the results of clay mineralogy can only be used very indicatively and that many other parameters are of (greater) importance.

Conclusion

Regarding the clay content, one can conclude that a higher clay content will result in a more erosion resistant soil due to the higher inter-particle forces. This is also already done in several design codes (albeit the Dutch code works the other way around, dismissing clays with a too large sand content). Further, using the clay mineralogy in the assessment of its erosion resistance is not possible due to the non-conclusive results. However, research might shine a better light on the effect of the clay mineralogy on a clay's erosion resistance. This will however not be done in this research.

2.2.2. Density

Another topic of importance that contributes to the erosion resistance of clay is the density according to (R. Fell (2013)). This is also kind of acknowledged by the current dutch guidelines by stating that a soil must at least have 97 % proctor density when compacted which is a method of incorporating the density as a measure for erosion resistance. Also, obviously, the density is a measure of the quality of compaction. However, the bulk density on its own does not necessarily give a good indication if something is erosion resistant, only when comparing it to for instance a proctor test. Proof of that can be seen by looking at the erosion classes as set up in (CROW (2010)). Here it can be seen that soils with a higher bulk density generally have a lower resistance to erosion. This is because clays with a higher sand content (and thus are less erosion resistant) have a higher bulk density. However, as is proven in the section below concerning compaction, a higher compaction effort, which will lead to a different density, will result in a higher erosion resistance in general.

Conclusion

Using the bulk density as a measure for erosion resistance is a good way of doing so. To do this properly however, one must compare the bulk density measurement against the results of a standard compaction test before a conclusion can be drawn. Also, one must not forget that to truly understand the compaction state of a soil it must be considered in the proctor plane where the density is a combination of the water content and energy level.

2.2.3. D_{50}

Describing the erosion resistance using the D_{50} has already been done for a long time, especially when describing the erosion of sand, as has been done by (Shields (1936)). This resulted in a graph as presented in figure 2.3.

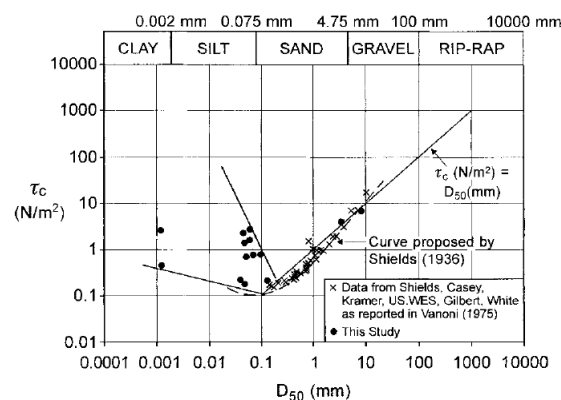


Figure 2.3: Shields-curve (Briaud (2001))

For sand this also makes sense, because erosion of sand is mostly a problem involving sand grains eroding individually, with a certain shear force imposed by the flowing water, and a certain weight to resist these forces. For clay this makes less sense, but it can also apply and can be used as seen in (Zhang and Yu (2017)). The reason why it makes less sense for clay is because there are a lot of internal/contact forces which come into play because of its fine-grained nature. However, it can be a well-educated first guess. This can be seen in figure 2.3, here (Briaud (2001)) plotted the results from erosion testing in the shields diagram and found that low, but conservative estimation of the possible critical shear stress.

Conclusion

Determining if a soil is more or less erodible based on the measurement of the D_{50} could be a possible way of giving a first, conservative crude estimation of its erodibility. However, caution should be exercised.

2.2.4. Liquid limit and plastic limit of the soil

Integrating the liquid limit and plastic limit of the soil in the erosion resistance is something that has been proposed and done by (Gibbs (1962)), (Kruse (1988)) (Briaud (2001)) and (R. Fell (2013)). Its importance has also been acknowledged by (Hughes (1981)) and (R. Crowley and Robeck (2012)). This because if a soil has a high range between these 2 limits, it will be influenced less in its strength parameters than a soil that has a lower margin. The results can then be plotted in a figure with the plasticity index (PI) on the x-axis and the critical shear stress at which the soil starts eroding on the y-axis, or plotting the plasticity index versus the initial erodibility of the soil. This has been done by (J.L Briaud and Shaffi (2017)) in figure 2.4 and figure 2.5.

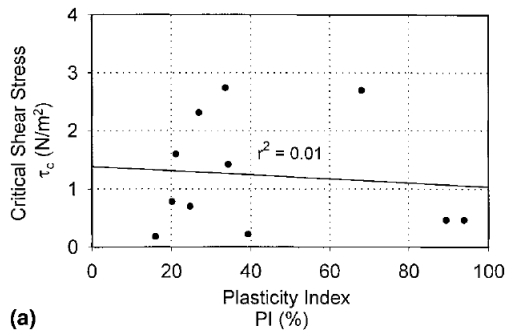


Figure 2.4: Relationship PI and Critical shear stress (Briaud (2001))

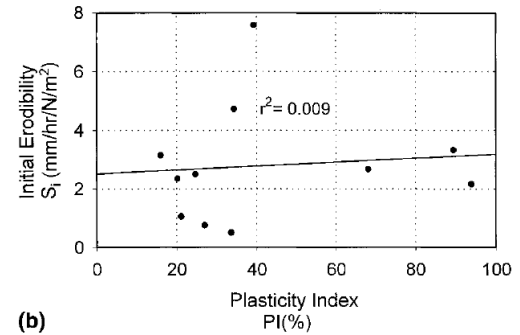


Figure 2.5: Relationship PI and initial erodibility (Briaud (2001))

From these graphs one cannot say that there is a clear-cut relationship between plotting the plasticity index versus erosion parameters, but rather shows a more random fit. It may be noted however that these 11 results have been obtained by testing samples procured from widely differing regions of Texas leading to many factors being different, e.g. mineralogy or the geological history it has endured. This could then mean that a relationship may be present, but be obscured by the widely varying backgrounds of the samples.

Therefore, also data acquired by Kruse (1988) has been used, and this gives the results given in figure 2.6 and figure 2.7.

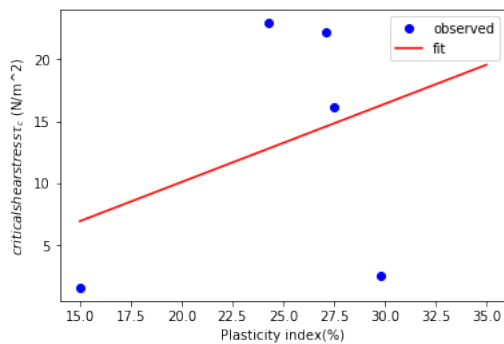


Figure 2.6: Relationship PI and Critical shear stress

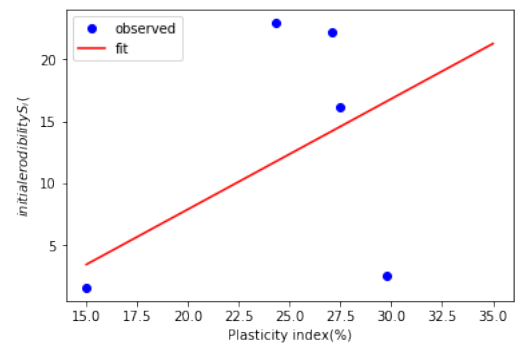


Figure 2.7: Relationship PI and initial erodibility

Looking at this data one would also not suggest there is a good relationship between PI and the critical shear stress or its initial erodibility, albeit all samples have a similar geological history (all samples were taken in the Dutch delta area). And although the geological conditions in the Dutch delta area are not homogeneous and the area is fairly large, it is much smaller and much more homogeneous on a geological scale than the entirety of Texas.

It might therefore be a good reason also to try and correlate the results obtained by Kruse against the Consistency and Liquidity Index, which are defined in equations 2.2 and 2.3.

$$CI = \frac{LL - w}{LL - PL} \quad (2.2)$$

$$LI = \frac{w - PL}{LL - PL} \quad (2.3)$$

The liquidity and consistency index are supposed to show how near or far a soil is to being liquid or plastic. This is then also a good indicator if a soil is more or less likely to swell or shrink (Kruse (1986)), which will affect the possibility of the material to erode.

This gave the following results with the data of Kruse (the data of Briaud has been left out due to the heterogeneous origin of the soils as mentioned above):

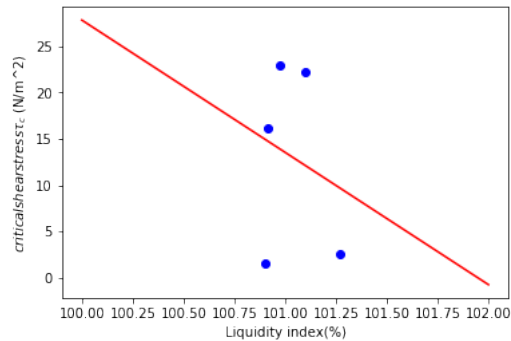


Figure 2.8: Relationship Liquidity index and Critical shear stress

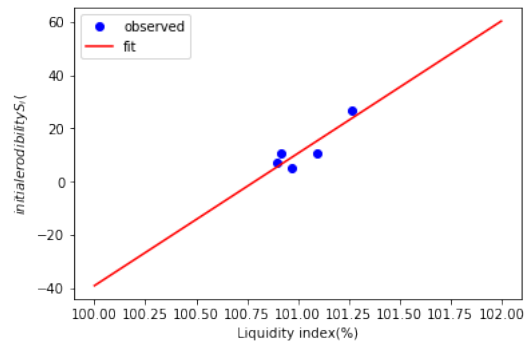


Figure 2.9: Relationship Liquidity index and initial erodibility

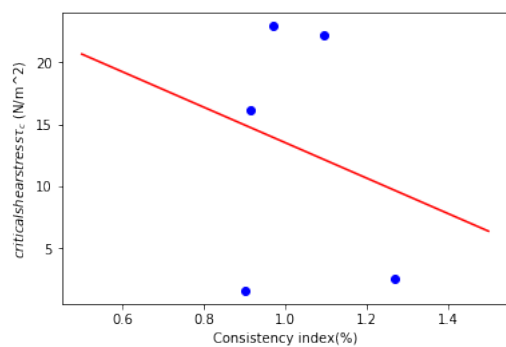


Figure 2.10: Relationship consistency index and Critical shear stress

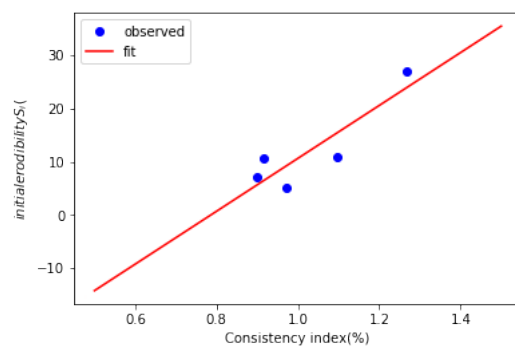


Figure 2.11: Relationship consistency index and initial erodibility

When looking into these graphs it seems that both the liquidity index and consistency index give a good fit when looking at what the initial erodibility of the soil, however it does give a poor fit of estimating the critical shear stress. It might therefore be a good idea to also use either the consistency or liquidity index in the rest of this research. That there is a correlation between the consistency/liquidity index is in line with suggestions proposed by Kruse, but which has not been looked into further detail by Kruse.

Another possibility, which has been done by Kruse, is make a LL/PI plot and see how the erosion resistance develops, which has been done in figure 2.12.

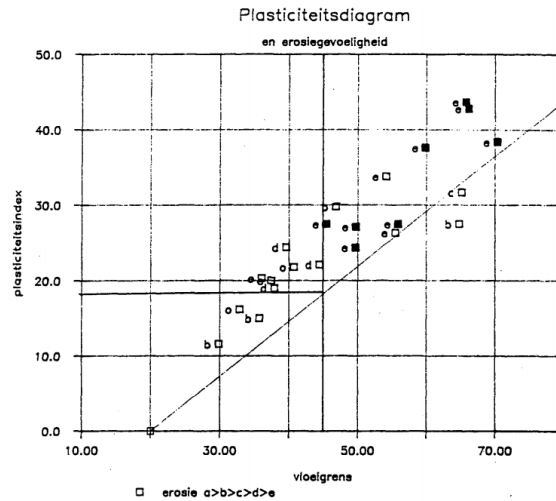


Figure 2.12: Erosion class division based on testing by (Kruse (1988))

With the help of figure 2.12 it is shown that samples which have a higher liquid limit and plasticity index have a higher erosion resistance in general. From his tests classes were drawn which are incorporated in the Dutch guidelines with respect to clay erosion and thus will not be further discussed in this section, but can be looked into in section 2.6.1.

Up to now no strength parameters have been taken into account when looking at erosion, but also has an influence, which is why people have also tried to correlate the erosion resistance to the so-called activity of a soil, which is defined as such:

$$a = \frac{PI}{\% < 2\mu m} \quad (2.4)$$

Where in this equation a represents the activity of a soil, and PI the plasticity index. According to (Waterloopkundig Laboratorium (1985)) it incorporates a strength parameter in a certain way, because a higher clay content will result in a soil which is more erosion resistant. However, no results are available that it gives a good fit and will therefore not be used in any further research.

Further along, there has been tried to create a so-called erosion factor (Waterloopkundig Laboratorium (1985)), which has been defined as such:

$$C_e = \frac{G_e}{\frac{A * v^2 * t}{\gamma_b * PI}} \quad (2.5)$$

In this equation C_e is the erosion factor, G_e the mass lost in the erosion process, A the area exposed to erosion, v the speed of fluid flow, t the time that erosion took place, γ_b the bulk density of the soil eroded and PI the plasticity index.

However, it also delivers widely varying and inconsistent results and therefore will not be used anymore.

However, based on reasoning the influence of the liquid and plastic limit is definitely there.

A way of still underlining the necessity of this parameter is including certain threshold values to the clay when classifying it as being sufficient or not as has been done by (Nguyen (2014)) based on Gibbs. But what also has been done is for instance

Conclusion

Use of the Liquid and Plastic limit is a reasonably straightforward method of assessing the erodibility of soils. However, solely using the liquid or plastic limit to assess the erodibility of a soil seems a fairly poor way of doing so. Using the combination of liquid and plastic limit (as done by Kruse) seems to be a better approach in general. Further, the use of the liquidity index (or consistency index) seems to yield promising results and the use of the liquidity index will also be used in the remainder of this report. The added benefit of using the liquidity index in combination with the liquid and plastic limit is that the liquidity index is a parameter which reflects the state of the soil. However usage of only the liquidity index is not advised because this does not reflect how far the liquid and plastic limit are from each other.

2.2.5. Undrained shear strength C_u

Making an estimation of the erodibility of the soil based on the undrained shear strength has 2 distinct benefits: it includes strength parameters and can be executed fairly easily. This has been tried to be done by (Nguyen (2014)) and (Independent Levee systems investigation team Hurricane Katrina (2006)) and gave results as represented in figures 2.13 and 2.14 (Briaud (2001)).

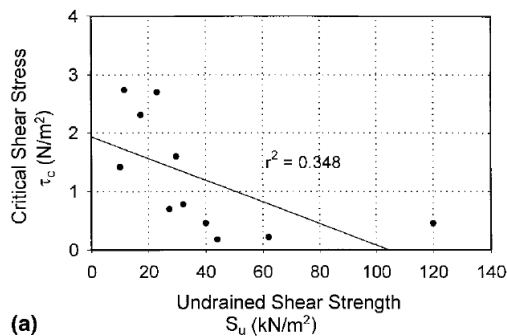


Figure 2.13: Relationship undrained shear stress and and critical shear stress

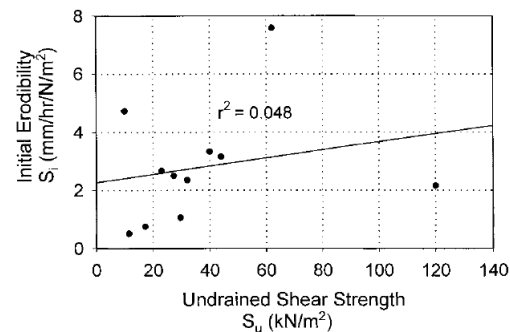


Figure 2.14: Relationship undrained shear stress and initial erodibility

Looking at these results (of different types of clays, all non-compacted) it seems that there an increasing undrained shear strength results in a higher erodibility. This can be explained when thinking what the undrained shear strength is related to. This is related to (not meant be an extensive list) the angle of internal friction, the relative density, cohesion, degree of saturation and permeability. This means that a more sandy clay will have a higher undrained shear strength due to its higher angle of internal friction and higher permeability, but it will be more erodible. However, a more compacted soil will also have a higher undrained shear strength. This means that when comparing between clays it can be said that a higher undrained shear strength will result in a higher erodibility. However, when comparing within one clay type compacted in different water content/energy level combinations a higher undrained shear strength will result in less erodibility. This is also something that can be observed in (B. Kerssens (2017)).

Conclusion When comparing different types of clay one can conclude that a higher undrained shear strength will result in less favorable erosion characteristics. However, when comparing within one clay a higher undrained shear strength will result in less erosion in general.

2.2.6. Lime content

The lime content is of influence because it has a positive effect on the inter-particle forces between the clay particles according to (Wouters (1981)). However, this statement is based on a very limited amount of research, and there is ample concern that a very high amount of lime might be undesirable due to possible dissolution through meteorological conditions (e.g. acid rain). Because of this uncertainty a cautious limit of 25 % lime in the clay has been imposed.

2.2.7. Organic matter

Organic matter is of influence with respect to the erosion resistance of clay because it grants extra structure to the soil according to (Wouters (1981)). However, when looking at the long-term effects there is concern that this organic matter will rot away. Because of this uncertainty also a cautious 5 % limit on the amount of organic matter is imposed, although its effect is not clearly understood.

2.2.8. Conclusion on different soil parameters

As can be seen before, a lot of research has already been performed trying to correlate the erodibility of soil to different parameters, however none of this research has been able to give a good fit to soil data. This is obviously due to the complex property set of clay in general. However, trying to correlate a soils erodibility to different soil parameters is indisputably the easiest way to get a quick estimation for the erodibility of soil rather than immediately start erosion testing in a device as has already been pointed out by (Arulanandan and Perry (1983)). Therefore, these correlation will be kept in mind when setting up testing to get good first estimations, and wherever possible further improve correlations.

2.3. Cyclic loading effects

Further the effects of cyclic loading are discussed. Cyclic loading means that the soil is repeatedly dried and wetted. This occurs in a clay cover of dike due to the repeatedly changing weather conditions while being sufficiently far above the ground water to prevent capillary action from keeping the soil wet.

This repeatedly drying and wetting of soil leads to changes in soil structure, its water retention capabilities as well as several other parameters (Azizi (2017)). These changes lead to a more open soil structure, which also leads to a lower ability for the soil to retain water and an increased hydraulic permeability. Obviously, this leads to a significant change in the hydro-mechanical behaviour of the soil as also can be seen in (C. Airò Farulla (2005)), (J.M Fleureau et al. (2005)).

When talking about the erosion resistance 2 main processes occur that negatively influence the erosion resistance:

- Structure change and cracking
- Overall drying of superficial soil layer

The repeatedly wetting and drying of the soil will lead to a more open structure, resulting in a less aggregated structure causing that small chunks of the soil will tend to fail, rather than particle by particle. Further this more open structure will allow the superficial layer to dry-out more easily. This then results in a superficial clay layer that is drier than the optimum water content and has a different behavior than when it was compacted initially.

This effect was also clearly seen when visiting a dike revetment project, the first 20/30 centimeters of the soil were extremely cracked and dry. These observations are discussed more in detail in Appendix D.

2.4. Effects of Compaction

In this section the effects of compaction will be discussed. The method of compaction that will be used is Proctor Compaction. This because it is the main way to test a compacted soil in the laboratory and can be executed relatively easily. The procedure of proctor compaction is given in Appendix D.

The standards regarding the Proctor test are mostly given in (NEN (2010)) (Briaud (2013)). It is normal that the effect of compaction is presented in a proctor curve, an example of which is given in figure 2.15.

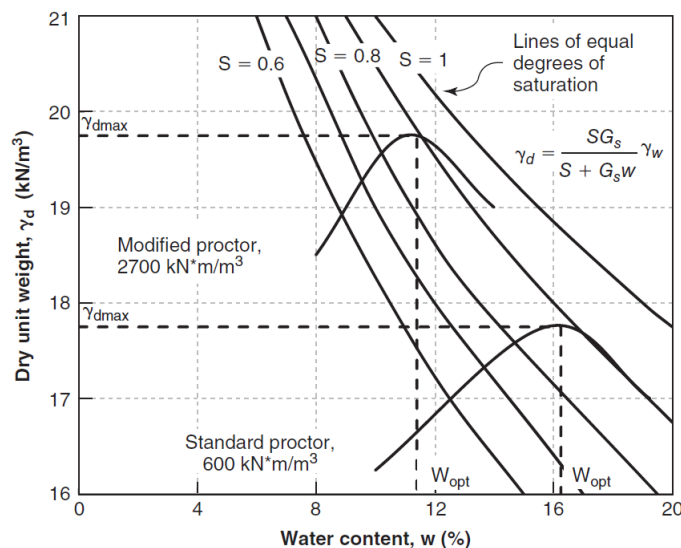


Figure 2.15: Example of a proctor curve (Briaud (2013))

It can thus be seen that at a given energy level significant differences can occur in dry density when the water content is changed, thus resulting in different strength, stiffness and eventually erosion resistance. But it can also be seen that at a given energy level the dry density can differ significantly. This can be due to the lack of moisture present making it more difficult to mold the clay to a high density or the excess amount of moisture being trapped in the soil limiting the ability for compaction. Therefore, tests will be conducted taking a soil at different compaction levels and different moisture contents into account.

For an example of how the erosion resistance can differ when compacted at different water contents can be observed in figure 2.16. It correlates the detachment coefficient (how fast soil erodes) to water content (United States Federal Bureau of Reclamations (2014)).

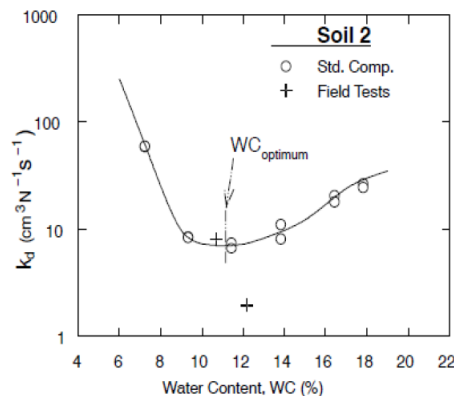


Figure 2.16: detachment coefficient versus water content at a given energy level (United States Federal Bureau of Reclamations (2014))

It is obvious that the soil has an optimum water content that limits the erodibility of the soil, but it can also be seen in figure 2.17 that different energy levels lead to different detachment coefficients. Similar effects can be seen in the study performed by (Yasufuku (2018)).

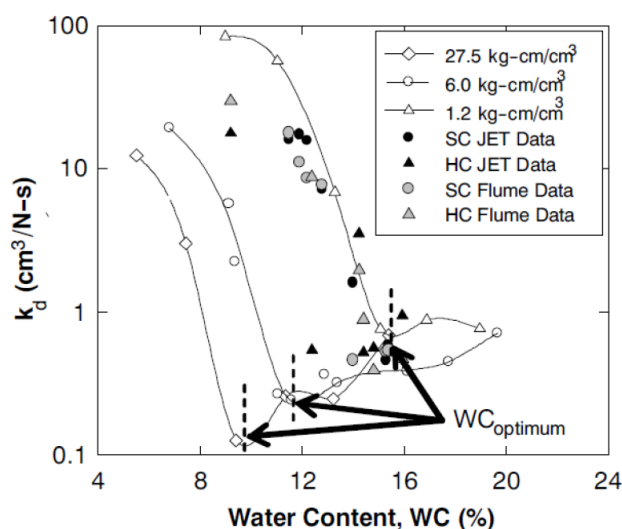


Figure 2.17: Detachment coefficient at different energy levels(United States Federal Bureau of Reclamations (2014))

Here the effect of compaction on the erosion resistance of clay can clearly be observed and thus it makes clear that it is of importance to better grapple with the issue.

To take this effect into account a set of guidelines and practices have been set up by (adviescommissie voor de waterkeringen (1996)), (T. Pullen et al. (2007)) and (US Army Corps of Engineers (2000)) that the fill of embankments must be at least (dependent on the region) 95 % or 97% proctor density (dependent on the country). However, no further studies have been found concerning this topic.

Conclusion The effect of compaction on the erosion resistance of clay can clearly be seen. The combination of water content and energy level at which a soil is compacted can dramatically increase its performance an order of magnitude. To at least have some guideline what minimum level of compaction is needed, there has been stated to have at least 95 % proctor density. However, there is room for improvement to have a more thorough quantification of the effects of compaction.

2.5. Influence of Soil Structure and Salt/Fresh water interaction

Also of influence is the soil structure and the effects of salt and fresh water. Generally speaking the structure of soil can be divided in the following types as given in figure 2.18 (figure modified from Mitchell and Soga (2005)).

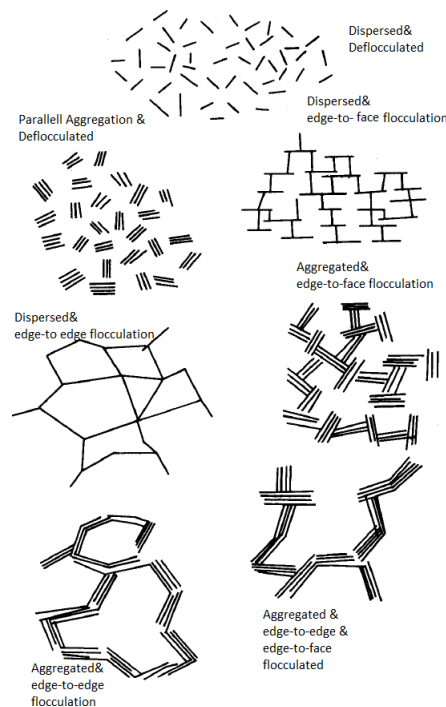


Figure 2.18: Structural alignment possibilities soil Mitchell and Soga (2005)

From this graph one can see that there are 2 main possible ways to distinguish the structure of a soil: if it is aggregated or not (i.e. the particles stick together) and if the particles are flocculated or not (i.e. do the groups of particles group together). The reason why this is of importance is because flocculated soils are less erosion resistant than deflocculated soils due to the more open structure that they tend to form (Mitchell and Soga (2005)), (Mitchell (1960)). Further, it has been assessed that aggregated soils tend to be more erosion resistant than dispersed soils due to the larger 'van der Waals forces' that can be developed in aggregated soils. This would then mean that one would like to get an aggregated and deflocculated structure, which is more easily obtained if the soil is better compacted.

The importance of the structure of the soil has been observed by (Independent Levee systems investigation team Hurricane Katrina (2006)) that samples that have been compacted at a non-optimal water content have less erosion resistance. One of the reasons for this is because the soil tends to aggregate less and a less dense structure will form.

However, one must also take into account the effects of salt/fresh water because this will affect the structure of the soil (as also mentioned in section 2.2.1). As stated by (Waterloopkundig Laboratorium (1985)) it can be expected that a soil in a fresh water development will develop a totally different structure than a similar soil which is deposited in a salt water environment (being more flocculated), as can be seen in figure 2.19 (modified from (Waterloopkundig Laboratorium (1985))).

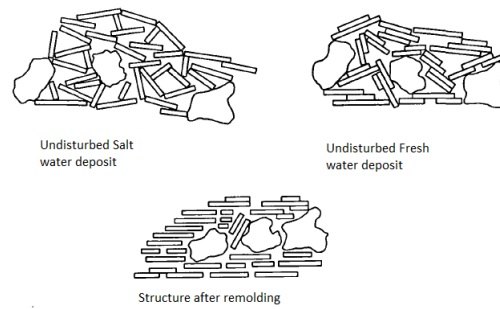


Figure 2.19: Effects of salt/fresh water environment Mitchell and Soga (2005)

Conclusion All in all the structure of the sample and the fresh/salt water effects are important to take into account. It is definitely not the main parameter that contributes to a soil being erosion resistant, but it has a positive impact. The most important lesson from this is that a proper compaction is critical to getting a good clay structure resulting in a well resistant soil. Further, it might be of interest to take extra care when using clay's of marine origin because these will tend to possess a more flocculated structure.

2.6. Current assessment Standards

2.6.1. Dutch Standards

The current standard in the Netherlands is based on extensive research conducted in the 1980's by Grondmechanica Delft. This research can be found in (Kruse (1986)) and (Kruse (1987)). Later on this resulted in the assessment standard presented in (CROW (2010)). In this research an erosion centrifuge was used. In this centrifuge a soil sample is placed after which water is rotated at a certain speed after which the mass loss is measured and an evaluation is made if failure has occurred. Based on the speed of the centrifuge a determination is made if the soil is prone to erosion or not. This classification is presented in table 2.2.

Class	Speed	Erosion Potential
A	<0.7 m/s	Very high potential
B	0.7 - 4.0 m/s	High
C	4.0 - 6.0 m/s	Limited
D	6.0 - 8.0 m/s	Low
E	>8.0 m/s	Very low

Table 2.2: Erosion classes according to Kruse

This resulted in the following guidelines given in table 2.3. This has been based on the many tests, a brief overview of which was presented earlier in figure 2.12 in section 2.2.4.

Parameter	Cat. I clay (well suited)	Cat. II clay (mediocre)	Cat. III clay (poorly suited)
LL (liquid limit)	>45 %	<55%	<0.73*(LL-20%)
PI	>0.73*(LL-20%)	>18	<18
Sand	<40 %	<40 %	>40 %

Table 2.3: Dutch erosion guidelines

But these guidelines also always have the following additional requirements, presented in table 2.4.

Soil parameter	Limit
Organic matter	<5 %
Lime content	<25 %
Salt concentration	<4 g/L
LI clay cover	>75 %
LI clay core	>60 %

Table 2.4: Additional requirements Dutch erosion guidelines

It is good to note that this classification of erosion resistance does not take into account the effect of the grass cover (if present) and that this will not be taken into account at all during the thesis.

Conclusion The current Dutch assessment standards do properly take into account the effects of the liquid and plastic limit, it takes into account that the soil becomes less erosion resistant with an increasing sand fraction, and does somewhat take into account the effects of water content.

However, the current assessment standard only divides the soil in classes based on soil parameters and no specific erosion testing. Further there is a limited understanding of how the properties really change and impact the erosion resistance. There is just a division of the soils in classes based on the tests performed by Kruse (1988) with limited knowledge about the effects of compaction.

Because of the above points all laboratory testing will also be checked with the Dutch assessment standards, but it will mostly be used as a reference framework and not as a main guideline.

2.6.2. German Standards

The only other country in Europe that has guidelines in place which could be found is in Germany, which are summarized in (T. Pullen et al. (2007)) and (Zentrum Geotechnik Deutschlands (2002)). The guidelines are in nature quite similar to those of the Netherlands in the sense that soils are classified based on their liquid limit and plasticity index. The limit values that come with these guidelines are given in table 2.5 (Wiersma (2011)).

German guidelines	Limit values		
	Well suited	Suitable	Poorly suited
Clay-% ($d < 0.002\text{mm}$)	20-40	15-20	10-15
Sand-% ($d > 0.063\text{mm}$)	10-40	25-50	30-50
Liquid limit (%)	35-70	30-55	25-40
Plasticity index (%)	20-45	15-20	10-15
Water content \ during placing (%)	25-60	25-50	25-45
Dry density ($\frac{Mg}{m^3}$)	1.1-1.45	1.15-1.50	1.25-1.55
Undrained shear strength c_u (kPa)	>25	>30	>40
Weight loss (%)	<10	<10	<5

Table 2.5: German erosion guidelines

When these standards are compared it is clear that the guidelines thoroughly disagree when graphically represented as is done in figure 2.20.

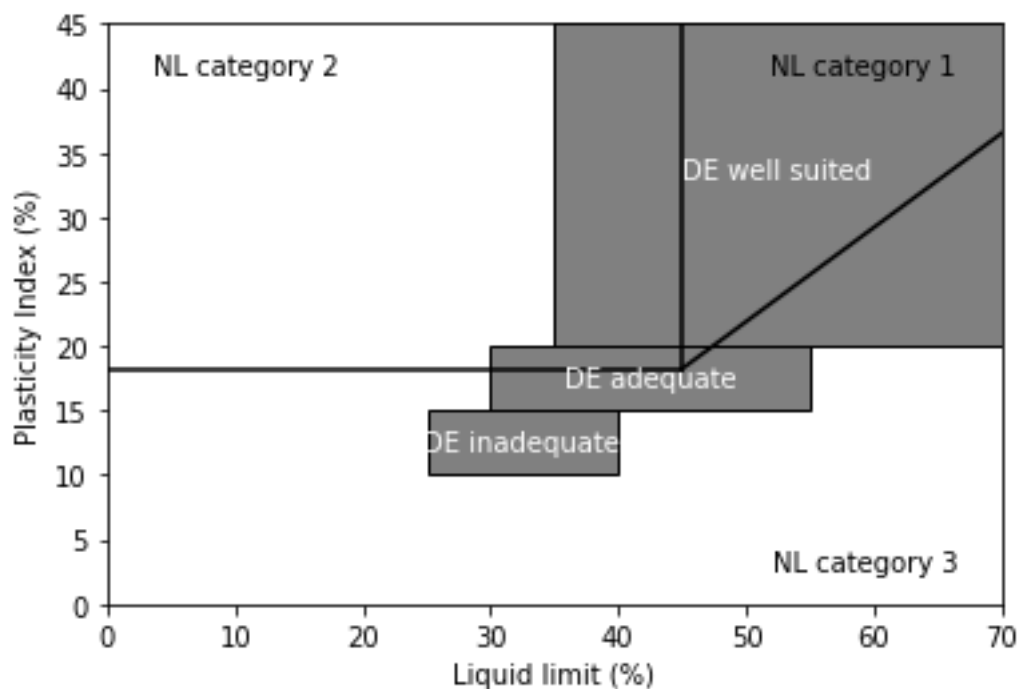


Figure 2.20: Difference German/Dutch guidelines

Now that these norms are known, we can keep these in mind while looking at the other available literature.

Conclusion

The set-up of the German erosion guidelines is very similar to those in The Netherlands, albeit with slight distinctions in classes in comparison to The Netherlands. This is an extra confirmation that the use of soil parameters to classify clay is only an approximation of the erosion resistance. Therefore more research is needed.

2.6.3. Proposed Practice in California, US

In California a different approach is proposed, which is mostly based on testing the erodibility directly in the laboratory. Here a certain load is applied to the clay and then the shear stress and rate of erosion is measured. From this a classification is made if a soil is erosion resistant, this is largely based on the research performed by Briaud in (Briaud (2001))(J.L. Briaud (2005))(J.L Briaud and Shaffi (2017))(Briaud (2008)). This is in contrast to the Dutch and German guidelines, which correlate its liquid and plastic limits to its erodibility. This practice is proposed in (S. Shewbridge (2010a)) & (S. Shewbridge (2010b)) by the Californian department of Water Resources when assessing levees.

It states that erosion can be defined by an erosion function, defined as follows:

$$\epsilon = s * (\tau - \tau_c)$$

In the equation the symbols represent:

ϵ = rate of erosion ($\frac{mm}{hr}$)

s = detachment coefficient ($\frac{m^3}{Nh}$)

τ = shear stress ($\frac{N}{m^2}$)

τ_c = critical shear stress when erosion starts ($\frac{N}{m^2}$)

Correlating the erosion rate to shear stress is also more accurate than correlating it to several soil parameters according to (Arulanandan and Perry (1983)). However, it is of course much more economical to make a pre-selection by saying that a clay is more or less erosion prone based on some soil parameters.

Because shearing is the driving force behind erosion, this then can be represented in an erosion curve as given in figure 2.21 .

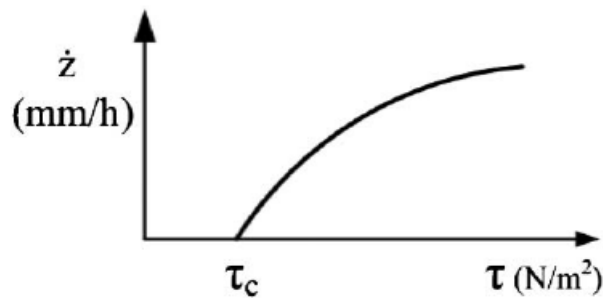


Figure 2.21: Proposed erosion function (Briaud (2001))

Because an erosion curve can be drawn a prescriptive erosion diagram has been drawn by the authorities in California. This diagram is given in figure 2.22.

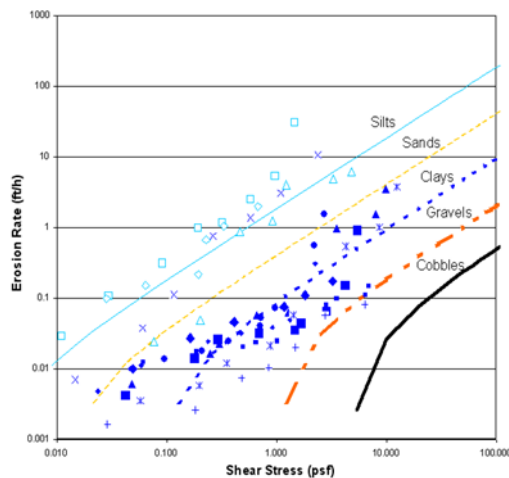


Figure 2.22: Possible erosion curves US guidelines (S. Shewbridge (2010a))

This then finally leads to a categorization of 6 classes for all soils. This can be seen in 2.23.

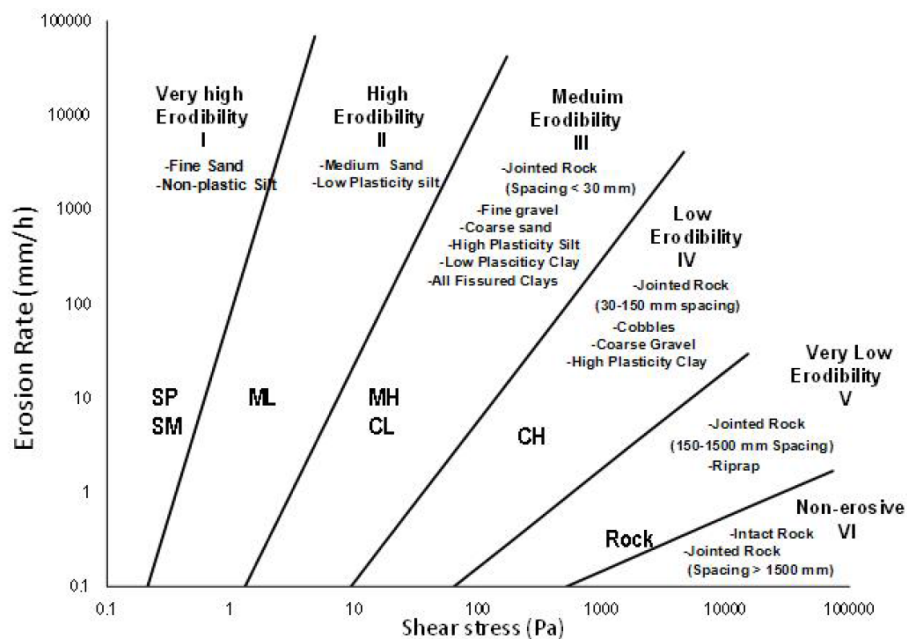


Figure 2.23: erosion class division (J.L. Briaud and Shaffi (2017))

According to (Federal Highway Administration (May 2015)) most clay's will fall in class 3 and thus it will be interesting to look into the class changes. (J.L. Briaud and Shaffi (2018b)) (J.L. Briaud and Shaffi (2018a)).

Now it is useful to look into the different types of devices that are available to conduct erosion tests which is done in the next section.

Conclusion

The approach to divide the soil in erosion classes is largely based on experimental testing. To classify a soil lots of tests are needed, which means that the shear stress at which a soil starts eroding is known as well as its erosion rate. However, this is obviously a very costly approach. On the other side the Dutch approach makes it very simple to classify a soil, but the true erosion rate etc. are not known.

It is therefore a good idea to bundle the knowledge of the Dutch/German guidelines and this guideline. The Dutch/German guidelines could make a pre-selection of the more or less suitable soils and the Californian approach could create more insight between the differences of suitable soils. Then based on the testing results a comparison could be made between guidelines where there are similarities and where there are differences and try to relate them. It is also possible to make a comparison based on the testing results from the work of Briaud which is given in (J.L. Briaud and Shaffi (2017)), (J.L. Briaud and Shaffi (2018b)) and J.L. Briaud and Shaffi (2018a).

2.7. Types of Erosion devices

To perform testing on the erosion resistance of clay a device must be built. Therefore, there will be looked into the different types of devices that are used to determine erosion resistance. Many types are erosion devices are available, however when regarding erosion concerned with wave overtopping of dikes, in general it can be stated that there are 2 machines most customary (R. Crowley and Robeck (2012)). These are the following:

- Erosion Centrifuge
- Erosion Function Apparatus

These devices will be discussed after which a decision will be made on which one to use. The other types of machines will be touched upon in section D.5.

2.7.1. Erosion Centrifuge

The erosion centrifuge (or also known as Rotational Erosion Testing Apparatus or RETA) is an apparatus in which a cylindrical soil specimen is placed and water is rotated around the sample. By measuring the weight loss of the sample the erosion resistance can be measured. This apparatus has been widely used worldwide and this apparatus is available at Deltares.

A figure of the Erosion Centrifuge is given in figure 2.24



Figure 2.24: Photo of Erosion centrifuge at Deltares (Alkemade and Kruk (2018))

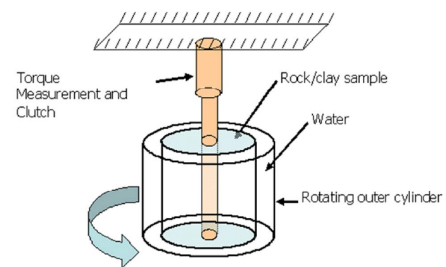


Figure 2.25: Schematic figure of erosion centrifuge (R. Crowley and Robeck (2012))

The use of this machine obviously comes with its own advantages and disadvantages. A large benefit of this machine is that higher speeds can definitely be reached. Also a continuous measurement of the mass loss is possible, this in comparison to the erosion function apparatus which is general a discrete measurement. This is definitely a benefit when there is a sudden mass/volume loss. A large disadvantage is however that no direct measurement of the shear stress can be performed, only a measurement of speed in the centrifuge through which an indirect calculation of shear stress can be performed. This is obviously a drawback.

Something else that has to be taken into account is that when a clay is compacted, it tends to orient itself in the horizontal plane, which is also the direction of the applied shear stress during overtopping. However, during testing the flow is around the circumference of the sample, leading to a wrong erosion pattern than would occur outside in the field. It can also be argued that soil tested in the erosion centrifuge will show a weaker response compared to a sample with flow over the top due to the orientation of the soil structure.

Finally there are boundary effects at the top and bottom of the sample leading eventually to an hourglass shape of the sample at the end of the test.

The final decision on which apparatus to use is done in section 2.7.3 after having discussed the benefits and drawbacks of the Erosion Function Apparatus.

Overview of main advantages and disadvantages

- | | |
|--|---|
| +Higher speeds are possible | -Not very accurate flow direction |
| +Mass loss can be measured more easily | -Difficult to measure shear stress |
| +No problems when chunks fail | -Difficult to get continuous flow over height of sample |

2.7.2. Erosion Function Apparatus

The Erosion Function Apparatus is proposed by (J.L. Briaud (2005)) and is in essence a flume from which below clay is fed and then eroded away. A schematic overview is found in the figure below.

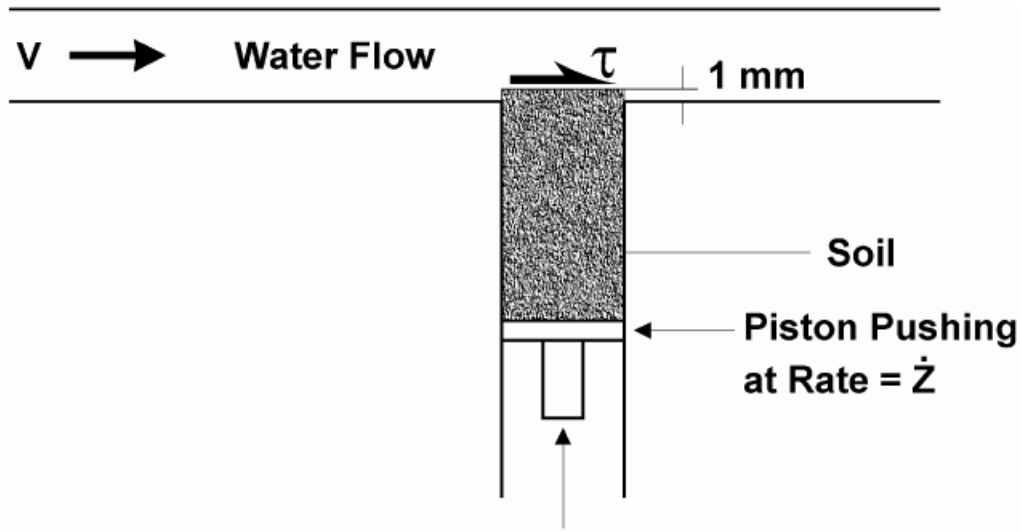


Figure 2.26: Basic functioning of Erosion Function Apparatus

A photo of erosion function apparatus is given in figure 2.27:



Figure 2.27: photo of Erosion function apparatus (M.E. Walker III (2013))

However, this machine also has its (dis)advantages which will be discussed below. This set-up is a better representation of wave overtopping in comparison to the erosion centrifuge, however it is not at present available in The Netherlands. It is also positive that shear stress can be measured more easily. This can be done by measuring the head in front and behind of the sample. From this difference the shear stress the sample encounters can be measured. What is however different from the erosion centrifuge is that a volume loss is measured, instead of a mass loss. This is not necessarily a problem, but it requires an equal distribution of mass through the sample, which does automatically happen during compaction with a proctor

mold. This will be discussed in detail during the proctor compaction section. Further there is more data available internationally about the use of the Erosion Function Apparatus.

The erosion function apparatus then has the following pro's and con's:

- | | |
|--|---|
| +More accurate representation of wave over-topping of a dike | -Heterogeneous failure can prove troublesome |
| +Measurement of shear stress is possible | -Has to be built from scratch |
| +Design is fairly straightforward | -Mass loss can not be measured, only volume loss. |

2.7.3. Decision between erosion centrifuge and erosion function apparatus

After taking into account the benefits and drawbacks of both machines the Erosion Function Apparatus has been chosen as the machine to go forward. This is mainly because of the following items:

- More accurate representation of outdoor situation
- Possibility of measuring shear stress of soil sample
- More international literature available

Obviously the Erosion Function apparatus has its disadvantages such as that it has to be built from scratch. However, because Boskalis wants an erosion set-up in their laboratory this argument would also apply to building an erosion centrifuge.

Further matters concerning the design of the Erosion Function apparatus is done in chapter A.

3

Erosion Function Apparatus overview

The aim of this chapter is to give a general overview of the design of the Erosion Function Apparatus as well as the capabilities. For a detailed description of how the device was designed and built reference is made to Appendix A. Regarding the proof of concept testing reference is made to Appendix C.

The goal of designing this EFA is to be able to measure the erosion rate while relating this to a quantity which can reflect the driving force of the erosion. This means that by designing the set-up several parameters have to be controlled, and several parameters are subsequently measured/derived. These are listed below in table 3.1

Controlled parameter	Measured parameters
Flow rate	Velocity
Initial protrusion	Pressure drop sample
Compaction condition sample	Absolute pressure

Table 3.1: Controlled and measured parameters Erosion Function Apparatus

Using the controlled and measured parameters an average erosion rate is estimated by using the initial protrusion and the time necessary to erode the soil away at a given flow rate.

The flow rate is controlled by controlling the operating frequency of the pump and the velocity is then measured by means of a pitot tube. Further the initial protrusion is controlled to be as close to 1 millimeter as possible. Finally the compaction conditions of the sample are controlled. From these tests then the pressure drop over the clay sample is measured in order to back-calculate a shear stress and the absolute pressure is measured in order to compare the testing results to those of the Computational Fluid dynamics model that was made in order to design the EFA. Finally the (average) erosion rate is measured by precisely determining the initial protrusion and the time that it has taken to erode away the protrusion (or stop the test if it takes longer than 1 hour). The shear stress that is associated with this average erosion rate is the average shear stress that occurred during the interval in which erosion took place.

The final result of the erosion function apparatus is given below in figure 3.1 with letters to explain what each specific part does. In figure 3.1 the following elements can be recognized:

- | | |
|---------------------------------|---|
| A: Pump | F: pitot tube |
| B: Main flow tube | G: Differential pressuremeter (Rosemount) |
| C: Filling cap | H: Absolute pressuremeter (Rosemount) |
| D: Transition round/rectangular | I: Soil feeding mechanism |
| E: Valves and hoses | J: Polyflow connections |

Finally it is also useful to note the capabilities and accuracy of the set-up as it currently stands, which is presented in table 3.2.

Further the erosion rate can be measured between 0 and approximately 300 mm/hr, but as this is not truly a capability of the EFA it is not listed in the table above. The accuracy of this erosion rate is then +/-2% for the more erosion resistant clays and +/-10% for the least erosion resistant clays.

Parameter	Measurable range	Accuracy
Operating velocity	2-4.5 m/s	+/- 1.5% deviation
Pressure drop (resulting in shear stress)	0-0.1 bar (from 9 Pa and up)	+/- 7% deviation
Absolute Pressure	0 bar to 4 bar	+/- 0.1% deviation

Table 3.2: Capabilities and accuracy EFA

The operating velocity is between approximately 2 m/s and 4.5 m/s due to the instability of flow below this 2 m/s limit and the maximum capacity of the pump is reached at 4.5 m/s. It is perceived to have an accuracy of +/- 1.5 % of the mean measured value. Explanations how this and other values are obtained is given in the Appendix. Further the range of shear stresses that can be measured is very large, due to the very accurate and very large range the differential pressure sensor can operate in. It can only not measure shear stresses below an approximate 9 Pa, because the pump can not go to such low velocities to get a shear stress below this 9 Pa. The upper bound of the shear stresses is not mentioned because it far exceeds the shear stresses associated with flow rates of 4.5 m/s. It has a +/- 7% deviation of the mean, which is so large due to the very small pressure drops that are measured. The absolute pressure can be measured from 0 bar up to 4 bar, which is a value that very much exceeds the pressures that may be expected, and measures it very accurately.

Finally, the erosion rates that reasonably can be measured are from 0 up to approximately 300 mm/hr. This upper limit is due to the length that a test takes. If the erosion rate is upwards of 300 mm/hr the length of a test drops below 12 seconds, which is too little to have a fair test reading. It is expected to have an accuracy of +/- 10%, however a lot depends on the clay tested. As can be seen in the Appendix, repeatability tests have been run on the Boom clay (the erosion resistant clay) and the Kampen III clay (the very erodible clay) a test becomes less repeatable if a soil becomes more erodible (+/- 2% deviation for the Boom clay and +/- 10% for the Kampen III clay). It is thought that this is due to the differences in structure and the increased sand content leading to the development of preferential erosion planes.

For further explanations how the EFA was designed reference is made to Appendix A, for reference to the full-page design drawings reference is made to appendix E, for the result pictures of the EFA reference is made to appendix H and for the proof of concept testing reference is made to appendix C.



Figure 3.1: End result Erosion Function Apparatus

4

Soil characterization, clay compaction and erosion testing method

This chapter will focus on the following topics:

- The soil types that have been investigated
- The index tests that have been conducted and their results
- Discussion on the index testing results
- The compaction curves of the clays
- Discussion on the compaction curves
- Erosion testing method

4.1. Soil types tested

3 different soil types have been tested during this study, being Boom clay, Kampen II clay and Kampen III clay.

The Boom clay used in this study originates from Schelle, Belgium (15 km south of Antwerp) and has been under consideration for use by Boskalis. It has been dug up 25 meters below surface level and is a high plasticity clay with a low sand content and has low amounts of calcite and organic matter and looks visually homogeneous. It will therefore be a class I erosion clay according to the Dutch guidelines. In the Unified Soil Classification system it is designated as a high plasticity clay.

The Kampen II clay used in this study originates from "het Reeve" several kilometers south of Kampen. The Reeve is a side channel of the IJssel that flows to the IJsselmeer. The Kampen II clay is won at the beginning of this branch of the IJssel and is a clay with a moderate plasticity, some sand in it and classifies as a class II erosion clay and some heterogeneity. In the Unified Soil Classification system it is designated to be a low plasticity clay.

The Kampen III clay of this study also originates from "het Reeve", but is found near the estuary where it flows into the IJsselmeer. This clay also has a moderate plasticity, but a noticeably higher sand content (it falls apart fairly quickly) and is fairly heterogeneous. It is therefore classified to be a class III erosion clay. It is also designated to be a low plasticity clay in the USCS system.

4.2. Index testing

For each type of clay the following soil parameters have been chosen to test for:

Plastic Limit	Percentage of particles $< 2\mu m$
Liquid Limit	Organic content
Bulk Density	Undrained shear strength
Grain density	Salt concentration
Sand content	Lime content
Percentage of particles $< 63\mu m$	

However, many of these parameters have already been tested for the Kampen II and Kampen III clay during the research of (Alkemada and Kruk (2018)) and will be used.

The reason to perform most tests are based on the guidelines as set out for instance in CROW (2010). This guideline prescribes that the Bulk density, Plastic limit, Liquid limit, Sand content, Organic content, Lime content and Salt content must be determined. That these parameters have to be determined is mostly in line with the findings of the literature study.

Further the choice has been made to also determine the grain density, clay content and undrained shear strength. The grain density has been determined in order to say something about the degree of saturation the clay is at. Further the undrained shear strength has been determined in order to see how it correlates with the findings correlating the undrained shear strength to the erosion resistance. Finally also the entire sieve curve is determined to properly know how the soil is built up.

The results of these index tests are then presented in table 4.1.

	Boom Clay	Kampen clay II	Kampen clay III
Plastic limit (%)	28	19	11
Liquid limit (%)	80	38	31
Plasticity index (%)	52	19	17
Grain density (kg/m ³)	2652	2689	2676
Salt concentration (g/L pore fluid)	0.13	0.10	0.10
Lime content (%)	7.2	11.0	11.2
Organic content (%)	0.9	0.3	0.6
Sand content (%)	0.4	14.0	49.0
Silt content (%)	26.3	66.7	39.7
Clay content (%)	73.3	19.7	11.3
Undrained shear strength (kPa)	15	10	8

Table 4.1: Index testing results tested clays

The implications of these results are then discussed below and correlated to the literature of the previous chapter.

4.3. Discussion on Index Testing tests

According to the Dutch design codes it appears that the Boom clay is a class I clay, Kampen clay II is a class 2 clay and Kampen clay III is a class III clay as can be seen in figure 4.1.

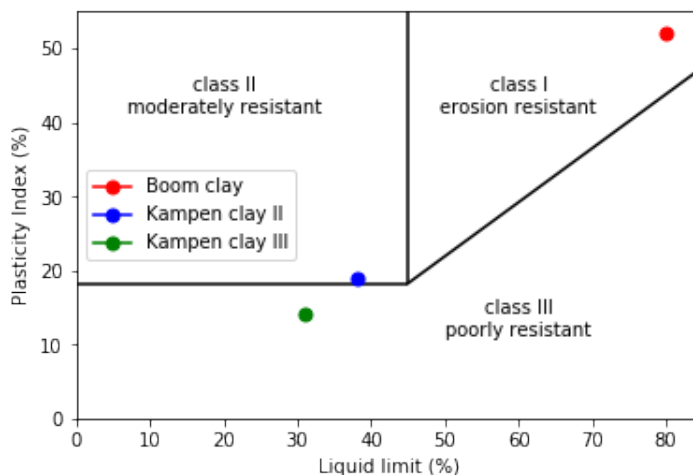


Figure 4.1: Erosion class designation tested clays

Further all clay's comply with the additional demands that are set by the CROW (2010), which also have been discussed in 2. Something that stands out quite clearly is the huge amount of particles under $2 \mu\text{m}$ and $63 \mu\text{m}$ in the Boom clay is very large, when comparing this to the Kampen clay's, Further, the limited amount salt and lime is something to note.

It is also good to compare how these index testing results compare to the findings correlating the different soil parameters to the erosion resistance. As a reminder, this means that the following soil parameters will be discussed:

- Clay content
- bulk density
- D_{50}
- c_u

The effect of the consistency and liquidity index are not discussed in this chapter because it is dependant on the water content of the soil. This means that each sample has a different liquidity index and each soil has a wide range of liquidity indices. The effect of the liquidity index will be discussed in the erosion testing results chapter.

The clay content of the Boom clay is highest, followed by the Kampen II clay and lastly by the Kampen III clay. This is thus in accordance with what may be expected. Concerning the D_{50} , the Boom clay has the lowest D_{50} , then the Kampen II clay and the Kampen III clay. According to literature, for clays, there is an inverse relationship between the D_{50} and the erodibility and thus it suggests that the Boom clay must be least erodible, then the Kampen II clay and then the Kampen III clay. This thus is as expected. What concerning the bulk density, literature suggests that a higher bulk density results in a higher resistance to erosion. Also, this is somewhat incorporated in the current guidelines by placing a density requirement on the clay. However, something odd happens here, what is displayed clearly in table 4.2.

Clay	$\gamma_{proc,max}(Mg/m^3)$	$w_{opt,proc}(\%)$	Erosion class
Boom clay	1.46	0.30	I
Kampen II	1.72	0.185	II
Kampen III	1.87	0.145	III

Table 4.2: Clay dry densities, optimum water contents and erosion classes

Here it can be seen that what is perceived as the most erosion resistant clay actually has the lowest dry density. However, it will appear in the next chapters after erosion testing has occurred that an increase of the dry density within one clay type will generally result in a lower erodibility. It is unwise however to purely focus on the dry density alone, because as can be seen here, the dry density of more erodible clays is generally higher, it can only be adequately compared to for instance the proctor density of that specific clay when analyzing the erodibility.

Finally also the undrained shear strengths of the different clays are compared. Literature suggests that a decrease of the undrained shear strength would result in a lower erodibility. However, as seen with the index tests above the Boom clay has the highest undrained shear strength whilst in definitely is the most erosion resistant (i.e. the opposite of what may be expected by literature). It is thought that this is because the literature does not take into account that the Boom clay is heavily over-consolidated and therefore has a higher undrained shear strength. It is therefore advised not to use this correlation.

Concluding the comparison between the index testing data en the comparison what may be expected by literature the results of the clay content D_{50} are in accordance whilst the comparison between bulk density and the undrained shear strength was off. This once again proves that these correlations must be used with caution.

4.4. Proctor curves

All clays have been compacted at at least 2 different energy levels and at each energy level there has been at least 3 water contents that have been compacted at. This led to the following initial compaction curve plan:

Boom Clay					
Energylevel	Far drier than opt.	Drier than opt.	Optimum	Wetter than opt.	Far wetter than opt.
0.3 MJ/m ³	✗	✓	✓	✓	✗
0.6 MJ/m ³	✓	✓	✓	✓	✓
2.7 MJ/m ³	✗	✓	✓	✓	✗

Table 4.3: Testing Programme Boom clay

Kampen II clay					
Energylevel	Far drier than opt.	Drier than opt.	Optimum	Wetter than opt.	Far wetter than opt.
0.3 MJ/m ³	✗	✓	✓	✓	✗
0.6 MJ/m ³	✓	✓	✓	✓	✓
2.7 MJ/m ³	✗	✓	✓	✓	✗

Table 4.4: Testing programme Kampen II clay

Kampen clay III					
Energylevel	Far drier than opt.	Drier than opt.	Optimum	Wetter than opt.	Far wetter than opt.
0.3 MJ/m ³	✗	✗	✗	✗	✗
0.6 MJ/m ³	✓	✓	✓	✓	✓
2.7 MJ/m ³	✗	✓	✓	✓	✗

Table 4.5: Testing programme Kampen III clay

There has been chosen to do a 5 point test at the proctor energy level (for each soil), as to get a good shape of how the proctor curve looks, but there has been chosen not to do this for each level as to limit the work (in that case a 3 point proctor curve has been produced).

There has been chosen to perform the tests for the Kampen II and Boom clay at 3 different energy levels in order to properly see how erosion resistance will also vary with differing energy levels. This was not possible for Kampen III clay, because it would fail at the very lowest energy level just standing on the table.

However, due to arbitrary quirks when performing these compaction tests, this resulted in several more samples which eventually yielded the compaction curves as as presented in figures 4.2, 4.3 and 4.4.

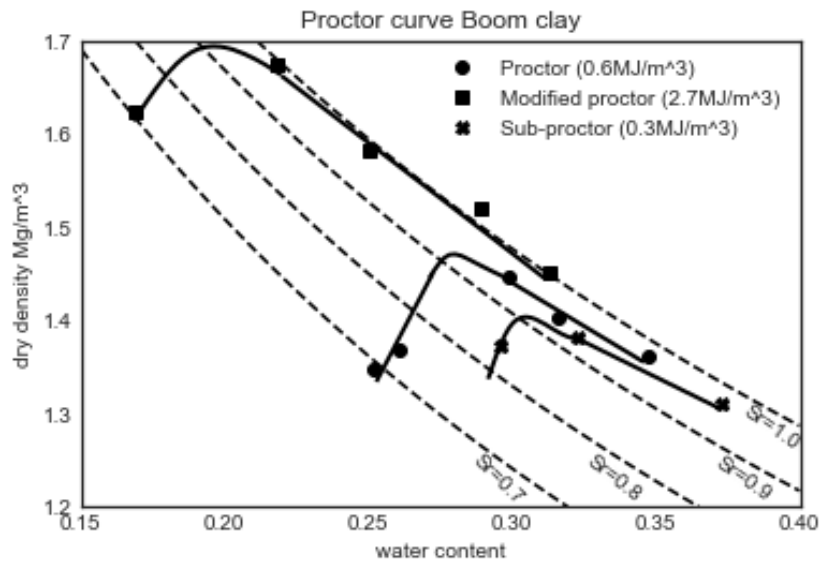


Figure 4.2: Proctor curve Boom clay

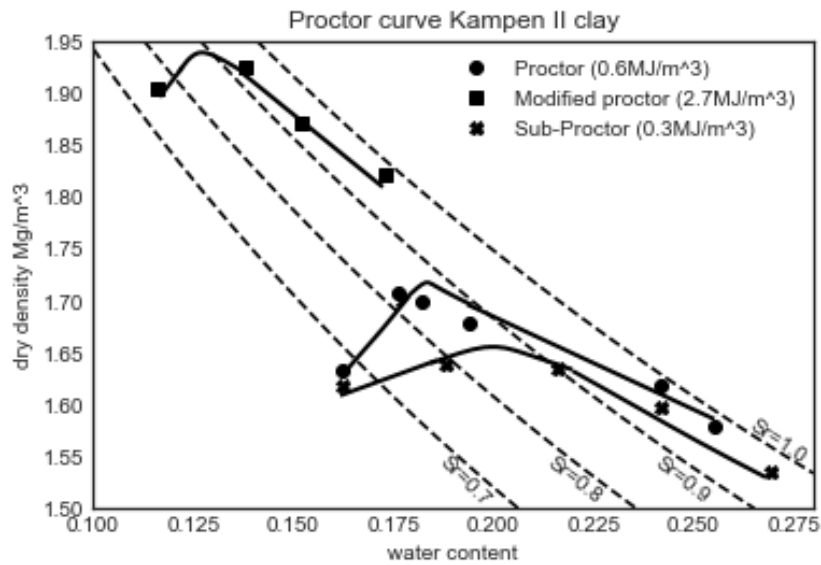


Figure 4.3: Proctor curve Kampen II clay

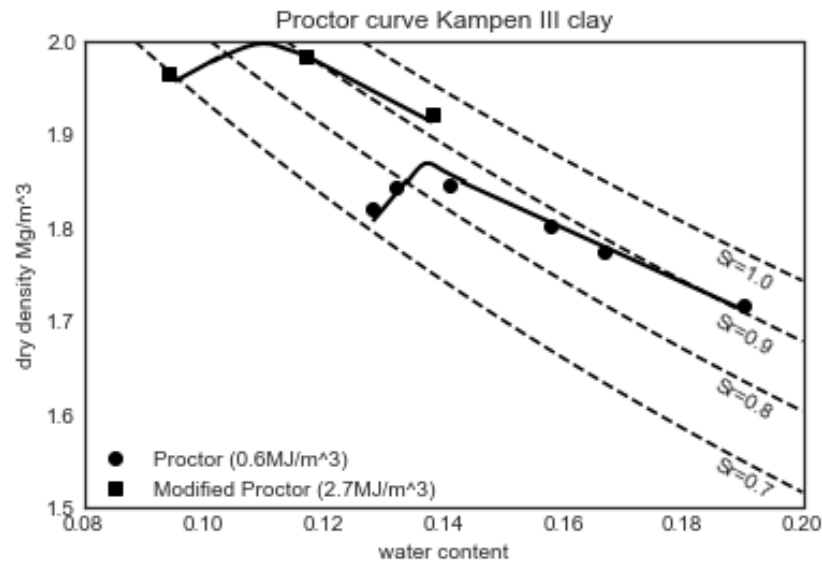


Figure 4.4: Proctor curve Kampen III clay

This part discusses several observations that were made while assessing the proctor curves.

The first observation is that there is a relatively good fit of the proctor data and that 2 of the proctor planes (the Boom clay and the Kampen III clay) have a significant asymptotic behavior towards a level of saturation (the Boom clay being 100 % saturation, the Kampen III clay being 90 % saturation). Secondly it can also be seen that the maximum density of all clays corresponds towards being approximately 85 to 95 % saturated, which seems to be something that is material specific. These numbers will be kept in mind while assessing the something that is also obvious is that the modified proctor curve of the Boom clay goes slightly over the 100 % saturation line which should definitely not be the case. This implies that there is either a slight deviation in the grain density, which is more than likely, or the measured density is slightly higher than it should be. This means that in this case the saturation lines must be considered as roughly. The results from these proctor curves will be used in the discussion when considering the results from the EFA testing and thus this part is now concluded.

4.5. Erosion testing method & Interpretation

4.5.1. Erosion testing method

All samples will be tested at several velocities, the amount is dependant on the size of the sample, the amount of erosion tests with zero erosion and the velocity limit. The aim is to get 3 points for each clay sample and determine an erosion curve from these points. Albeit there is a Working Protocol in place, as described in Appendix J it is good to go over the results of how a test is executed and the erosion parameters determined.

As an example sample γ is taken, which is a Kampen II, sub-Proctor, just below optimum water content sample. It has the following water content, dry density characteristics: $(w, \rho_d) = (0.188, 1.640)$. The sample is then undergoes several erosion tests, each described below.

First Run

The sample is cut to fit in the sample container, and after having measured the protrusion at 6 different points with a precision caliper (0.01mm precision) it protrudes 1.31 millimeter into the erosion flume. The pump has been set at 25 Hz (+/-3.2 m/s) and the erosion flume filled. The pump was started and the waiting began. However, unfortunately after 1 hour no measurable erosion had occurred which meant that the test was discontinued. During this 1 hour, an average pressuredrop-output of 4.1469 mA was measured, an average absolute pressure output was measured of 8.2581 mA and a velocity-output of 4.872mA.

These outputs are then converted into an (average) shear stress measured in Pa, an average absolute pressure in bar and a velocity in meter per second. This can be done by knowing that the rosemounts always operate (linearly) between 4 and 20 mA, and that 4 mA corresponds to the lower bound the rosemount is set at (0 bar for all sensors) and 20 mA to the upper bound the rosemounts are set at (1 bar for the pressure drop sensor and pitot tube, 4 bar for the absolute pressure sensor).

Taking into account that the erosion flume is 5 centimeters high, 6 centimeters wide and 15 centimeters between the points where the pressure drop is measured between, this means that this pressure drop can be translated to a an average shear stress with the following method:

$$P_{pressuredrop} = (4.1469 - 4) / 16 * 1 = 0.0092bar \quad (4.1)$$

$$\tau_{avg} = 0.0092bar * (0.05m * 0.06m) / (2 * 0.05m * 0.15m + 2 * 0.06m * 0.15m) = 10.23Pa$$

The absolute pressure output can be translated to a pressure as follows:

$$P_{abs} = (8.251 - 4) / 16 * 4 = 1.06bar \quad (4.2)$$

And the velocity can be determined because the pressure difference between the static pressure and dynamic pressure is determined with the Rosemount/pitot tube combination. This means that the velocity can be calculated as follows:

$$h = (4.872 - 4) / 16 * 10 = 0.545m(\text{head difference}) \quad (4.3)$$

$$u = \sqrt{0.545 * 2 * 9.81} = 3.27m/s$$

This then concludes the first run. This means that the first point on the erosion curve has been found. The next run is now explained.

Second run

The pump frequency is now raised to 30 Hz and a part of the sample is now prepared and placed in the soil container. The soil protrudes 1.21 mm this time. The pump is started and it takes 654 seconds to erode this sample. This means that there is an average erosion rate during this time frame of 6.66 mm/hour, with the erosion rate being slightly higher in the begin of this time frame than towards the end (the shear stress as well). Given the method as prescribed before the shear stress is determined to be 26.45 Pa, the velocity is 4.43 m/s and the absolute pressure is 1.08 bar.

Third run

The pump frequency is now raised to 40 Hz, and the sample protrudes 1.07 mm and it takes 175 seconds to erode, resulting in an erosion rate of 22.05 mm/hr. The velocity at which this took place is 4.14 m/s, the shear stress is 50.78 Pa and absolute pressure of 1.13 bar.

Fourth and final run

The pump frequency is raised to 50 Hz (full speed), the sample protrudes 0.95 mm and erosion takes 128 seconds, resulting in an erosion rate of 26.7 mm/hour at a velocity of 4.47 m/s, shear stress of 62.70 Pa and an absolute pressure of 1.18 bar. These four points are then the points to be used in the interpretation.

4.5.2. Interpretation of erosion characteristics sample

As a recap, during this test the following points were obtained:

Velocity (m/s)	Shear stress (Pa)	Erosion rate (mm/hr)
3.27	10.2	0
3.61	26.5	6.66
4.14	50.8	22.05
4.47	62.7	26.70

To interpret these results 2 methods are available: the SRICOS model as proposed in (J.L. Briaud et al. (1999)), or the methodology as proposed in the NCHRP report (Briaud et al. (2019)). Both models are discussed and worked out using the results from test sample γ as example. Finally a decision is drawn which of the models is used and how these results are bounded.

SRICOS model

The SRICOS (Scour Rate in Cohesive soils) model is actually more a methodology and proposes to tests soils in the EFA (exactly as done in this study) and plot the shear stress on the x-axis and the erosion rate on the y-axis in an arithmetic space, interpolate with a best fit (log-)function and then determine the following properties:

- A critical shear stress $\tau_c(Pa)$
- A (shear stress driven) detachment coefficient $S_i(mm/hr/Pa)$

The erosion curve of sample γ as described above is plotted according to the SRICOS model in figure 4.5.

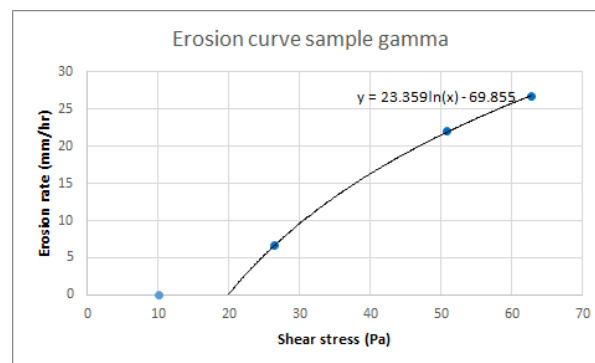


Figure 4.5: Erosion curve sample γ SRICOS model

With the best-fit function being determined to be $\epsilon = 23.359 * LN(\tau) - 69.855$ the critical shear stress is determined to be 19.9 Pa, because the erosion is just 0 at that shear stress. The detachment coefficient by definition the slope of the erosion function at the critical shear stress. Therefore first the derivative of the erosion function is determined after which the detachment coefficient is determined by filling in the derivative at the critical shear stress, as is done below:

$$\epsilon' = \frac{23.359}{\tau}$$

$$S_i = \frac{23.359}{19.9} = 1.17 mm/hr/Pa \quad (4.4)$$

Further, the author also chose to determine **back-calculated** erosion rates at the benchmark shear stresses of 3.2, 7.0, 15.0 and 32.4 Pa. This was no part of the scheme in (J.L. Briaud et al. (1999)). These shear stresses have been chosen because they reflect overflow rates of 0.1, 1, 10 and 100 l/s per meter dike of overflow and

they correspond to insignificant, limited, severe and catastrophic dike overflow rates. This way a good quantitative comparison can be struck between samples.

This thus yields the following erosion rates:

$$\begin{aligned}
 \epsilon_{3.2Pa} &= 0 \text{ (under critical shear stress)} \\
 \epsilon_{7.0Pa} &= 0 \text{ (under critical shear stress)} \\
 \epsilon_{15.0Pa} &= 0 \text{ (under critical shear stress)} \\
 \epsilon_{32.4Pa} &= 23.359 * LN(32.4) - 69.855 = 11.4 \text{ mm/hr}
 \end{aligned}
 \tag{4.5}$$

The benefit of using the SRICOS model is that it always will yield a result a critical shear stress and a detachment coefficient. Further, it is a relatively easy model to understand and looking at the points in arithmetic space it (intuitively) makes sense to use a log-function. However, because it is always possible to get a (fairly good) fit with this model, it can sometimes yield fairly arbitrary results, which is also observed in the testing results. The quality of the fit therefore depends a lot on the amount and quality of the data points which is fairly limited in this study. Also, this model does not take velocity into account at all, although this is a much more clear parameter to measure than the shear stress of the sample. In general this model has yielded higher critical shear stresses and higher detachment coefficients than the methodology as proposed in the NCHRP report.

NCHRP report model

In the NCHRP report (Briaud et al. (2019)) a large range of tests are combined, not only EFA testing, but also Jet erosion tests and several other tests as well. This report proposes to plot the points on the erosion curve in 2 log-log space graphs in which the Briaud erosion categories are drawn. 1 graph is a plot of the velocity on the x-axis and the erosion rate on the y-axis, as presented in figure 4.6 and the other graph has the shear stress on the x-axis and the erosion rate on the y-axis as seen in figure 4.7. From these graphs the following erosion parameters are determined:

- A critical shear stress $\tau_c(Pa)$
- A critical erosion velocity $v_c(m/s)$
- A (shear stress driven) detachment coefficient $S_i(mm/hr/Pa)$
- A (velocity driven) detachment coefficient $S_{iv}(mm/hr/m/s)$

These parameters have been determined by drawing a linear line through the data points obtained during testing in this log-log space. The point where this line intersects the 0.1mm/hr limit is considered the critical shear stress or critical erosion velocity respectively. Then the slope of both lines are calculated to determine the (shear stress) detachment coefficient and velocity detachment coefficient. This approach is in completely identical to the approach as proposed in Briaud et al. (2019). How this methodology works is illustrated in figures 4.6 and 4.7.

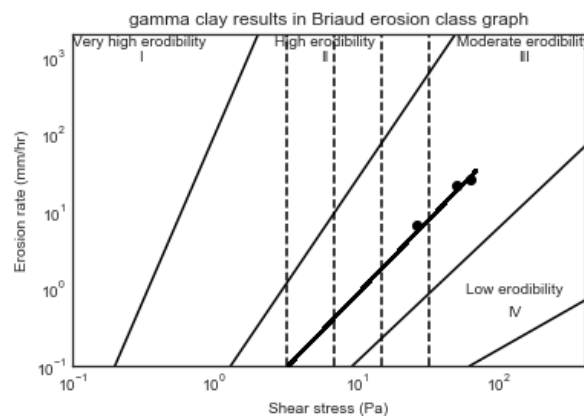


Figure 4.6: Shear stress/erosion rate plot in log/log space

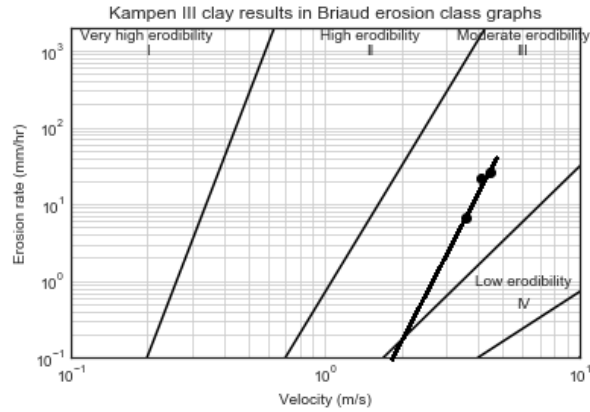


Figure 4.7: Shear stress/erosion rate plot in log/log space

From the above graphs it can be concluded that the critical shear stress is around 3.2 Pa and the critical erosion velocity is 1.8m/s. The detachment coefficients are then calculated as follows:

$$S_i = \frac{\Delta \epsilon}{\Delta \tau} = \frac{22.05 - 6.66}{50.8 - 26.5} = 0.63 \text{ mm/hr/Pa}$$

$$S_{iv} = \frac{\Delta \epsilon}{\Delta \tau} = \frac{22.05 - 6.66}{4.14 - 3.61} = 17.69 \text{ mm/hr/m/s}$$
(4.6)

Finally, also here the (predicted) erosion rates at 3.2, 7.0 , 15.0 and 32.4 Pa are back-calculated in order to be able compare the erosion rates of the samples with each other . This sample is expected to have the following erosion rates at these benchmark shear stresses:

Benchmark shear stress (Pa)	Back-calculated erosion rate (mm/hr)
3.2	0
7.0	0.5
15.0	2
32.4	8.5

Further of every sample the number of non-zero erosion rates will be noted in order to distinguish between samples of which the erosion curve is better known and samples of which the erosion curve is less well known.

The benefit of using this model is that it removes the possibility of a rather arbitrary, however it has downside that it will not always yield a critical shear stress and thus yields the test worthless. This also has an upside because the tests that have the "arbitrary results" of the SRICOS model are mostly the one's where there is no critical shear stress in this model. Thus it is a good method of filtering out the tests with outlying results. Further, the NCHRP model incorporates the velocity into the analysis of erosion. This is a benefit, because velocity is a much easier to measure quantity, and shear stress can only be back-calculated or estimated. This method also produces in general lower critical shear stresses and a lower detachment coefficient than the SRICOS model, and thus is generally a more conservative model. This can especially be seen when looking at the back-calculated erosion rates at the benchmark stresses, the erosion rates calculated by the SRICOS model are lower than the erosion rates calculated by the NCHRP model. That the NCHRP model is more conservative is rather obvious, because it is a linear model rather than a logarithmic model. This also makes clear why the SRICOS model yields higher critical shear stresses and higher detachment coefficients. This means that in low shear stress ranges the NCHRP model will yield higher erosion rates, and in higher (very unlikely) shear stress ranges the SRICOS model will yield lower erosion rates.

Choice between models

Both models have their benefits and their disadvantages: using the SCIRO model is an easy model, relatively straightforward, produces well-fitting results but has the possibility of producing weird testing results. The method proposed by the NCHRP report is fairly conservative method, has only a limited arbitrary interpretation method and it incorporates velocity in the analysis.

There has been chosen therefore to present the values of both models in order to see how large the possible range is of erosion properties, with the NCHRP model values being leading in analysis. Also, these results are also bounded as much as possible by the testing results as possible.

For the critical shear stress this means the following:

-According to the SRICOS model the critical shear stress is 19.9 Pa, which is the highest estimate, according to the NCHRP model it is 3.2 Pa. However, from the testing data it is seen that there is no erosion at 10.2 Pa. The critical shear stress is therefore considered to be between 10.2 and 19.9 Pa, with 10.2 Pa being the lowest, conservative estimate used in analysis. However, in the table of testing results the range of 10.2-19.9 Pa is given as range of critical shear stress.

For the critical erosion velocity, this means the following:

-The critical erosion velocity is determined to be 1.8 m/s according to the NCHRP model, it is not determined with the SRICOS model. However, taking into account the testing data, there is also no erosion at 3.27 m/s so the critical erosion velocity is set at a minimum of 3.27 m/s and below 3.61 m/s, because at that specific velocity erosion occurs.

For the detachment coefficient, this means the following:

With the SRICOS model a detachment coefficient has been found of 1.17 mm/hr/Pa and with the NCHRP model a detachment coefficient has been found of 0.63 mm/hr/Pa. Here there will be continued with the 0.63mm/hr/Pa, however given the closeness of these 2 values, it is known that a relatively high trust can be placed in the accuracy of the value.

For the velocity detachment coefficient, this means the following:

A value of 17.69 mm/hr/m/s has been found, and this will be continued to be used in analysis.

For the benchmark shear stress of 3.2 Pa this means:

A value of 0 mm/hr was found for both models, and is used in analysis.

For the benchmark shear stress of 7.0 Pa this means:

A value of 0.5 mm/hr was found with the NCHRP model, 0 mm/hr with the SRICOS model. Taking into account that at 10.2 Pa no erosion occurred during a test, 0 mm/hr is used in analysis.

For the benchmark shear stress of 15.0 Pa, this means:

A value of 2 mm/hr erosion was found using the NCHRP model, 0 mm/hr with the SRICOS model. Here as a conservative estimate (and because the NCHRP model is assumed to be leading) the 2 mm/hr is used in analysis.

For the benchmark shear stress of 32.4 Pa, this means:

8.5 mm/hr was found using the NCHRP model, and 11.4 mm/hr was found using the SRICOS model. In analysis this means that 8.5 mm/hr is used in analysis, because the NCHRP model is used as primary model. However, the fact that the 11.4 mm/hr of the SRICOS model is relatively close a relatively high amount of trust in this back-calculated erosion value can be placed.

Overall, this means that in analysis the following parameters are used:

	Range [min-max]	Use in analysis
$\tau_c(Pa)$	[10.2-19.9]	10.2
$v_c(m/s)$	[3.27-3.61]	3.27
$S_i(mm/hr/Pa)$	[0.63-1.17]	0.63
$S_i v(mm/hr/m/s)$	[17.69-17.69]	17.69
$\epsilon_{3.2Pa}(mm/hr)$	[0-0]	0
$\epsilon_{7.0Pa}(mm/hr)$	[0-0.5]	0
$\epsilon_{15.0Pa}(mm/hr)$	[0-2]	2
$\epsilon_{32.4Pa}(mm/hr)$	[8.5-11.4]	8.5

This is then done for all samples tested. This then concludes the erosion testing and interpretation method.

5

Testing Results erosion testing

This chapter will present the results of the erosion testing, the method of interpretation and the analysis. To this end this chapter will cover the following aspects:

- Results erosion testing
- Erosion analysis in the context of the proctor plane
- Erosion in context with other research
- Observations during testing

5.1. Results erosion testing

First of all an overview of all testing results is given below in the table below in table A.1. The testing results are then interpreted in table 5.2.

Using the procedure interpretation procedure this leads to the following interpretation:

Clay	Energy level	w	$\rho_d(Mg/m^3)$	S_r	Test #1			Test #2			Test #3			Test #4			N	N>0
					v (m/s)	$\tau(Pa)$	$\epsilon(mm/hour)$											
Clay	Modified Proctor (2.7MJ/m ³)	0.169	1.624	0.708	4.47	76.26	2.19	4.16	55.27	0.54	n.a.	n.a.	n.a.	n.a.	n.a.	n.a.	2	2
		0.218	1.675	0.991	4.47	91.04	3.24	4.16	67.79	1.52	n.a.	n.a.	n.a.	n.a.	n.a.	n.a.	2	2
		0.25	1.583	0.982	4.47	95.24	0.47	4.16	47.64	0	n.a.	n.a.	n.a.	n.a.	n.a.	n.a.	2	1
		0.289	1.52	1.029	4.47	89.74	1.50	4.15	43.70	0.87	n.a.	n.a.	n.a.	n.a.	n.a.	n.a.	2	2
		0.252	1.347	0.69	3.6	26.44	45.09	4.17	43.7	60	4.47	85.44	62.6	n.a.	n.a.	n.a.	3	3
	0.261	1.369	0.739	3.6	14.42	0	4.14	46.06	16.91	4.47	93.61	43.85	n.a.	n.a.	n.a.	3	2	
	0.299	1.446	0.951	3.7	30.76	0	4.17	62.61	0	4.34	79.19	0	4.47	90.59	7.56	4	1	
	0.316	1.403	0.941	4.17	62.42	0.24	4.47	89.45	0.3125	n.a.	n.a.	n.a.	n.a.	n.a.	n.a.	2	2	
	0.347	1.361	0.97	3.60	28.11	0	4.18	50.19	5.80	4.47	70.55	7.56	n.a.	n.a.	n.a.	3	2	
	0.296	1.374	0.844	3.62	26.11	24.68	4.17	51.55	106.2	5.05	55.65	125.68	n.a.	n.a.	n.a.	3	3	
Boom clay	Sub-Proctor (0.3MJ/m ³)	0.323	1.383	0.934	3.99	27.02	0	4.20	51.55	9.64	4.40	63.95	15.26	n.a.	n.a.	n.a.	3	2
		0.373	1.31	0.966	3.59	21.29	16.87	4.17	62.30	14.86	4.47	110.72	67.32	n.a.	n.a.	n.a.	3	3
		0.116	1.905	0.758	n.a.	14.24	51.25	n.a.	40.23	103.7	n.a.	49.19	118.85	n.a.	n.a.	n.a.	3	3
		0.138	1.924	0.933	3.82	22.48	0	4.16	40.24	1.82	4.47	86.10	6.96	n.a.	n.a.	n.a.	3	2
		0.152	1.871	0.935	3.59	25.87	8.95	4.16	50.25	11.10	4.47	67.24	11.57	n.a.	n.a.	n.a.	3	3
	0.173	1.821	0.976	3.24	15.47	24.18	4.14	47.80	31.10	n.a.	n.a.	n.a.	n.a.	n.a.	n.a.	2	2	
	0.162	1.633	0.674	3.24	4.96	45.68	3.95	36.46	190.42	3.34	60.56	198	n.a.	n.a.	n.a.	3	3	
	0.176	1.708	0.824	3.21	6.72	2.34	3.89	29.88	10.17	4.33	60.95	10.925	n.a.	n.a.	n.a.	3	3	
	0.182	1.7	0.841	3.61	19.32	3.50	4.22	37.64	97.87	n.a.	n.a.	n.a.	n.a.	n.a.	n.a.	2	2	
	0.194	1.678	0.866	n.a.	37.29	58.66	n.a.	57.85	64	n.a.	7067	390.6	n.a.	n.a.	n.a.	3	3	
Kampen II	Proctor (0.6MJ/m ³)	0.242	1.619	0.985	3.26	6.72	0	3.57	16.58	10.84	4.15	60.95	61.66	n.a.	n.a.	n.a.	3	2
		0.255	1.579	0.975	n.a.	11.53	254.7	n.a.	19.76	350.6	n.a.	44.01	444	n.a.	n.a.	n.a.	3	3
		0.162	1.619	0.659	3.23	10.29	5.06	3.95	37.33	94.41	4.31	65.47	112.37	n.a.	n.a.	n.a.	3	3
		0.188	1.64	0.79	3.27	10.23	0	3.61	26.45	6.66	4.14	50.78	22.05	4.47	62.70	26.7	4	3
		0.216	1.636	0.902	3.61	26.27	9.44	4.19	55.44	13.6	4.47	72.57	59.47	n.a.	n.a.	n.a.	3	3
	0.242	1.597	0.952	3.26	19.86	0	3.93	33.75	15.38	4.36	69.20	83.20	n.a.	n.a.	n.a.	3	2	
	0.269	1.536	0.964	3.59	25.87	8.95	4.16	50.25	11.58	4.47	67.24	11.11	n.a.	n.a.	n.a.	3	3	
	0.094	1.966	0.687	3.59	25.63	8.95	4.18	50.33	12.5	4.47	63.54	13.4	n.a.	n.a.	n.a.	3	3	
	0.117	1.984	0.885	3.60	25.87	13.9	4.14	37.79	20.13	4.47	67.24	21.93	n.a.	n.a.	n.a.	3	3	
	0.138	1.921	0.928	3.28	8.09	12.14	3.96	39.15	27.18	4.36	60.01	47.35	n.a.	n.a.	n.a.	3	3	
Kampen III	Modified Proctor (2.7 MJ/m ³)	0.128	1.821	0.722	3.24	5.63	29.75	4.19	41.47	66.47	n.a.	n.a.	n.a.	n.a.	n.a.	2	2	
		0.132	1.843	0.773	3.61	19.32	3.50	4.22	37.64	97.87	n.a.	n.a.	n.a.	n.a.	n.a.	2	2	
		0.141	1.845	0.829	3.24	12.91	12.82	3.90	38.87	18.045	4.47	51.55	75.53	n.a.	n.a.	n.a.	3	3
		0.158	1.802	0.863	3.52	11.62	10.1	4.26	49.32	450	4.56	59.70	516	n.a.	n.a.	n.a.	3	3
		0.167	1.775	0.872	3.24	10.41	9.25	3.89	29.31	275	4.16	43.63	289.53	n.a.	n.a.	n.a.	3	3
	0.19	1.716	0.901	3.24	17	105	3.66	24.73	118.85	3.98	44.31	138.08	n.a.	n.a.	n.a.	3	3	

Table 5.1: Results erosion testing

Clay	Energy level	w	$\rho_d(Mg/m^3)$	S_r	N	N>0	τ_c [min-max] analysis value	v_c [min-max] analysis value	S_f [min-max] analysis value	S_{iv} [min-max] analysis value	Valid test? [Y/N]
Boom clay	Modified Proctor (2.7MJ/m ³)	0.169	1.624	0.708	2	2	[38-49.9] 38	3.8	[0.079-0.103] 0.079	5.55	Y
		0.218	1.675	0.991	2	2	[21-52.3] 52.3	4.16	[0.074-0.111] 0.074	5.32	Y
		0.25	1.583	0.982	2	1	[47.6-up] 47.6	3.3	[0.01-0.014] 0.01	1.52	Y
		0.289	1.52	1.029	2	2	[2-16.3] 2	3.2	[0.013-0.054] 0.013	1.97	Y
	Proctor (0.6MJ/m ³)	0.252	1.347	0.69	3	3	[NAN-2] NAN	[0.11-0.25] 0.11	NAN	NAN	N
		0.261	1.369	0.739	3	2	[1-17] 1	2.7	[0.66-higher] 0.66	81.6	Y
		0.299	1.446	0.951	4	1	[79.2-90.5] 79.2	[4.34-4.47] 4.34	[0.57-1.33] 0.57	58.15	Y
		0.316	1.403	0.941	2	2	[19-20] 19	3.5	[0.003-0.01] 0.003	0.24	Y
	Sub-Proctor (0.3MJ/m ³)	0.347	1.361	0.97	3	2	[0.2-27.3] 0.2	1.4	[0.086-0.308] 0.086	6.07	Y
		0.296	1.374	0.844	3	3	[1.8-27.3] 1.8	[1.2-2.2] 1.2	[3.2-4.75] 3.2	28.1	Y
		0.323	1.383	0.934	3	2	[4.5-35.7] 4.5	2.3	[0.453-0.731] 0.453	22.14	Y
		0.373	1.31	0.966	3	3	[0.35-27.3] 0.35	1.6	[1.74-2.04] 2.04	106.6	Y
Kampen II	Modified Proctor (2.7MJ/m ³)	0.116	1.905	0.758	3	3	[NAN-5.47] NAN	1.3	NAN	95.36	N
		0.138	1.924	0.933	3	2	[5.47-10] 10	3.5	[0.10-0.22] 0.10	1.52	Y
		0.152	1.871	0.935	3	3	[NAN-0.7] NAN	0.28	NAN	5.35	N
		0.173	1.821	0.976	2	2	[NAN-0.3] NAN	0.11	NAN	7.69	N
	Proctor (0.6MJ/m ³)	0.162	1.633	0.674	3	3	[NAN-2.36] NAN	1.5	NAN	203.86	N
		0.176	1.708	0.824	3	3	[0.3-3.4] 0.3	2.2	[0.34-1.21] 0.34	11.5	Y
		0.182	1.7	0.841	2	2	[8-18.8] 8	2.8	[5.15-7.52] 5.15	69	Y
		0.194	1.678	0.866	3	3	[4.5-36.1] 4.5	2.3	[9.94-12.09] 9.94	154.7	Y
		0.242	1.619	0.985	3	2	[0.4-12.6] 0.4	1.1	[11-13] 11	263.4	Y
		0.255	1.579	0.975	3	3	[0.1-1.75] 0.1	0.34	11.65	309	N
		0.162	1.619	0.659	3	3	[2-9] 2	2.4	[3.3-10.29] 3.3	124.1	Y
		0.188	1.64	0.79	4	3	[4.2-19.8] 4.2	2.9	[0.63-1.18] 0.63	19.6	Y
	Sub-Proctor (0.3MJ/m ³)	0.216	1.636	0.902	3	3	[3.3-23.7] 3.3	2.5	[1.08-1.68] 1.08	4.62	Y
		0.242	1.597	0.952	3	2	[2.6-28.6] 2.6	0.8	[1.10-1.90] 1.10	58.17	Y
		0.269	1.536	0.964	3	3	[NAN-0.7] NAN	0.7	NAN	75.63	N
		Kampen III	Modified Proctor (2.7 MJ/m ³)	0.094	1.966	0.687	3	3	[0.12-0.7] 0.12	0.55	[0.52-3.6] 0.52
0.117	1.984			0.885	3	3	[0.45-4.2] 0.45	0.60	[0.18-1.96] 0.18	7.46	Y
0.138	1.921			0.928	3	3	[0.1-4] 0.1	1.5	[0.67-3.85] 0.67	22.12	Y
Proctor (0.6MJ/m ³)	0.128		1.821	0.722	2	2	[1.2-6] 1.2	0.58	[1.18-15.32] 1.18	56.34	Y
	0.132		1.843	0.773	2	2	[9-18.8] 9	3.1	[1.02-7.52] 1.02	38.65	Y
	0.141		1.845	0.829	3	3	[NAN-10.4] NAN	2.8	NAN	7.92	N
	0.158		1.802	0.863	3	3	[2.7-11.2] 2.7	2.5	[11.67-27.43] 11.67	44.7	Y
	0.167		1.775	0.872	3	3	[1.8-8.9] 1.8	0.22	[14.06-20.33] 14.06	594.46	Y
0.19	1.716	0.901	3	3	[0.8-2.6] 0.8	0.11	[1.79-42.99] 42.99	408	Y		

Table 5.2: Interpretation of erosion testing results

Clay	Energy level	w	$\rho_d(Mg/m^3)$	$\epsilon_{3.2Pa}$	$\epsilon_{7.0Pa}$	$\epsilon_{15.0Pa}$	$\epsilon_{32.4Pa}$
Boom clay	Modified Proctor (2.7MJ/m ³)	0.169	1.624	0	0	0	0.27
		0.218	1.675	0	0	0	0
		0.25	1.583	0	0	0	0
	Proctor (0.6MJ/m ³)	0.289	1.52	0.15	0.25	0.4	0.65
		0.252	1.347	10	17	30	50
		0.261	1.369	0.35	1.1	3.3	10
		0.299	1.446	0	0	0	0
	Sub-Proctor (0.3MJ/m ³)	0.316	1.403	0	0	0	0.15
		0.347	1.361	0.7	1.5	2.5	4
		0.296	1.374	0.3	1.8	8	38
		0.323	1.383	0	0.23	0.9	3.5
		0.373	1.31	1.5	4	10	8
	Kampen II	Modified Proctor (2.7MJ/m ³)	0.116	1.905	20	35	50
0.138			1.924	0	0	0.25	1
0.152			1.871	6	7	8.5	10
Proctor (0.6MJ/m ³)		0.173	1.821	1	20	23	27
		0.162	1.633	35	60	100	180
		0.176	1.708	1.2	2.5	4.5	11
		0.182	1.7	0	0	0.9	33
		0.194	1.678	0	0	3.4	35
		0.242	1.619	1.4	3.5	9	37
Sub-Proctor (0.3MJ/m ³)		0.255	1.579	130	200	280	400
		0.162	1.619	0.3	1.8	11	70
		0.188	1.64	0	0.18	1.5	6
		0.216	1.636	0	0.75	3	10
	0.242	1.597	0	0.5	2.7	12	
Kampen III	Modified Proctor (2.7 MJ/m ³)	0.269	1.536	2.2	5	7	10
		0.094	1.966	1.5	2.7	7	20
		0.117	1.984	0.5	1.8	4.5	8.5
	Proctor (0.6MJ/m ³)	0.138	1.921	1.05	2.6	5.5	18
		0.128	1.821	25	32	45	60
		0.132	1.843	0	0	1.5	35
		0.141	1.845	8	10	15	20
		0.158	1.802	0.2	2	18	150
		0.167	1.775	0.2	2.5	30	140
		0.19	1.716	60	80	100	300

Table 5.3: Back-calculated erosion rates at benchmark shear stresses

5.2. Erosion analysis in the context of the proctor plane

This section looks in possible trends by plotting the results in the context of the proctor plane.

First an overview is given by plotting the (velocity) detachment coefficient and critical shear stress/velocity of the Kampen III clay in the proctor plane, as is done in 5.1, 5.2, 5.3 and 5.4. In these graphs the gray lines are the results from the erosion tests, namely the critical shear stress, critical erosion velocity, detachment coefficient or velocity detachment coefficient respectively. And in black the proctor curve is drawn. The axis of the proctor curve is drawn on the right hand side, whereas that of the result curve is drawn on the left-hand side. Finally the saturation lines for 70%, 80%, 90% and 100% have been drawn in the figure.

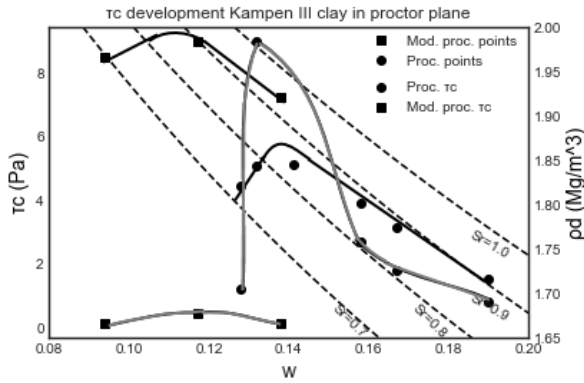


Figure 5.1: Critical shear stress Kampen III clay

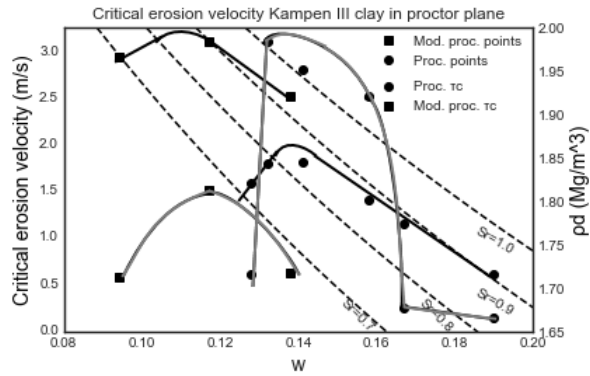


Figure 5.2: Critical erosion velocity Kampen III clay

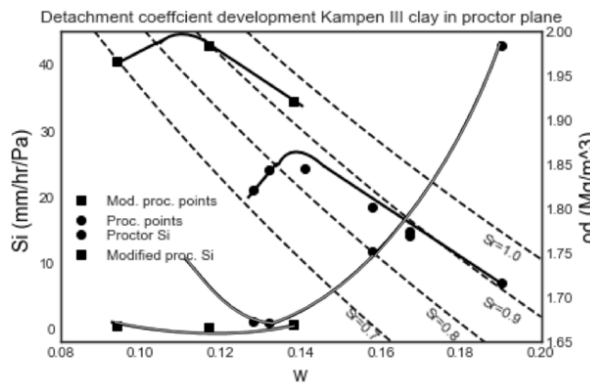


Figure 5.3: Detachment coefficient Kampen III clay

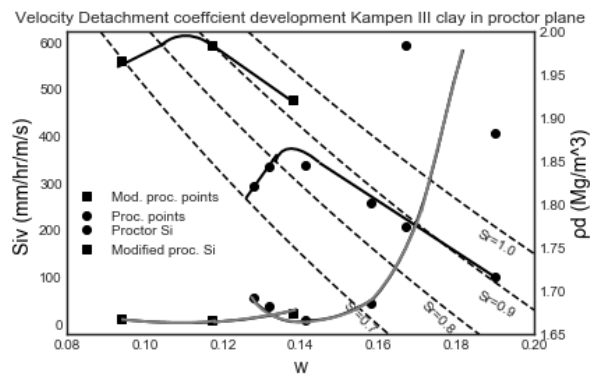


Figure 5.4: Velocity Detachment coefficient Kampen III clay

From figures 5.1 and 5.2 it can be seen that the critical shear stress/velocity (i.e. the point where erosion starts) is a variable of the energy level and water content at compaction. This point reaches its maximum at the optimum water content and decreases as the water content deviates further from the optimum. This is in line with the results from the literature study. Also it seems that compaction at a higher energy level does not result in a higher critical shear stress/velocity, but this statement does not hold when looking at the results of the other clays. It is suspected that the critical shear stress is lower due because it has a lower water content resulting in less suction of the sample. Suction could be of influence, because it results that the sample is subjected to a higher effective stress which could reasonably lead to less erosion.

Further in figures 5.3 and 5.4 it is seen that the detachment coefficient is lowest at the optimum water content and also decreases if the soil is compacted at a higher energy level. This seems logical, because it means the erosion increment (i.e. how much a soil extra erodes if the shear stress is above the critical shear stress) is lowest at the optimum water content and lower at a higher energy level (i.e. the soil is most erosion resistant at the optimum water content and more erosion resistant at a higher energy level). Finally it is also observed that the optimum behavior of both clay occurs at 85 % saturation.

From figure 5.3 it can be seen that the detachment coefficient becomes lower if the clay is compacted at higher energy levels (i.e. the soil is more erosion resistant) and that the detachment coefficient is also lowest at the optimum water content (once again, this is around 85 % saturation).

To see if these trends are true in a more general sense, the results for the other clays are also plotted.

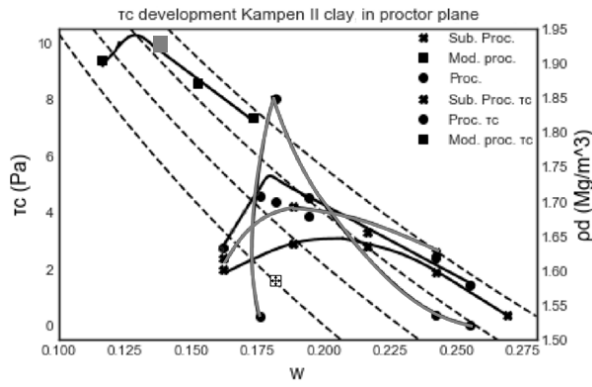


Figure 5.5: Critical shear stress Kampen II clay

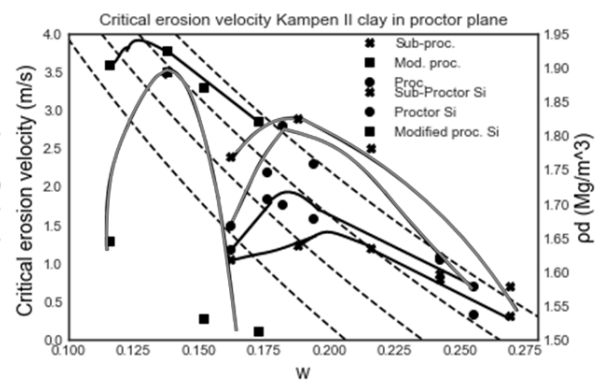


Figure 5.6: Critical erosion velocity Kampen II clay

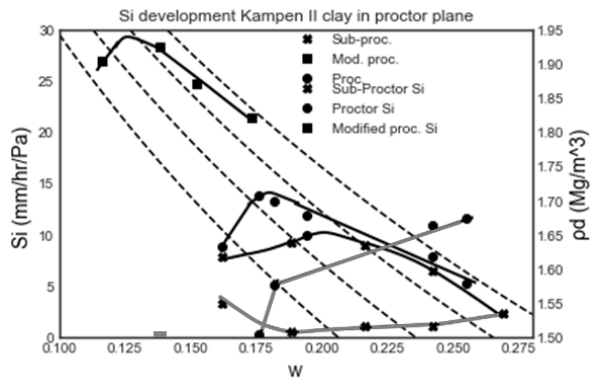


Figure 5.7: Detachment coefficient Kampen II clay

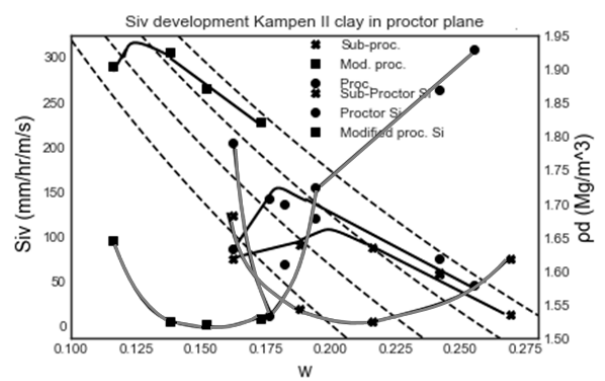


Figure 5.8: Velocity detachment coefficient Kampen II clay

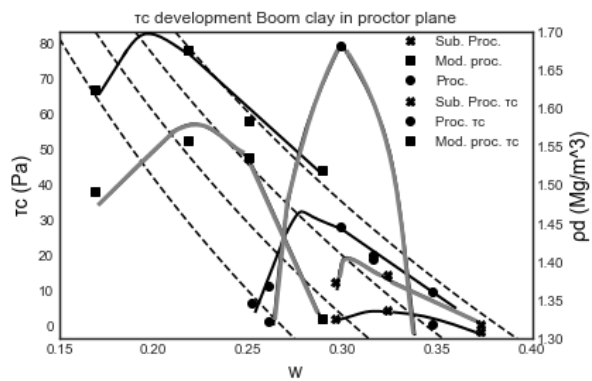


Figure 5.9: Critical shear stress Boom clay

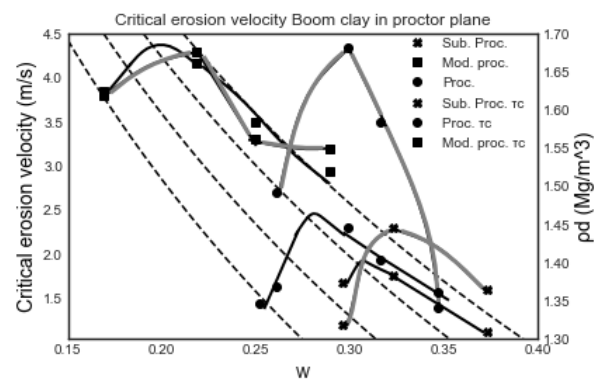


Figure 5.10: Critical erosion velocity Boom clay

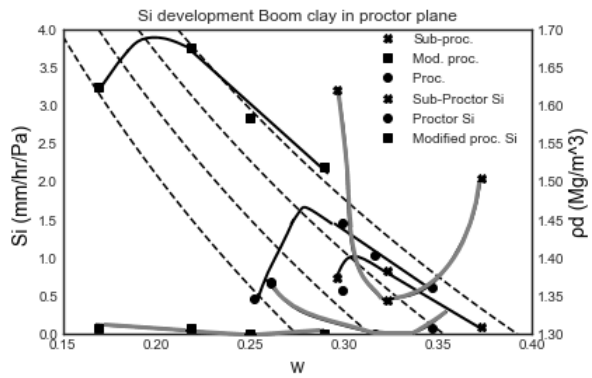


Figure 5.11: Detachment coefficient Boom clay

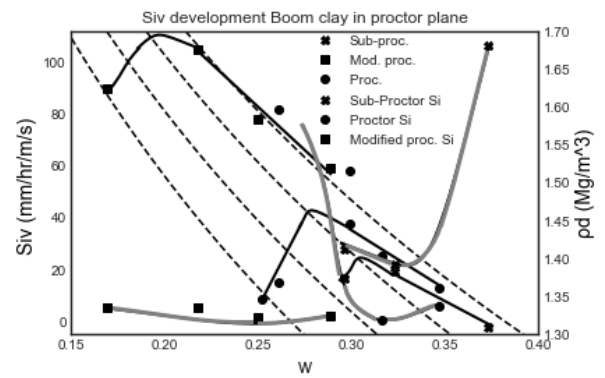


Figure 5.12: Velocity Detachment coefficient Boom clay

Looking at the graphs displayed on the previous page it is clear that a change from Kampen III to Kampen II to Boom clay consistently results in an increase of performance, which is what to be expected because it is going from a class III poorly suitable clay, to a class II clay to a very erosion resistant class I clay. To prove this an overview is made of what range of results were obtained during testing with the different types of clay in the table below.

ranges erosion parameters	Boom clay	Kampen II clay	Kampen III clay
$\tau_c(Pa)$	0-80	0-10	0-9
$v_c(m/s)$	0-5	0-4	0-3
$S_i(mm/hr/Pa)$	0-4	0-30	0-50
$S_{iv}(mm/hr/m/s)$	0-100	0-300	0-600

Table 5.4: Ranges erosion parameters different clays

That the Boom clay performs better than the Kampen II clay and even better than the Kampen III clay is even more clear when bounding the erosion parameters of each clay. This is done for each clay at each energy level. Here an estimation is made of what the most conservative value of the critical shear stress/erosion velocity/detachment coefficient or velocity detachment coefficient is in the range of the optimum minus 1 % water content or the optimum plus 1 % water content. This range is taken to account for the inaccuracies of compaction.

Clay	Energy level	$\tau_c(Pa)$	$v_c(m/s)$	$S_i(mm/hr/Pa)$	$S_{iv}(mm/hr/m/s)$
Boom clay	Modified proctor (2.7MJ/m ³)	55	4.2	0.01	2
	Proctor (0.6MJ/m ³)	70	4.4	0.02	5
	Sub-Proctor (0.3 MJ/m ³)	10	2.2	0.5	25
Kampen II	Modified proctor (2.7MJ/m ³)	10	3.2	0.1	1.5
	Proctor (0.6MJ/m ³)	6	3	0.3	11
	Sub-Proctor (0.3 MJ/m ³)	4	2.8	1	20
Kampen III	Modified proctor (2.7MJ/m ³)	0.5	2	0.2	11
	Proctor (0.6MJ/m ³)	8	1	1	30

Continuing on with the analysis of figure 5.5 through 5.12. Here the conclusions drawn with the Kampen III clay are confirmed. Also here the detachment coefficient is lowest at or close to the optimum water content and the detachment coefficient also reduces with an increasing energy level. This effect is quite dramatic, because in the worst case the detachment coefficient can differ 2 orders of magnitude between a properly modified compacted sample and a poor compacted sub-proctor density sample, even when using the same clay to start with! This trend also holds for the velocity detachment coefficient. What concerning the critical shear stress and critical erosion velocity also here are highest close to the optimum water content and do not necessarily increase at a higher energy level. However, it also striking here to see the differences that occur when comparing well compacted soils at a proper water content versus samples that have not been compacted in such a manner, here there is also a difference of 2 orders of magnitude. Finally, also here the best erosion parameters occur around 85 % saturation.

To further then investigate the performance of the samples back-calculated erosion rates have been determined at the benchmark shear stresses of 3.2, 7, 15 and 32.4 Pa. The results of this are presented in table 5.3. Here it can be observed that despite the initial difference in erosion characteristics the (currently deemed unsuitable) Kampen II clay shows only slightly more erosion than the well performing Boom clay (whereas the

Kampen III clay still performs below standard). For instance, when considering the optimum water content, proctor density samples of the Boom clay and Kampen II clay, the Boom clay shows 0 mm/hr erosion at the (catastrophic) shear stress level of 32.4 Pa whereas the Kampen II clay shows a very limited 6 mm/hr of erosion. If the Kampen II clay is compacted at a modified proctor energy level it shows only 1 mm/hr of erosion. This implies that during a catastrophic storm a dike which has a Kampen II clay dike cover can withstand several days of catastrophic overflow without the structural integrity of the dike being at stake. When considering (more likely) lower values of shear stress (and overflow) this period becomes even longer. Considering the low erosion rates that are associated with the Kampen II clay, it can be concluded that Kampen II clay can be reasonably considered as a dike cover if compacted at or very close to the optimum water content and at a sufficiently high energy level. This energy level should be at or higher than Proctor density. Expanding these conclusions towards all category II clays is probable, however this delivered with some caution, because not all possible combinations of category II clays have been investigated. The Kampen III clay on the other hand has proven not be acceptable under any circumstance, especially as it seems to erode away "in one go" when tested.

5.3. Erosion in context with other research

In this section the results of this study are put into context with results obtained in the studies performed by Briaud. This is done by plotting the results in the Briaud erosion class graphs and then further elaborated. First the results of the Kampen III clay are presented in figures 5.13 and 5.14. In the left graph the results of the Kampen III erosion tests are displayed in a shear stress/erosion rate figure with the Briaud erosion classes drawn out, whilst on the right hand side the same graph is drawn but now in a velocity/erosion rate plane. Please note that these graphs are zoom-ins of the original Briaud erosion class division.

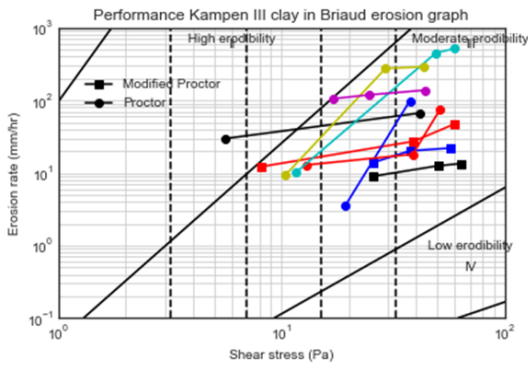


Figure 5.13: Kampen III shear stress/erosion rate results in Briaud erosion graph

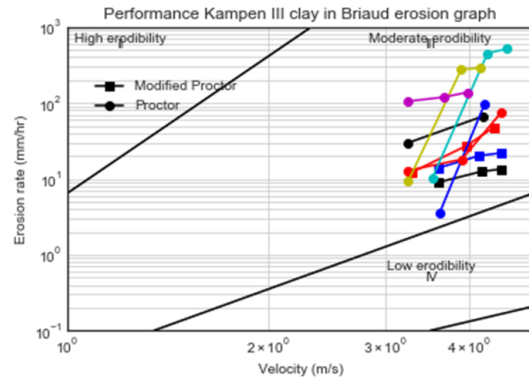


Figure 5.14: Kampen III velocity/erosion rate results in Briaud erosion graph

From the figures above it can be seen that the Kampen III clay falls in the Moderate erodibility range, which may be expected when considering what is a low plasticity clay. This is clearer when in figures 5.15 and 5.16 the suggested erosion ranges for a low plasticity clay are drawn in as suggested in (Briaud et al. (2019)).

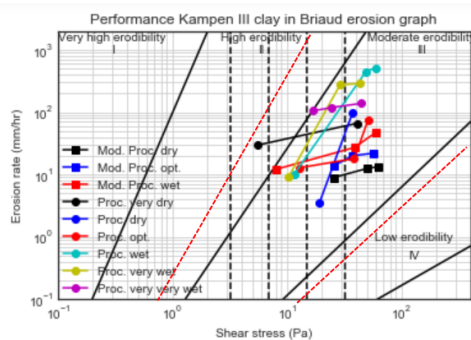


Figure 5.15: Kampen III low plasticity clay ranges

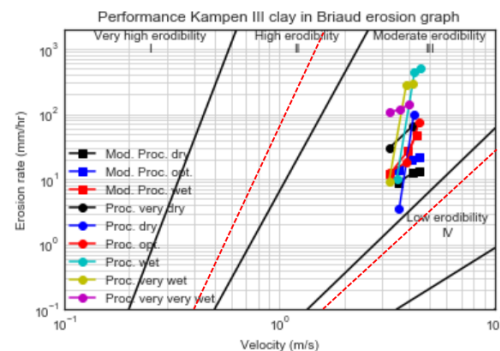


Figure 5.16: Kampen III low plasticity clay ranges

Looking at these graphs the following things are clear:

- The Kampen III clay fully fits in the ranges proposed by Briaud for low plasticity clays
- Also here the effect of differing energy level and water content are visible
- Samples have been investigated for fairly limited shear stress/velocity ranges

The second point noted, that the effects of compaction is visible because the modified proctor samples show less erosion at comparable shear stress/velocities. Also the better compacted samples have a lower erosion increment, which is totally in line with the findings in the proctor plane, because the erosion increment is basically the detachment coefficient. Further, it is clear that in comparison with the testing of Briaud there has been tested for a fairly limited range of shear stress and velocities. This is due to the nature of the machine that was built but also due to the expected the overflow rates that are to be expected in the case of overflow of a levee. These ranges were tailored in the design of the machine in order to produce the most relevant tests.

These conclusions can also be extrapolated for the other clays, the results of which are displayed in figure 5.17,5.18,5.19 and 5.20

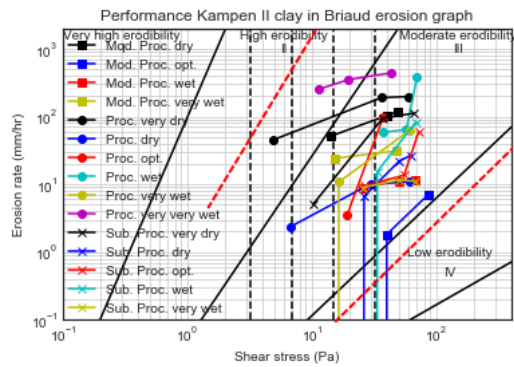


Figure 5.17: Kampen II low plasticity clay ranges

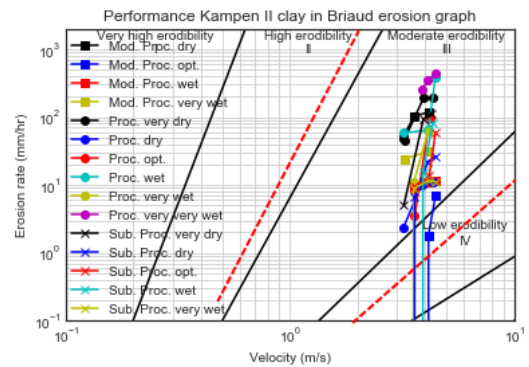


Figure 5.18: Kampen II low plasticity clay ranges

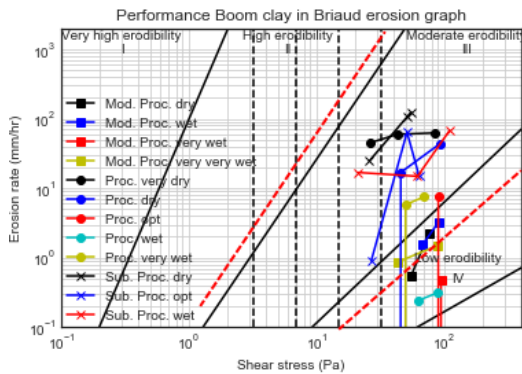


Figure 5.19: Boom high plasticity clay ranges

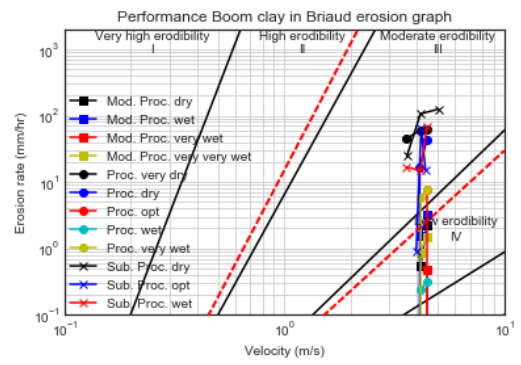


Figure 5.20: Boom high plasticity clay ranges

Most conclusions from the Kampen III clay also hold up here, but it is good to note that the Boom clay which has undergone a modified Proctor compaction are so erosion resistant they fall outside of the High plasticity clay range for erosion results as proposed by Briaud.

In essence the conclusion from comparing the results of the erosion tests to the erosion tests carried out by Briaud are that they largely overlap, although it is not always easy to compare due to the difference of tested shear stress/velocity ranges.

5.4. Analysis in different manners

Finally, the erosion results were also analyzed in several different manners that were not successful, but are nevertheless listed as reference to analysis methods that did not work:

- Comparing erodibility and Liquidity index
- Comparing erodibility and Degree of Saturation
- Comparing erodibility and the associated erosion energy

The first comparison was undertaken because the requirements by (adviescommissie voor de waterkeringen (1996)) require the clay layer of a dike to have a consistency index at compaction above 0.75. However, even applying such high consistency indices would result in compacting the clay at a far too high water content when considering the results from the previous sections. For instance, compaction of Boom clay ought to then be at a water content above 41% whilst based on the analysis in the proctor plane it should be at about 30% water content. The same holds for the other clays. Further, plotting the erosion parameters against the consistency index did not yield any significant result.

Finally, also there was looked if it was possible to find a trend between the energy that was necessary to erode the sample and the energy that was put into compacting the sample. This did not yield any significant result with a correlation between the amount of energy put into erosion and the amount of energy put into compaction. This was done by estimating the amount of shear stress the sample was subjected to during erosion and the amount of material eroded in order to determine an amount of energy put towards eroding the sample and comparing the energy level during compaction it was subjected to.

5.5. Observations during testing

2 main observations have been gleaned during testing: 1 concerning the failure mode of the samples and the other in the failure progresses during testing. Each will be discussed and used in analysis.

Concerning the failure mode it is observed that the Category III clays fail in a much more granular way (i.e. larger parts fail at once) than the Kampen II clay which fails more granular way than the Boom clay. This can be explained fairly well because the Kampen clays contain more sand and therefore have lower inter-particle forces and will fail more at once. On the other hand the Boom clay fails much more gradual and more individual "flocks" of matter erode away. Note that this is only the case for very carefully prepared samples (which have been crumbled carefully and then compacted). Otherwise it was observed that the samples failed along the boundaries of the chunks that have been compacted resulting in higher erosion rates. This means that care must be taken outside to compact the clay layer in such a way that the clay does not fail along the predetermined chunk lines.

What has also been observed is the way in which the sample fails. During the beginning of testing the sample hardly erodes at all. However, during testing first the front end fails, the rear end fails it the sample will start protruding more as a semi-circle. A schematization of the stages that failure goes through (starting from 1 going to 4) is given below in figure 5.21.

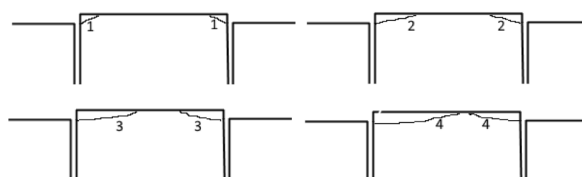


Figure 5.21: Progression of failure during testing

This is in start contrast with the idealisation thought upfront that the sample will erode top-down. Something else that is clear is that the shear stress decreases considerably during the eroding of the 1 millimeter of soil.

This implies that the assumption during CFD modelling that the shear stress will not decrease significantly during testing is false. Also the previously mentioned failure mode suggests that the saturation of the soil is correlated to when the soil fails. This idea arises from the fact that during the entire test the most exposed part to the water only fails.

This then concludes the results and analysis chapter, now a continuation will be made with a discussion chapter which puts the results in context. Then a conclusion chapter will follow and end with recommendations.

6

Discussion

This chapter discusses the differences between the results obtained in the laboratory and how they might differ outside. This can then be used to properly put the results in context and draw appropriate conclusions and recommendations

It will mainly focus on the following aspects:

- Differences in overflow regime
- Overtopping effects
- Erosion stages
- Scale effects
- Remoulding effects
- Time-effects
- Dry/wet cycles

The effects of these aspects will then be put into context with the results obtained.

First of all it is important to note the difference in overflow regime: in an EFA a constant overflow takes place in time and space whereas in reality the overflow of a dike will be more in waves with the overflow rate being not constant and resulting in a non-homogeneous shear stress on the clay. This is especially clear when looking at video's of levee overflow (one which is in the graduation presentation). Due to this method of overflow there will be a certainty of unhomogeneous erosion which is and can not reasonably be accounted for in the EFA and can not be dealt with. This is a topic that might be of interest to better understand.

Further, it is important to note that this thesis has mainly dealt with overflow and not overtopping effects. The main difference is that overtopping will not only result in "smooth" erosion due to water passing by over the surface of the clay but also that the clay must sustain some impact. This will result in more erosion and though this study has crudely tried to capture this effect (as explained in Appendix A) it can be safely assumed that erosion results found in this study are a lower bound of the erosion that can be found outside.

Another topic of importance when relating the laboratory tests with the reality outside is the scale of testing. This arises from the fact that the samples that are tested are much obviously much smaller than the clay cover that is potentially eroded away outside. This has 1 massive implication:

The area to volume ratio's of the samples are very different to outside

This will mean that water infiltrates relatively quicker into the sample compared to outside, because there is more surface area exposed (in contact with water from the top and the perimeter compared only to the top). Because the water infiltrates quicker the sample will become saturated easier and as has been discussed above full saturation will result in failure of the sample.

This means that it is very probable that a slight overestimation of the erosion rate of the clay is made. However, further the method of erosion, and the orientation of the compacted clay is correct with respect to flow direction of the water. This means that the method of testing is a valid method.

Further the effects of remoulding must not be forgotten. With the effects of remoulding is meant that all samples (and the clay cover as well) are built up from clay blocks. As has been observed during practicing the tests, samples that have been constructed from coarse clay crumbs fail faster and fail at the interface between the clay crumbs. This means that there is a significant effect of remoulding of the clay that must be kept in mind.

This is important because during testing with the EFA the samples are created in such a manner (with very small clay crumbs) that the entire clay is remoulded to a single, solid block as much as is possible. Outside the clay is constructed however from larger blocks, but also correspondingly larger machines. It is therefore good to see if this still then molds to 1 large block.

This question can be answered however by the knowledge gained during the site visit done to Delfzijl (of which further details are given in Appendix D). A cross-sectional photo is presented and it can be seen that although the top-layer is very cracked the deeper clay layers are more or less one solid block. In other words the sample structure observed during testing in the laboratory is similar to the structure in the dike and probably will yield similar results. Nevertheless, it is very important to try and compact the soil as much as possible as one single block in order to enhance the erosion resistance as much.

On the other hand it is seen that the top layer is cracked and dry can be ignored during this study because it is the layer that will contain the grass (roots) and therefore will behave very differently. Also the effect of grass on the erosion resistance is not in the scope of this research.

During proof of concept testing also a mention was made of the effect of time on the testing results. During proof of concept testing this was done in order to see how the time effect influenced the results. It can be seen from these tests that prolonged periods of testing will cause an increase of the erosion rate due to the saturation of the sample during testing. However, a devastating storm obviously lasts longer than the several minutes it might cost to erode away a single millimeter of clay, a devastating storm can easily last several hours. This means that it is important to determine the length of a normative storm and the shear stress that occurs in such a case. In this research a well-educated assumption of 32.4 Pa of shear stress has been taken and a length of 6.25 hours (one high tide cycle) but further research might be considered.

Unfortunately it was not possible to have an in-depth research concerning the cyclic effects of erosion. Nevertheless, it is unquestionable that the continuous drying and wetting of the clay on a levee will have significant impact on its erosion properties. However, this study has only looked into the erosion resistance of soils after compaction. It is therefore a good idea to look into this more.

Something that also must be considered is the difference between mass versus volume erosion. During tests with the EFA volume erosion has been tested for, and with an erosion centrifuge mass erosion has been tested. Now these results can not be compared in any way, due to the intrusion of water during the test. It is good to compare these 2 by adding a mass-measurement system in the set-up.

Finally, time-effects are to be discussed. Although briefly touched upon in Appendix B its full effects are not well known. What did appear however is that testing for prolonged stretches of time did result in an increase of the rate of erosion. This is probably because there is a certain infiltration of water during the process reducing the erosion resistance of the soil. However, to well estimate the erosion of a levee that is usually subjected to prolonged stretches of overflow it is of utmost importance to better understand how the amount of erosion develops over time. This is especially the case because the current erosion rates are in essence a baseline erosion rate which will increase over time.

Overall, looking at all factors that contribute to the difference between erosion in the laboratory and outside it can be seen that there still is a lot to further research. This mainly concerns the effects of wet-dry cycles, remoulding effects, scale effects, time effects and the overtopping effects. This is not surprising, because no deep investigative research has been conducted into these topics has been found whilst conducting the literature study, nor were these topics found to be of importance upfront when designing the set-up.

7

Conclusions

This chapter will discuss the conclusions that can be drawn from this thesis. This will be done by taking each sub-question and answering it and then answering the final research question.

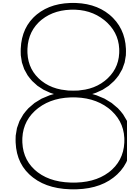
What effect does compaction have on the erosion resistance of clay in the unsaturated zone, when used as a dike cover, and how can this be measured and analyzed?

To answer this question first of all an Erosion Function Apparatus was built, proof of concept tests were conducted and then finally erosion tests of several types of clay have been executed. This research performed these tests on clays with several different initial erosion characteristics and showed that the current guidelines are right in appointing which clay will overall perform best. In this way the functionality of the current erosion guidelines have been proven.

Further, this research proved that compaction at or close to the optimum water content reduced the rate of erosion significantly (or let it stop all-together), as well as compacting at a higher energy level. Also, it is concluded that the results of the erosion tests conducted in this study fit well into the conclusions drawn by studies carried out by Briaud in the United States. However, the results obtained in this study are in more narrow shear stress/velocity ranges because these have been tailored to be representative of the velocities and shear stresses that may be expected with dike overflow. Also, when the erosion rates of the various clays are compared it can be concluded that the category II Kampen II clay performs almost as good as the category I Boom clay when subjected too relevant levels of shear stress.

This means that this research can conclude that by developing the Erosion Function Apparatus in this study it has been proven that the (currently perceived) unsuitable Kampen II clay can be used as clay cover if compacted at the optimum water content and at a sufficient energy level (preferably at Proctor compaction level or higher).

Finally, this research has also left some topics open for further research, which also have been elaborated a bit upon in the previous chapter, and these mainly concern investigating the effects of wetting drying cycles and getting a more in depth understanding of the differences between the erosion process outside and in the laboratory.



Recommendations

This chapter will sum up the recommendations that can be made for further research. Generally speaking these recommendations can be split in two categories:

- Recommendations regarding the EFA/sample preparations
- Recommendations regarding further testing possibilities

8.1. Recommendations regarding the EFA/sample preparations

Regarding the EFA several recommendations are made which can enhance the practical use of the EFA. These consider the following:

- Incorporate a continuous measurement system that weighs the sample
- Make an alternative pitot tube
- Place the erosion flume on different supports
- Make compaction procedure more efficient

All the individual recommendations will now be elaborated on.

It is proposed to incorporate a continuous measurement system that weighs the sample during testing. This will aid in understanding the process by which the sample gets more and more saturated and ultimately erodes away. Properly understanding this helps in 2 ways: coming one step further in understanding the erosion process, but also bridging the gap between mass and volume erosion. In fairness, in the beginning of the research the same recommendation was made to incorporate a mass measurement system. However, at first this difference between mass and volume erosion was deemed to be limited.

To incorporate this in the set-up it is proposed put the erosion flume on different block and between these blocks place a Z-type hydraulic load-cell . These devices are very accurate (error in range of 0.03 % FS) and are then connected to a Rosemount and is then finally connected to the readily present OPTO-22 box. This type of set-up has already been used several times with success in the laboratory of Boskalis, albeit with different set-ups. The cases in which this has been done successfully include (Heijmeijer(2019)) and (Noorman(2019)).

Also a proposal is made to make an alternative pitot tube. In this research use has been made of a pitot tube used from a previous set-up, as described in (Heijmeijer(2019)). However during this research it has occurred frequently during a test that the pitot tube became clogged due to clay debris and making it impossible to measure the speed in the erosion flume for the remainder of the test. Also extreme care had to be taken that there were no air intrusions messing up testing results, due to the unnecessary long length of the pitot tube.

Further, it is proposed to place the erosion flume on different supports. Up to now the set-up has been resting on the water basin (which also contains the pump). However, at higher speeds the pump starting

vibrating significantly. This makes filming the erosion process more difficult and having less clear camera footage to interpret.

Finally, a suggestion is made to investigate if the compaction procedure can be made more efficient. In this research a full proctor mold was compacted (diameter 100 mm, 100 mm high), after which a relatively modest sample of diameter 38mm, 80 mm high is extracted. This means that a significantly higher amount of clay has to be crumbled and compacted in order to get a sample.

However, it would be much more efficient if the samples could be compacted in such a manner that only a limited amount of clay has to be prepared. Compacting the samples in such a manner has been done in Alkemade and Kruk (2018), however it was decided against at first, because it was (and is) uncertain if this will not lead to an uneven level of compaction and give non-consistent results. The reason for this belief is because this is something that is observed during compaction with a regular proctor mold. At the edges of the sample only a limited amount of remoulding is observed and the sample has more voids compared to the middle of the sample. The suggestion is made therefore to see if this is truly the case.

8.2. Recommendation regarding further testing

The recommendations regarding further testing consist of the following items:

- Proceed with testing more clays
- Investigate effects of water infiltration in more detail (after having added mass measurement system)
- Investigate effects of cyclic loading
- Better investigate differences between outside erosion and laboratory erosion

The first recommendation is to test more types of clays. The reason for this is very simple: only a few types of clay have been tested in this research, which is too limited to draw widespread conclusions. However, the following 2 recommendations are in the opinion in of the author more important to understand rather than just test more clays. This is because the following 2 recommendations really enhance the understanding of erosion whereas this recommendation is more to check if the findings are universal.

Further a recommendation is made investigate the effects of water infiltration. This is however more or less the same as described above by adding a mass system to the EFA and will therefore not be discussed again.

Further it is suggested to look into the effects of cyclic loading. This is something that has only been looked into on a theoretical scale during this research. However, to know the full implications of using different clay types/compaction levels on dikes it also necessary to understand the effects over time on the erosion behavior.

Finally it is advised to obtain a more in-depth understanding of the differences between the outside and laboratory erosion processes. This has already been discussed in detail in the Discussion chapter and therefore will not be repeated here.

Bibliography

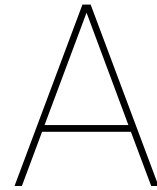
- Technische adviescommissie voor de waterkeringen. Technisch rapport klei voor dijken. Technical report, Technische adviescommissie voor de waterkeringen, 1996.
- Q. Alkemade and N. Kruk. Erosiebestendigheid van klei in dijken. Afstudeeronderzoek Hanzehogeschool, Groningen in opdracht van Hydronic B.V., 2018.
- K. Arulanandan and Edward Perry. Erosion in relation to filter design criteria in earth dams. *Journal of Geotechnical and Geoenvironmental Engineering*, 109:682–698, 1983.
- Autodesk CFD. Governing equations autodesk cfd. <https://knowledge.autodesk.com/support/cfd/learn-explore/caas/CloudHelp/cloudhelp/2018/ENU/SimCFD-Learning/files/GUID-83A92AE5-0E9E-4E2D-B61F-64B3696E5F66-htm.html>, 2017.
- Jommi Azizi, Musso. Effects on repeated hydraulic loads on microstructure and hydraulic behaviour of a compacted clayey silt. *Canadian Geotechnical Journal*, pages 1–42, 2017.
- B. Kerssens. Mass flow excavation of a cohesive soil. Graduation thesis, Delft University of Technology, 2017.
- J.A. Battjes. Vloeistofmechanica. Collegedictaat TU Delft, 2002.
- J.L. Briaud. Erosion function apparatus for scour rate predictions. *Journal of Geotechnical and Geoenvironmental Engineering*, 127:105–113, 2001.
- J.L. Briaud. Levee erosion by overtopping in new orleans during the katrina hurricane. *Journal of Geotechnical and Geo-environmental Engineering*, 134:618–632, 2008.
- J.L. Briaud. *Geotechnical Engineering Unsaturated and Saturated Soils*. John Wiley & Sons, Hoboken, NJ, United States of America, 2013.
- Briaud et al. Relationship between erodibility and properties of soils. Technical report, National cooperative highway research programme, 2019.
- C. Jommi C. Airò Farulla. Suction controlled wetting-drying cycles on a compacted scaly clay. *Proceedings of International Conference on Problematic Soils*, pages 1–9, 2005.
- CROW. *RAW 2010*. CROW, 2010.
- Federal Highway Administration. Scour in cohesive soils. Technical report, Federal Highway Administration, May 2015.
- H.J. Gibbs. *A study of erosion and tractive force characteristics in relation to soil mechanics properties*. Division of Earth engineering laboratories US Army Corps, 1962.
- Imam Haghigi. Caractérisation des phénomènes d'érosion et de dispersion : développement d'essais et applications pratiques. Technical report, Université Paris-Est, 2013.
- A. Hughes. Erosion resistance of compacted clay fill in relation to embankment overtopping. Technical report, University of Newcastle upon Tyne, 1981.
- Independent Levee systems investigation team Hurricane Katrina. Erosion tests on new orleans levee samples. Technical report, US Army Corps of Engineers, 2006.
- A. Govindasamy J.L Briaud and I. Shaffi. Erosion charts for selected geo-materials. *Journal of Geotechnical and Geo-Environmental Engineering*, pages 10–13, 2017. doi: DOI:10.1061/(ASCE)GT.1943-5606.0001771.
- A.V. Gavindasary J.L. Briaud and A. Shaffi. Closure to "erosion charts for selected geomaterials". *Journal of Geotechnical and Geo-environmental Engineering*, 145:213, 2018a.

- A.V. Gavindasary J.L. Briaud and A. Shaffi. Discussion of "erosion charts for selected geomaterials". *Journal of Geotechnical and Geo-environmental Engineering*, 144:1–5, 2018b.
- Chen J.L. Briaud. The efa, erosion function apparatus: An overview. *Proceedings of the 16th international conference on Soil Mechanics and Geotechnical Engineering*, pages 479–481, 2005. doi: doi:10.3233/978-1-61499-656-9-479.
- J.L. Briaud et al. Sricos: Prediction of scour rate in cohesive soils at bridge piers. *Journal of Geotechnical and Geo-Environmental Engineering*, 237:237–246, 1999.
- J.M. Fleureau et al. Aspects of the behaviour of compacted clayey soil on drying and wetting paths. *Canadian geotechnical journal*, 39:1341–1357, 2005.
- G. Kruse. Onderzoek van kleibekleding van dijken langs ijssel en pannerdens kanaal voor het ontwikkelen van keuringseisen van klei. Technical Report CO-275921/47, Grondmechanica Delft, 1986.
- G. Kruse. Onderzoek van kleibekleding van dijken aan zout en brak water in friesland, zuid-holland en zeeland voor het ontwikkelen voor keuringseisen van klei. Technical Report CO-275923/29, Grondmechanica Delft, 1987.
- G. Kruse. Onderzoek naar het beoordelen van de geschiktheid van kleigrond voor bekleding van dijken met grasdekking. Technical Report CO-275925/14, Grondmechanica Delft, 1988.
- M.E. Walker III. Scour potential of cohesive soils. Graduation thesis, Auburn University, 2013.
- J. Mitchell. The fabric of natural clays and its relation to engineering properties. *US Army Corps of Engineers, Mississippi*, 1960.
- J. Mitchell and K. Soga. *Fundamentals of Soil Behaviour*. John Wiley & Sons, Hoboken, NJ, United States of America, 2005.
- Mostafa. Erosion resistance of cohesive soils. *Journal of Hydraulic research*, pages 777–787, 2008.
- NEN. Ongebonden en hydraulisch gebonden mengsels-deel 2: beproevingsmethoden voor het bepalen van de laboratoriumreferentiedichtheid en het watergehalte-proctorverdichting. *NEN-EN 13286-2*, 2010.
- Nguyen. Characterisation de l'érosion de soils par le jet erosion test. These Ecole central Paris, 2014.
- D. Bloomquist R. Crowley and C. Robeck. Description of erosion rate testing devices and correlation between rock erosion rate and cohesion. *ICSE6, Paris*, pages 205–213, 2012.
- G. Herrier D. Marot T. Wahl R. Fell, G. Hanson. Relationship between the erosion properties of soils and other parameters. *Erosion in Geomechanics applied to dams and levees*, 2013.
- J.D. Rice. Lecture external erosion. Lecture notes TU Delft, 2019a.
- J.D. Rice. Lecture internal erosion. Lecture notes TU Delft, 2019b.
- S. Hughes, J. Shaw and I. Howard. Earthen levee shear stress estimates for combined wave overtopping and surge overflow. *Journal of Waterway, Port, Coastal and Ocean Engineering*, 138:267–273, 2012.
- P. Mineart R. Millet W. Huag J. Vargas M. Inamine S. Mahnke S. Shewbridge, J. Perri. Levee erosion prediction equations calibrated with laboratory testing. *International Conference on Scour and erosion, ASCE*, 2010a.
- P. Mineart R. Millet W. Huag J. Vargas M. Inamine S. Mahnke S. Shewbridge, J. Perri. Levee erosion screening process. *International Conference on Scour and erosion, ASCE*, 2010b.
- A. Shields. Anwendung der aehnlichkeitsmechanik und der turbulenzforschung auf die geschiebebewegung. Technical report, Preussische Versuchsanstalt fur Wasserbau und Schiffbau, 1936.
- T. Pullen et al. Die kuste, archiv fur forschung und technik an der nordt und ostsee, eurotop wave overtopping of sea defences and related structures assesment manual. Technical report, Boyens Medien GMBH, 2007.

- United States Federal Bureau of Reclamations. Usbr best practices, erosion of soil and rock. Technical report, United States Army Corps of Engineers, 2014.
- United States Federal Bureau of Reclamations. Urs erosion guidelines chapter 7. Technical report, United States Federal Bureau of Reclamations, 2015.
- US Army Corps of Engineers. Design and construction of levees manual no. 1110-2-1913. Technical report, US Army Corps of Engineers, 2000.
- US Army Corps of Engineers. General design and construction considerations for earth and rock-fill dams no. 1110-2-2300. Technical report, US Army Corps of Engineers, 2004.
- G.A.M van Meurs and G.A.M Kruse. Update inzichten in gebruik van klei voor ontwerp en uitvoering van dijkversterking. Technical report, Deltares, 2017.
- Waterloopkundig Laboratorium. Klei onder steenzettingen, verslag literatuur en bureaustudies. Technical report, Waterloopkundig laboratorium, Laboratorium voor Grondmechanica en Deltadienst Rijkswaterstaat, 1985.
- E.M. White. *Fluid mechanics*. Mc Graw Hill, New York, NY, United States of America, 2011.
- K. Wiersma. Verschillen in dijkontwerp tussen Duitsland en Nederland, 2011.
- H.J. Wouters. Onderzoek naar de erosiegevoeligheid van baggerspecie. Ingenieursscriptie, Landbouwhogeschool Wageningen, 1981.
- Yasufuku. Compaction quality on the embankment slope and its evaluation method. *Japanese Geotechnical Society special edition*, pages 2622–2626, 2018.
- Zentrum Geotechnik Deutschlands. Klassifikation von Boden und Fels. Technical report, Zentrum Geotechnik Deutschlands, Lehrstuhl für Grundbau, Bodenmechanik, Felsmechanik und Tunnelbau, 2002.
- Zhang and Yu. Critical conditions for incipient motion of cohesive sediments. *Water resources research*, pages 7798–7815, 2017.

I

Appendices



Design Erosion Function Apparatus

This chapter discusses the design of the EFA, not only the final design but also which considerations were taken to get to this design. It will also discuss the extensive fluid dynamics modelling that has been performed, which has been used during the design and validation of the set-up. The set-up of this chapter will be as follows:

- General overview of design, with a Work Breakdown structure
- Discussion of the design of the pumping system
- Discussion of design of the flow tube with each of its individual parts
- Discussion of the measurement equipment
- Discussion of the other parts
- Discussion of the fluid dynamics modelling

A.1. General overview

In this section a general overview is given of the design of the erosion function apparatus, which has been done in figure A.1.

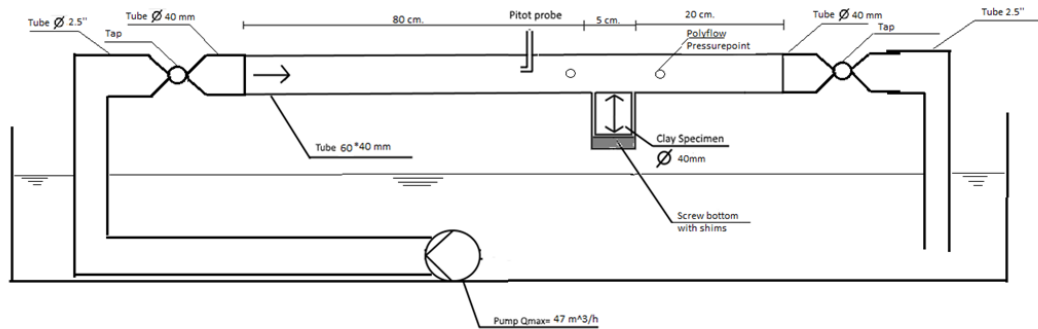


Figure A.1: Overview drawing Erosion Function Apparatus

A full-page version of this drawing is presented in Appendix H.

As already discussed in chapter 2 the Erosion Function apparatus is essentially a flume through which water flows as to erode a protruding soil sample measuring the time it takes to erode away.

This means that in general it would consist of the following elements:

- Flow tube
- Pump
- Measurement systems
- Some miscellaneous items

An overview photo of the final result is then given in chapter B and close-up photos of the individual parts in Appendix E.

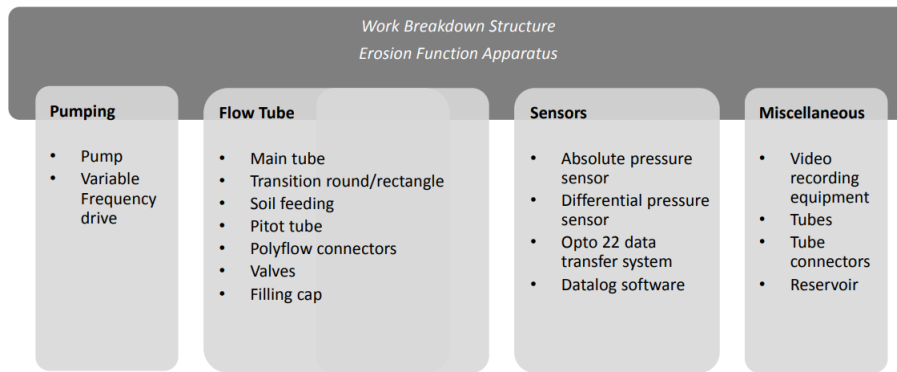


Figure A.2: Parts of Erosion Function Apparatus

To properly organize all parts of the set-up and work in a structured manner a Work Breakdown Structure was made which is given in figure A.2.

Now a systematic work-through of all parts will be done, starting with all items related to the pump, then the items connected to the flow tube, then to the sensors and finally the miscellaneous items.

A.2. Design Pumping system

Obviously in this set-up a pumping system is necessary and consists mainly of 2 parts:

- Pump
- Variable Frequency Drive

The Variable Frequency Drive is necessary to let the pump work at different flow rates. It works by taking regular power (230 V, 50 Hz) converts it from AC to DC current and then converts it from DC current to AC current at the required frequency (but below 50 Hz). By lowering power frequency the pump operates at a lower flow rate.

However, first the choice for the pump will be discussed.

When first looking for a pump the following criteria were used:

- The pump should be as large as possible
- Use a readily available pump if possible
- Limit the costs as much as reasonably possible
- The pump should readily come with a frequency drive or should be fit to be equipped with one.

Unfortunately, it was not possible to use any of the pumps available at Boskalis, they were either extremely large or relatively small and therefore unsuitable. Because of this an inventory was made of the different types of pumps and it immediately became clear that pumps with a power output above 1.5 kW became extremely expensive, and that pumps at or below 1.5 kW were reasonably affordable. Because of this the search was limited to pumps at or just below this 1.5 kW limit, and the limitation on flow rate was taken to compensate for as much as possible in the design of the erosion flume. The search came up with 5 suitable types of pumps, of which the preliminary flow rate calculations are given in F. The final choice for the pump is the Bedu DGX 200/2/65A0CM(T)50 pump which is able to generate a predicted flow rate of $41 \text{ m}^3/\text{h}$ resulting in a flow rate of 4.4 m/s.

This pump is able to be linked to a variable frequency drive as long as it operates at a start-up frequency of 20 Hz and a continuous operation frequency of 10 Hz.

A photo of the pump and the variable frequency drive are given further-on in Appendix B.

A.3. Design Flow tube

In this section the design of the flow tube is discussed, starting from the first starting point working step by step towards the final result. However, there will be first started with an overview of the final design of the flow tube and then a step-by-step explanation of each and every component.

A.3.1. Overview final design

The final design drawing of the flow tube is given below in figure A.3. It is to be constructed from acrylic sheet so that the entire erosion process can be observed and recorded on film.

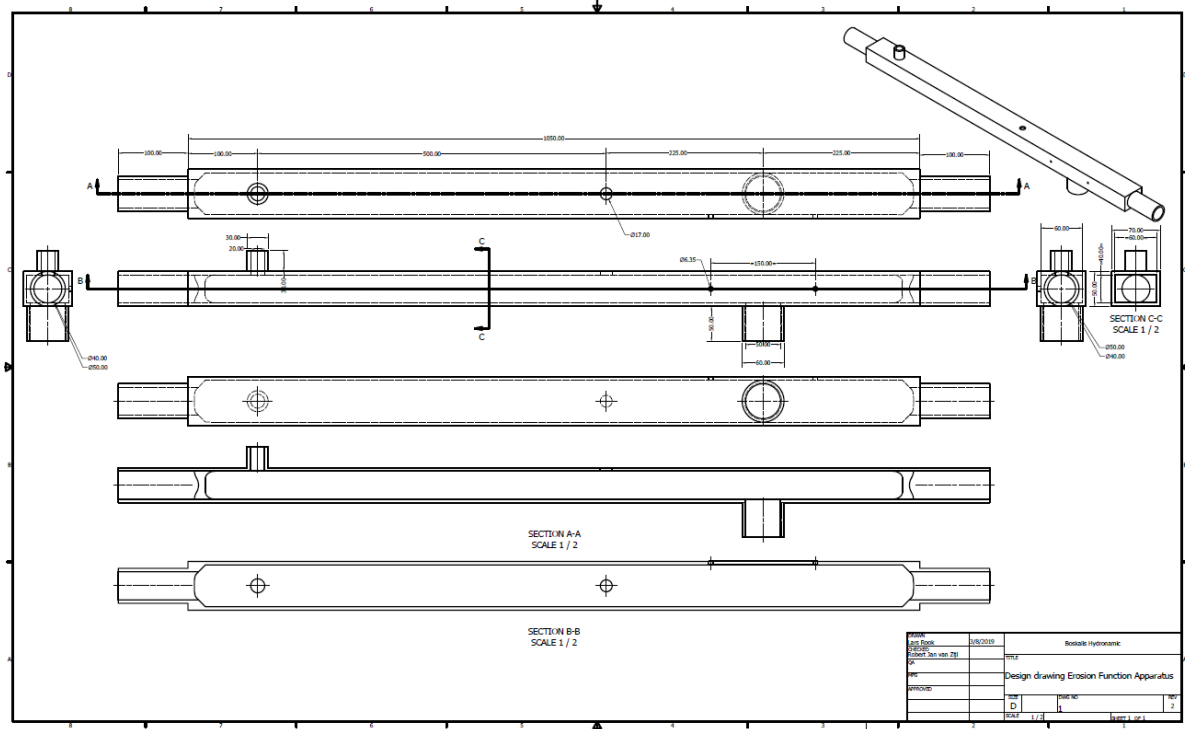


Figure A.3: Flow tube erosion function apparatus

A more large version of the Design drawing of the EFA flow tube is given in appendix E. The drawing represent the following views of the tube:

- Top-right: 3D overview
- Top: Overview of top of tube
- 2nd from top: Cross-section over the length, one side
- 2nd from bottom: Cross-section over length, other side
- Bottom: Overview of bottom of tube

From this drawing the following items can be distinguished:

- Erosion flume
- Soil feeding mechanism
- Transition piece round/rectangular
- Pitot tube
- Polyflow connections

- Pvc connectors to valve
- Valves
- Filling cap

Now all individual parts will be discussed.

A.3.2. Erosion flume

This part discusses the design of the erosion flume, which is split in the design of the cross-section of the flow tube and the longitudinal design.

Cross-sectional design erosion flume

The erosion flume that has been designed has to be as small as reasonably possible so that the speed in the tube is as high as reasonably possible, without causing too much resistance for the pump. Therefore a certain balance must be found. However, decreasing the cross-sectional area of the tube will also result in a sample size that decreases. It would be preferable however to have the sample size as large as reasonably possible. Therefore, to increase the speed as much as possible without limiting the sample size the decision was made to use a rectangular cross-section. This way a compromise is made between letting the flow speed be as high as possible and letting the sample be as large as possible.

To determine how wide the tube can be there was first looked what a normal diameter for a soil sample is. This is convenient because using a normal diameter soil sample would result in the possibility of using standard equipment for sample preparation. By looking in the laboratory of Boskalis it became apparent that most soil samples are either 38 mm or 50 mm in diameter. If one also leaves some space on either side of the sample in the flow tube to limit the unwanted boundary effects the tube width easily becomes 60 or 70 mm. To then get a proper speed (around 4 m/s) the tube must be 50 or 40 mm high respectively. However the combination 70 mm wide 40 mm will give trouble when connecting the round hose from the pump to the longitudinal flow tube (the hose has a diameter of 2.5"). That is why there was chosen to have a pipe which is 60 wide and 50 mm high.

Length longitudinal flow tube

The length of the flow tube must be designed in such a way that the transition from a round tube to a rectangular tube at the beginning and the end must not lead to an unstable flow regime at or near the sample. This means that the influence zone of these transitions must not extend into the zone where the pitot tube, the polyflow connections and the sample are. This is absolutely critical because it is necessary to have a stable flow regime to properly measure the speed in the tube, but also to measure the pressure differential over the tube and to let gradual erosion occur.

To get a first estimate of the length that is needed to get such a smooth transition a rule of thumb is used which is provided by Battjes (2002). This states that such a smooth transition is possible if a length is used that is 10 times the equivalent diameter. For the exit length there is stated that this is less, but not how much, therefore the author guesses this is about a third. This would mean that there should be at least 60 centimeters of entry length and 20 centimeters of exit length which has been used in design. To prove this a proof of design has been performed in the next part by using computational fluid dynamics software of which the results are given in section A.6. Not only a proof of design has been performed, but also a sensitivity analysis.

A.3.3. Soil Feeding mechanism

In the design for the EFA it is necessary to have some sort of soil feeding mechanism. This mechanism should be able to place a sample in the flume, and let the sample protrude in flume for 1 millimeter. This means that the soil mechanism should conform to the following requirements:

- The soil sample should easily be reached
- The protrusion should be able to be set accurately
- The soil sample ought to be placed and removed with no damage to the sample

To enable the sample to be easily reached it is deemed to easiest to use a screw-cap. However, when discussing the design with the supplier, they stated that it is not preferable to do this in acrylic. The reason for this is because it would need to be custom made, which is very expensive, but also the acrylic thread would deteriorate relatively quick. The solution therefore is to glue an acrylic tube to the erosion flume (inner diameter 50 mm, with an opening in the base of the erosion flume) and glue a more robust PVC tube (with an inner-diameter of 60 mm) with a screw-cap base over this. A detailed design drawing of this part is given below in figure A.4. Further, a photo of the result is given in Appendix H. This then concludes the part that allows the sample to be placed in and out of the EFA. However, this is not the full soil feeding mechanism, there is also a part that is supposed to contain the soil sample.

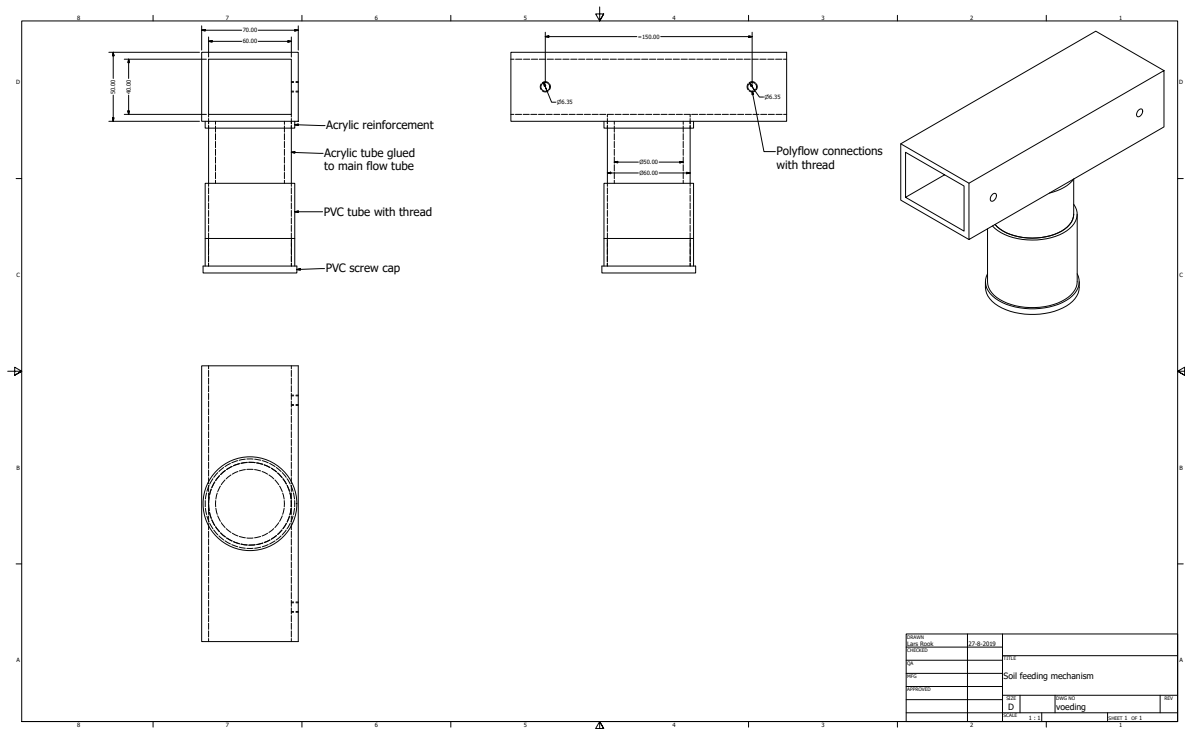


Figure A.4: Soil feeding mechanism EFA

A full-page version of this design can be found in Appendix E

To properly contain the soil sample a so called "soil container" is necessary to be able to place the sample without any damage. Further the length of the tube with screw-cap mechanism requires a platform to enable the sample to protrude in the erosion flume. Also the use of such a soil container should prevent the sample being flushed away in its entirety which was something observed in the first tests (as will be discussed in chapter C. A design drawing of the part is given below in A.5. Finally, a picture of the soil container and soil feeding mechanism is presented in appendix B.

This then concludes the design of the soil feeding mechanism.

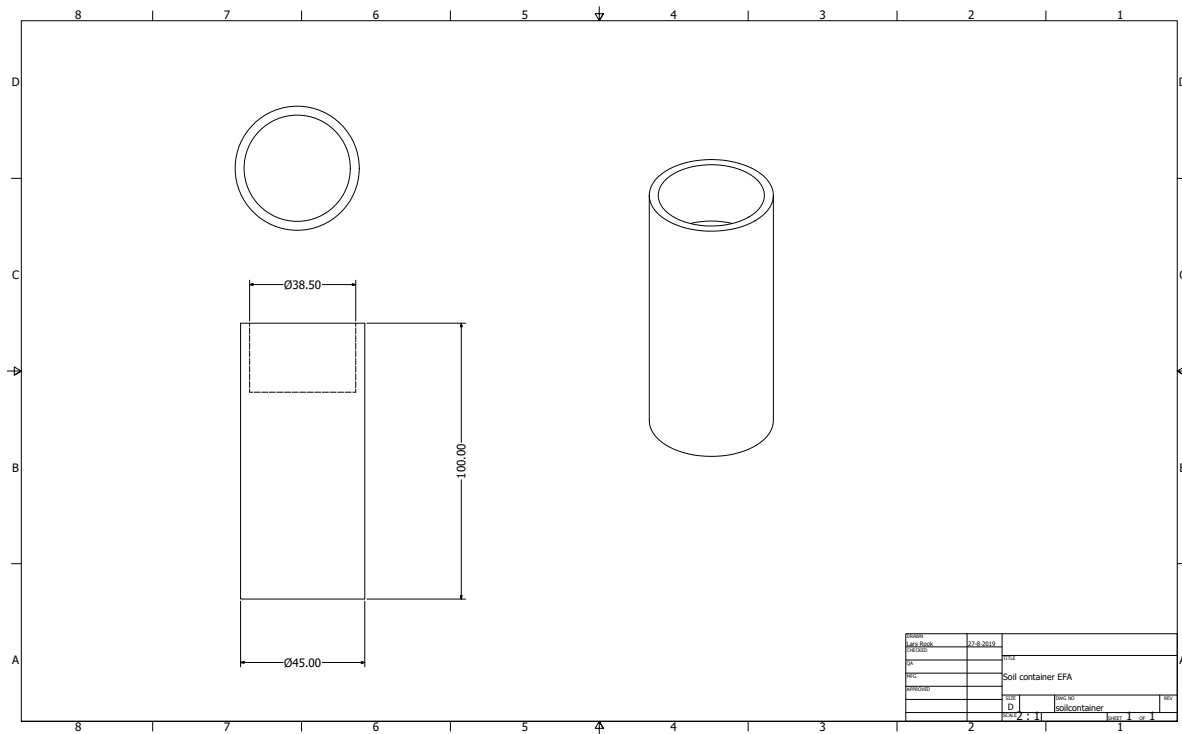


Figure A.5: Soil container EFA

A.3.4. Transition piece round/rectangular

There are 2 transition pieces from a round tube to a rectangular tube present in this design. This is because there is a round output from the pump which must be converted to a rectangle. Then at the end there is a similar transition in order to let the water flow back in the reservoir.

This transition consists of the following parts:

- The transition pieces to gradually change flow
- The connection of the round tube to the rectangular tube
- The PVC connection piece to add the valve
- The valve

For the acrylic parts (i.e. the transition pieces and the connection of the round tube to the rectangular tube) a design drawing was made which is presented in figure A.6.

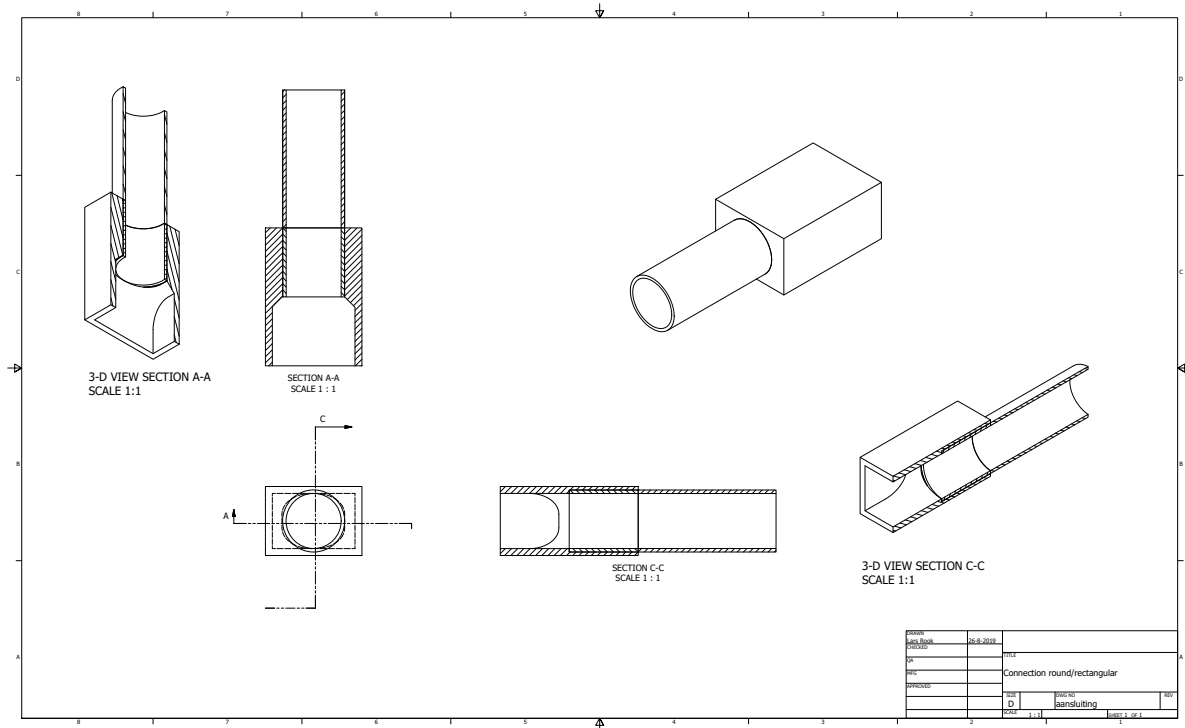


Figure A.6: Connection round tube to rectangular tube

Of the PVC connection piece and the valve no design drawing was made. Each item will now be discussed in turn. A full-page version of this design can be found in Appendix E, further a photo of the final result is presented in Appendix H.

Transition pieces to gradually change flow

To ensure the transition from round to rectangular to be as smooth as possible parabolic transition pieces have been made as can be seen in the design drawing above. After discussing this issue with the supplier it was found that this can be done by sawing several small cubes, drilling a cone out of the cube and then cutting the drilled out cube in four pieces which grants a very smooth transition if the are glued into the erosion flume. A photo of the result is given in Appendix H.

The connection of the round tube to the rectangular tube

Also a connection has been made from the round to the rectangular piece. However, this must be designed carefully because the tube is primarily 5mm thick acrylic sheet. To make this connection possible both ends of the main flow tube are solid acrylic blocks through which a cylinder is drilled. In this cylindrical opening a round tube can be placed and makes sure that it is connected in a sturdy manner to the main flow tube. This detail is presented in the design drawing above. Another important reason why this has been designed in this manner is because a (heavy-duty) valve will also be connected to this round tube causing a significant torque which must be carried by the erosion flume.

PVC connection to add the valve

Further a PVC connection was glued onto the acrylic plastic tube. This because the valve has a thread connection and as has been explained previously (with the soil feeding mechanism) it has been deemed not wise to use an acrylic thread connection because it is relatively weak. Therefore a 1-side threaded PVC connector is glued to the acrylic tube, and on the other side the valve is screwed in this piece. A photo of the result is given in Appendix H.

Valve

Finally a valve has been added at both ends of the set-up so that the erosion flume can be filled up with water gently (if both valves are closed) and thus that the sample will not erode away violently at the first gust of water from the pump. A photo of the result is also given in therefore designated appendix.

A.3.5. Pitot tube

In the design a pitot tube is used to measure the speed of flow. The pitot tube used is the same one as used in a previous set-up of Boskalis. To fasten this properly a screw connection is made with the erosion flume (which was not primarily foreseen, will be discussed in the next chapter). This screw connection is made out of acrylic because the accompanying fastening mechanisms that come with the pitot tube has an imperial tap that can not be regularly found in the Netherlands. Therefore, this piece has been custom-made and that can most easily be arranged with the supplier of the acrylic tube. It is deemed to be sufficient to make this connection out of acrylic because the amount of fastening and loosening of the system is extremely limited and it does not undergo large stresses during testing. The only reason for the screwed connection is that the pitot tube stays put even though there is a certain amount of over-pressure in the system. To then measure the speed there are 2 polyflow connections possible with the pitot tube. One measures the head without flow, the other with flow. This can then be measured with a rosemount, which will be discussed later. A design drawing of this detail is presented in figure A.7.

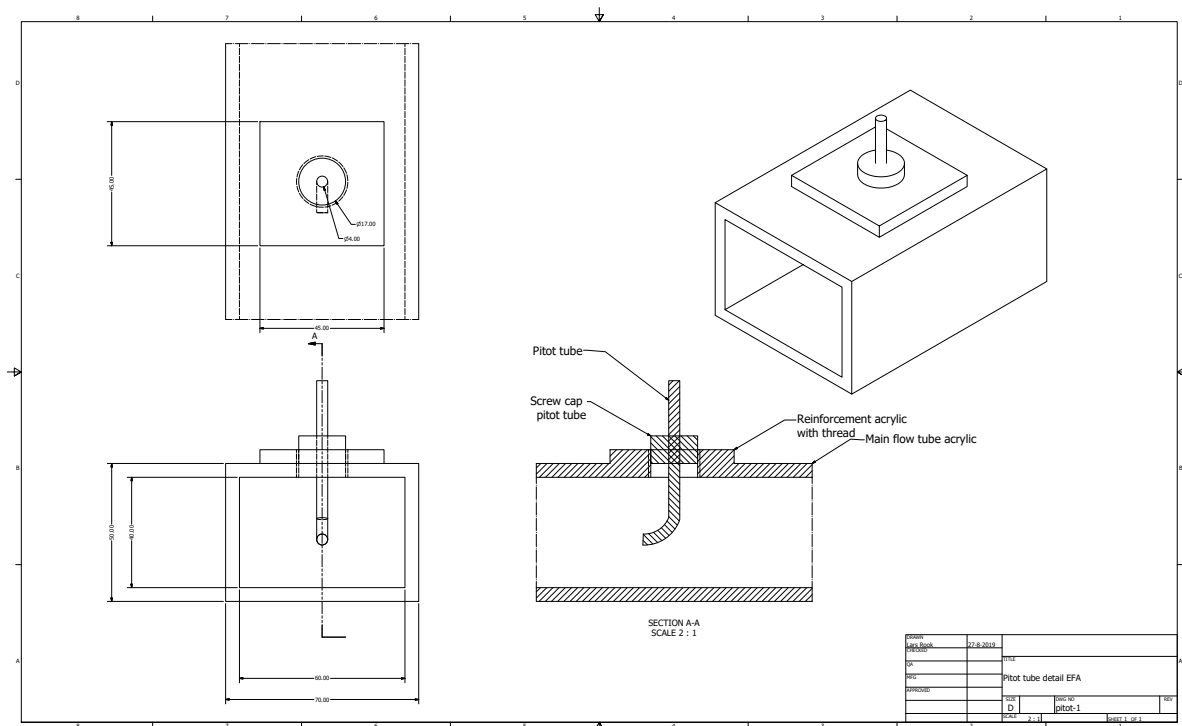


Figure A.7: Detail pitot tube

A full-page version of this design can be found in Appendix E.

A.3.6. Polyflow connection

Finally polyflow connections have to be attached in order to measure the pressure before and after the sample. These connections attach to polyflow tubes which are connected to the Rosemounts which measure the absolute or differential pressure. These connections also have an imperial thread and have to be custom made. This is also made out of acrylic, for similar reasons as with the connection with the pitot tube.

A.3.7. Filling cap

A filling cap has been added to the design so that if the valves in the design are closed the main flow tube can be filled with water in order to prevent erosion of the sample upon the first gust of water. The filling cap itself is made out of PVC because it has to be opened frequently and thus can not be made out of acrylic. This means that the cap is glued over an acrylic tube in order to connect it properly. A design drawing of this detail can be found below.

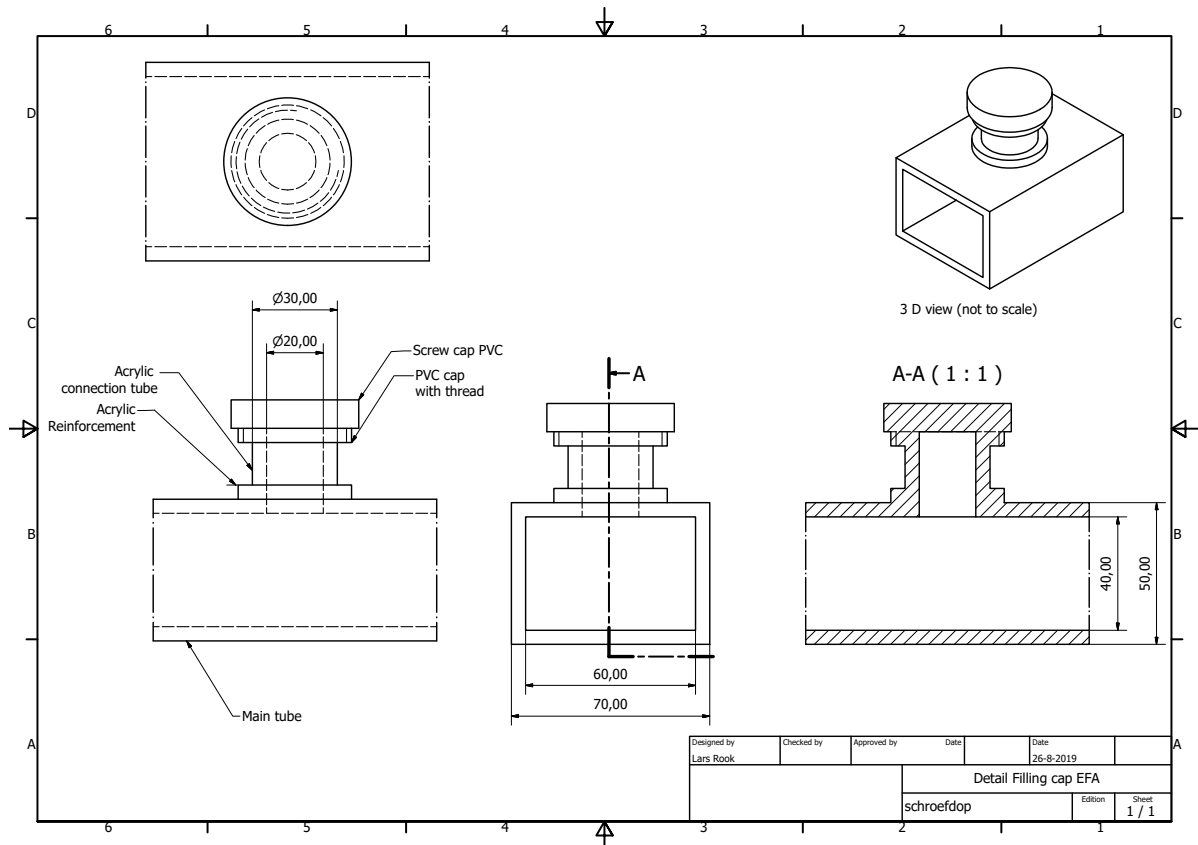


Figure A.8: Filling cap

A full-page version of this design can be found in Appendix E and a photo of the final result can be found in appendix H.

A.4. Sensors

In this design sensors are used to measure the speed, the absolute pressure in the tube and the differential pressure over the sample.

The speed is measured because it is an easy way of correlating the erosion rate to another parameter and it can be fairly easily measured using the right equipment. The absolute pressure in the tube is measured in order to monitor if the acrylic tube is not getting stressed too much as well. This data also gives the opportunity to verify if the results from the CFD modelling and the real thing are similar. Further the differential pressure over the sample is measured because it is a good way of estimating the shear stress the soil is encountering.

To measure this use has been made of the following equipment:

- 2 Rosemount 3051S1CD3A (Differential pressure)
- 1 Rosemount 2088A2S3 (Absolute pressure)
- 1 OPTO 22 datalogger box

Further, also data-logging software has been used. In this section the way these devices work is briefly explained as well as the manner they are connected to the system.

A.4.1. Differential pressure Rosemount

This Rosemount is used for measuring differential pressure and can be used to measure differential pressures up to 2.48 bar. One of the Rosemounts is used to measure the pressure difference over the pitot tube. The pitot tube here has 2 outputs through which water can flow. These outputs are then connected to the Rosemount with polyflow tubing and connectors. The other Rosemount measures the pressure differential over

the sample and is connected by tubes and the specially made polyflow connections in the flow tube of the EFA.

Now a brief explanation is given of how the Rosemount works. The Rosemount functions by containing 2 chambers separated by an impermeable membrane. In one of these chambers the pressure will be higher than the other causing the membrane to deform causing a certain strain. This strain is measured and then converted to a certain pressure differential.

This pressure differential is then converted to a signal which the Rosemount then sends to an OPTO 22 measurement box which can then be connected to a computer. The signal the Rosemount gives is in the range of 4 to 20 mA. Here 4 mA is the lower bound of operation, 20 mA the upper bound of operation with a linear relationship in pressure versus power output. Further, these limits of operation can also be set in order to maximize the resolution of the measuring data. For instance, the Rosemount connected to the pitot tube is set to work in the range between 0 and 1 bar differential pressure and the Rosemount measuring the differential pressure before and after the sample is between 0 and 0.1 bar.

A.4.2. Absolute pressure Rosemount

This Rosemount is used to measure the absolute pressure (with respect to 0 bar, not air pressure). It is connected to the first polyflow connector and is set to work between 0 and 4 bar absolute air pressure. It works by the same principle as the differential pressure Rosemount, however 1 chamber is under vacuum in order to measure the absolute pressure. In order to measure the over-pressure one has to compensate for the air pressure. This is done by letting the datalogging start before the erosion flume is filled with water. Then the normal air pressure is known when one is working out the data.

A.4.3. OPTO 22 datalogger box

An Opto 22 datalogger box has been used in this set-up in order to read out the electric signal sent out by the Rosemounts. This is then converted into a signal that can be read out by the computer. The computer is then equipped with datalogging software that can continuously register all rosemount data. This data will then be used in combination with the video recording data to analyze the soil's erosion resistance.

A.5. Miscellaneous parts

In this section the miscellaneous parts are discussed. These are the following:

- Reservoir
- Tubes
- Video recording equipment

Each part will now be discussed in turn.

A.5.1. Reservoir

A reservoir is used in this set-up. The reasoning of this is the following: using a reservoir makes it an open system, which has multiple advantages. An advantage for instance is that there is more water in the system, and therefore the water will get less murky during testing which is important to be able to film the erosion process. Also the eroded clay can hopefully settle down in the reservoir and does not continue rushing through the erosion flume. Further, it makes design much more easy: making closed systems means that everything has to be connected and be completely watertight (which is close to impossible). Finally, it also immediately a table to put the set-up on. A reservoir is used which is easily available in the laboratory of Boskalis and roughly contains 250 liter.

A.5.2. Video Recording equipment

Video recording equipment is added in order record how the erosion process takes place, as well as to initially measure how much the soil sample actually protrudes. This is done by taking a photo before the video recording and using photogrammetry. Then by recording the erosion process it can be looked back when exactly the millimeter of soil has been eroded away. It is also interesting to see if the samples erode away in a "chunk" fashion or rather a more smooth fashion.

A.5.3. tubes

In this design 2 tubes are included: 1 from the pump to the first valve connected to the erosion flume, and 1 other from the second valve back into the water reservoir. The tubes that are used are 2.5" (inch) because it is the output diameter of the pump. Also, it is also desirable to have the diameter in these tubes as high as possible, limiting the speed, to limit the resistance in this part of the set-up. It is also not really a problem limiting the speed here, because it is a long way away the soil sample that is being eroded.

A.6. Fluid Dynamics Modelling

In this section the results of the Fluid Dynamics Modelling will be discussed. This modelling has been done to aid the design process of the Erosion Function Apparatus. It has mainly aided in determining the dimensions of the apparatus so that the flow is stable in the zone where the clay is eroded, and not interfered by the transitions from a round tube to a rectangular tube. Further, it has been used to estimate the shear stress that the clay sample is being subjected to during testing as well as determining the pressures that occur in the tube. The results from this modelling can then be compared to the laboratory results: in the EFA the absolute water pressure is being measured before the soil sample and the pressure differential before and after the sample is being measured. These results can also be derived from the CFD modelling. Finally, also a precise speed profile can be derived from the CFD modelling.

This appendix will touch the following topics:

- Starting points and method
- Modelling results to prove design Erosion Function Apparatus
- Modelling results with different speeds
- Sensitivity analysis

A.6.1. Starting points and method

To model the fluid dynamics there has been chosen to use a quite common, intuitive program to model this, namely Autodesk CFD. To use this program a geometry must be imported which is made in another Autodesk program (Autodesk Inventor) after which the type of fluid, material constraining the fluid, boundary conditions and initial conditions must be implemented. Then the model calculates the flow conditions dependant on space and time.

Autodesk CFD is run by using a finite element modelling scheme. The general governing equations that is used for fluid flow is the Navier-Stokes equation Autodesk CFD (2017) (heat transfer is not considered in this problem). The Navier-Stokes equation is as follows:

$$\frac{\partial \rho}{\partial t} + \frac{\partial \rho u}{\partial x} + \frac{\partial \rho v}{\partial y} + \frac{\partial \rho w}{\partial z} = 0 \quad (\text{A.1})$$

Generally speaking the equation says that a change in the amount of momentum has to be compensated by a change in pressure and the dissipating viscosity forces. In order to limit the calculation time a different technique.

This main equation can then be split in 3 equations for the x, y and z axis respectively:

$$\rho \frac{\partial u}{\partial t} + \rho u \frac{\partial u}{\partial x} + \rho v \frac{\partial u}{\partial y} + \rho w \frac{\partial u}{\partial z} = \rho g_x - \frac{\partial p}{\partial x} + \frac{\partial}{\partial x} [2\mu \frac{\partial u}{\partial x}] + \frac{\partial}{\partial y} [\mu (\frac{\partial u}{\partial y} + \frac{\partial v}{\partial x})] + \frac{\partial}{\partial z} [\mu (\frac{\partial u}{\partial z} + \frac{\partial w}{\partial x})] + S_\omega + S_{DR} \quad (\text{A.2})$$

$$\rho \frac{\partial v}{\partial t} + \rho u \frac{\partial v}{\partial x} + \rho v \frac{\partial v}{\partial y} + \rho w \frac{\partial v}{\partial z} = \rho g_y - \frac{\partial p}{\partial y} + \frac{\partial}{\partial x} [\mu (\frac{\partial u}{\partial y} + \frac{\partial v}{\partial x})] + \frac{\partial}{\partial y} [2\mu \frac{\partial v}{\partial y}] + \frac{\partial}{\partial z} [\mu (\frac{\partial v}{\partial z} + \frac{\partial w}{\partial y})] + S_\omega + S_{DR} \quad (\text{A.3})$$

$$\rho \frac{\partial w}{\partial t} + \rho u \frac{\partial w}{\partial x} + \rho v \frac{\partial w}{\partial y} + \rho w \frac{\partial w}{\partial z} = \rho g_z - \frac{\partial p}{\partial z} + \frac{\partial}{\partial x} [\mu (\frac{\partial u}{\partial z} + \frac{\partial w}{\partial x})] + \frac{\partial}{\partial y} [\mu (\frac{\partial v}{\partial z} + \frac{\partial w}{\partial y})] + \frac{\partial}{\partial z} [2\mu \frac{\partial w}{\partial z}] + S_\omega + S_{DR} \quad (\text{A.4})$$

These equations basically the same as equation 3.1, but also has 2 sink terms S_ω and S_{DR} which are in there to account for rotating axis systems and non-homogeneous resistance terms.

One last important thing to note is the way in which there is dealt with turbulent flow. To properly model turbulent flow it is usually necessary to model with very small finite elements and time-steps. However, this would cause the calculation time very much and therefore there has been chosen to use time-averaged equations. This means that the speed is modelled as a 'mean speed' with a fluctuating value that is calculated with relatively small time steps.

A.6.2. Modelling results at different speeds

Then the fluid dynamics model is runned at the different speeds that the EFA will run. By doing this the shear stress at the sample can be estimated more accurately as well as the speed that will be measured at the pitot tube.

This led to the results given in table A.1.

Flowspeed v (m/s)	Shearstress at soil (Pa)	Pressure before sensor (Pa)	Pressure after sensor (Pa)
0.3	1.8	214	194
0.6	4.5	795	741
1.0	9.0	2130	2000
2.0	22.3	8280	7900
3.0	37.8	18900	18100
5.0	69.9	67500	65500

Table A.1: Shear stress development under different flow speeds CFD modelling

Discussion on results It is clear from table A.1 that the pressure drop that is measured before and after the sample is not merely due to the shear stress the sample is experiencing, but also due to the wall friction and turbulence that is occurring in the tube. Therefore it is very important to measure, ab initio, what the initial pressure drop is due to wall friction and turbulence (without a sample being present). Then it is able to measure what the extra pressure drop is due to the sample and is a good way of setting a baseline of the pressure drop.

Something important to note here is that the shear stress at the sample seems to grow less rapidly at increasing speed than the pressure drop over the sample. This can also be seen in A.9.

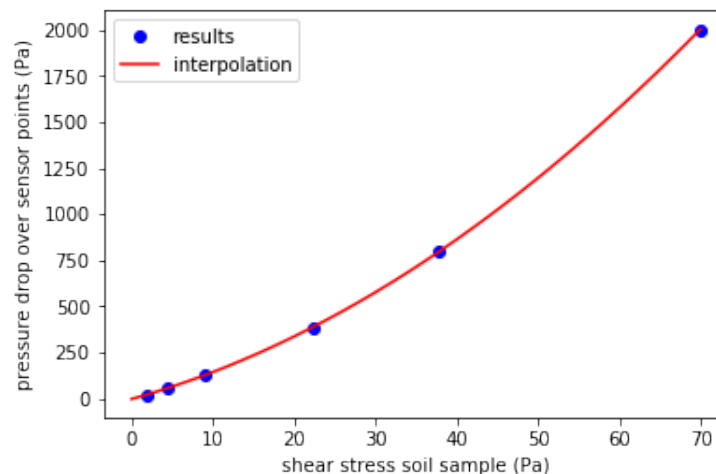


Figure A.9: Shear stress and pressure drop CFD modelling

N.B. It is known that pressures are being plotted, which should not ideally be done, but because both the area of the flow tube and the sample are identical this does not cause a significant difference in the type of relationship between data.

There seems to be a very good quadratic fit between this data, which can be explained well. As explained in D.3 the shear stress is the derivative of the velocity profile. It is known that the resistance (and if the area of a tube remains constant along its length) the pressure drop in a tube is quadratic correlated to the velocity (and thus the shear stress that the sample experiences). Because of this good fit, using this correlation to estimate the shear stress at the sample is also a good idea.

A.6.3. Sensitivity analysis

Finally a sensitivity analysis is carried out to see the effects of the following changing boundary conditions:

- Protrusion difference
- Size difference diameter

Protrusion difference There was chosen to differentiate in the protrusion because it is more than plausible that it is not possible to let the sample protrude exactly 1 millimeter, but rather protrudes e.g. 1.1 or 0.9 millimeter. It is then useful to know if this has a significant effect on the shear stress the sample experiences and the pressure in the tube. To this effect there has been chosen to take the model at which the fluid flow is 5 m/s and differentiate the protrusion from 0.8 to 1.2 mm in steps of 0.1 mm. The results of this analysis are given in table A.3.

Protrusion (mm)	Shearstress at soil (Pa)	Pressure before sensor (Pa)	Pressure after sensor (Pa)
0.8	68.6	67600	65700
0.9	68.3	67100	65200
1.0	69.9	67500	65500
1.1	69.3	67200	65300
1.2	69.0	62700	60700

Table A.2: Sensitivity analysis w.r.t protrusion

It can be seen that the change in shear stress and pressure is very limited and thus can be seen as constant. It is believed that these slight differences are due to either small numerical errors or slight perturbations due to the turbulence. If it is then well known what the protrusion is exactly the error in protrusion can be accounted for when calculating the erosion rate. To accurately know what the protrusion is a Go-Pro camera is used in combination with photogrammetry.

Sample diameter difference

Further a difference in sample diameter has been analyzed. This because it is impossible to get a sample with an exact diameter of 38 mm during preparation. There will always be some difference in the diameter of the sample. Therefore at a speed of 5 m/s there is taken a look if the shear stress at the sample differs significantly or the pressure drops vary significantly.

This resulted in the following:

Protrusion (mm)	Shearstress at soil (Pa)	Pressure before sensor (Pa)	Pressure after sensor (Pa)
37	66.8	66000	64200
38	69.9	67500	65500
39	71.3	69500	67400

Table A.3: Sensitivity analysis w.r.t diameter

From the sensitivity analysis with the diameter as varying parameter can be concluded that the shear stress varies unfortunately, albeit it is limited. This means that it is very important to try and get the sample diameter as close as possible to 38 millimeter. Further, the pressure drop that is associated with the difference in sample diameter is more or less quadratic (but only very crudely).

B

Build Erosion Function Apparatus

In this chapter several pictures are shown with the end result of the set-up as well as a discussion what happened during construction that differed from what was initially thought. This means that the chapter will consist of the following parts:

- Photo's of the results
- Discussions on what was different during the build

But first a start will be made with the end result of the set-up.

B.1. End result set-up

A final overview picture of the set-up can be found below in figure B.1. Letter have been added to the figure so that below the figure an explanation can be made of what part is what.

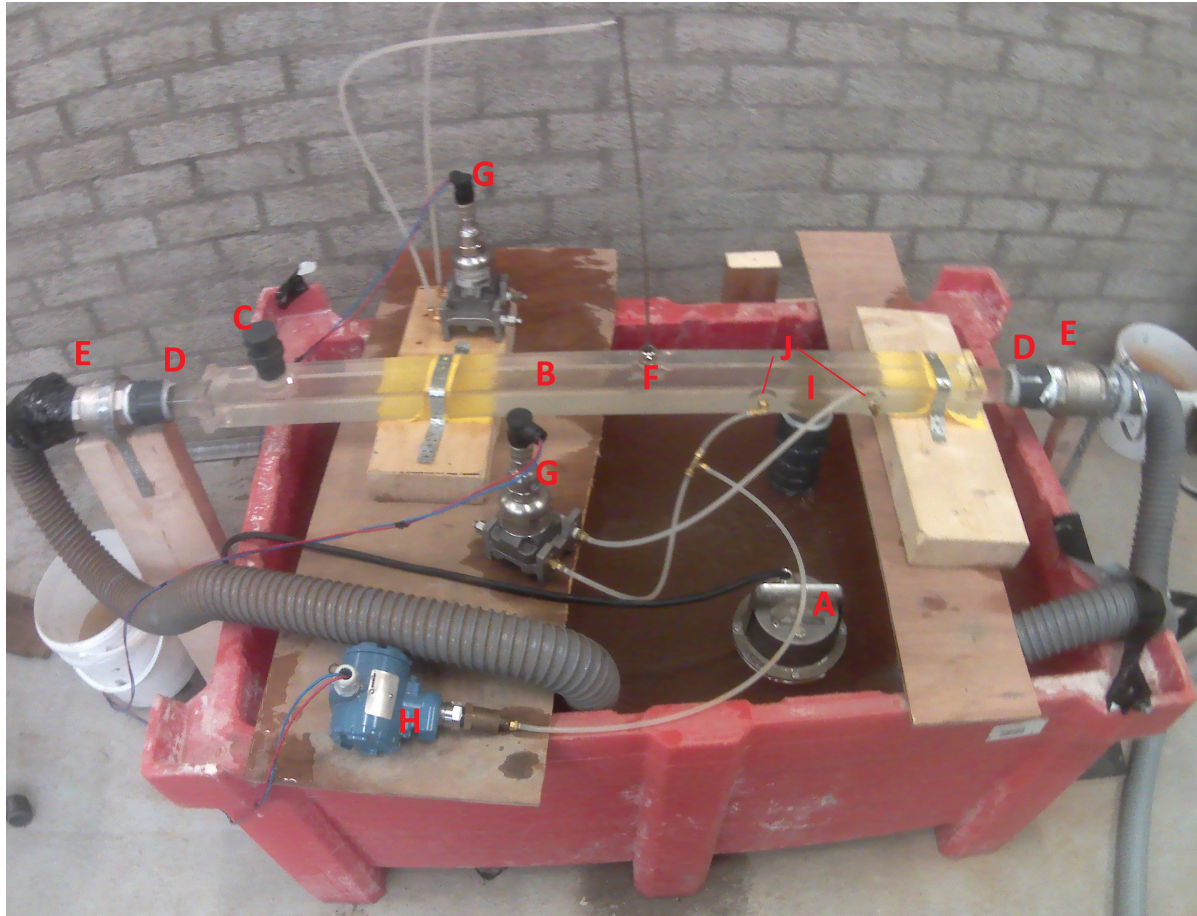


Figure B.1: End result Erosion Function Apparatus

In figure B.1 the following elements can be recognized:

A: Pump	F: pitot tube
B: Main flow tube	G: Differential pressuremeter (Rosemount)
C: Filling cap	H: Absolute pressuremeter (Rosemount)
D: Transition round/rectangular	I: Soil feeding mechanism
E: Valves and hoses	J: Polyflow connections

This photo in full-page size is given in Appendix H as well as further close-up photos. Now there will be continued with a section describing the unexpected effects during the build.

B.2. Unexpected events during the build

This section describes the unexpected events during the build, and has been written to describe what assumptions taken upfront were wrong and to fully learn from them.

The following unexpected events took place during the build:

- Change of pitot tube detail
- Leakage near the valves
- Change of soil container in soil feeder

These are now briefly discussed.

B.2.1. Change of pitot tube detail

The pitot tube detail as described in section A.3.5 was not as initially designed. This because there are 2 types of pitot tubes at Boskalis: 1 with a screw cap, and one with a rubber plug. First there was thought to use the one with a rubber plug. This because it would save making an expensive detail and one would need only a hole (diameter 17 mm) in the top of the erosion flume in which one presses a plug with the pitot tube. However, when conducting the first couple of tests it proved that at high speeds the plug shoots out and massive water flow occurs. This is due to the over-pressure that occurs in the erosion flume. Further the protrusion of the plug in the erosion flume interrupted the fluid flow in a bad way.

The solution for this is changing to the pitot tube with a screw cap. To make this happen an extra acrylic reinforcement piece was made with the special (imperial) thread and glued to the erosion flume. Further, the acrylic reinforcement is made sufficiently thick so that the plug that fastens the pitot tube does not protrude in the erosion flume.

When this was done it worked as it should.

B.2.2. Leakage near the valves

When connecting the hoses to the nozzle (which is connected to the valve) an unexpected large amount of leakage occurred. This is because the hoses that were bought are extremely smooth on the inside. This was done in order to limit the amount of resistance that the hoses cause. However, this means that the hoses were never intended to be used with a significant amount of over-pressure which they are however. This also means that the nozzle and the hose only have a limited amount of grip on each other. Therefore at the first tests the hoses slip of the nozzle and a huge amount of water leaked. This was resolved by gluing the 2 parts together. This resolved the issue mostly, however a small amount of leakage remains (roughly 10 liter per hour) which has been deemed to be no problem at all.

B.2.3. Change of soil container

First the idea for the soil container was to get a wooden round bar that precisely fits in to the soil feeding mechanism (thus 45 mm diameter) long enough too raise the clay into the erosion flume, but not too long. The idea then was to place pins in the top of the bar so that the clay has some kind of support. However trying this gave 2 problems: first the wood expands and came stuck in the flume. Secondly because the sample has a smaller diameter that the soil feeding mechanism there was a certain amount of flow around the sample. This caused that it was possible during one of the first tests that the sample was flushed away in its entirety.

To overcome this a soil container was designed as described in the previous chapter which has been made out of acrylic. This way there is no fluid flow around the sample and the material can not expand or retract.



Proof of Concept testing Erosion Function Apparatus

This chapter discusses the testing that has been performed in order to prove the design of the Erosion Function Apparatus. This will focus on the following aspects:

- Establishing a pumping curve
- System accuracy
- Repeatability of testing
- Protrusion effects
- Diameter effects
- Determining time-effects
- Validation of CFD modelling

First a pumping-curve will be established plotting the electrical frequency against the resulting flow rate in the flow tube. This is done to check if the performance of the pump is in accordance with the calculations made in Appendix F and to know upfront which operating frequency (roughly) corresponds to a certain speed. Secondly, from this data the accuracy of the measurement systems is determined, in order to know how accurate the measurement systems are. This has been done on 2 levels: the accuracy of the measurement system itself, and the accuracy of the entire EFA system.

After having determined the accuracy of the measurement systems, repeatability tests have been performed in order to see how similar the testing results will be with samples from the same proctor mold. This is very important to do, because if the testing results are non-reproducible, none of the results can be trusted at all. This has been tested by compacting clay at proctor density at its optimum water content, extracting 4 samples from the proctor mold and testing them all at the maximum speed. There has been chosen to test them at maximum speed because it is deemed to have the least reproducible results at high speeds (because granular failure is more likely to occur).

Also the effects of differing protrusion and differing diameter have been investigated. The reason for this is 2-fold: the first is to see how much the shear stresses and differential pressures change and thus how precise the sample diameter and protrusion must be during testing. Secondly it can be used to validate the results from the CFD modelling. To this end 3 samples of granite are prepared with diameters of 36,38 and 40 mm. These are then protruded 1 mm, 2mm and 4 mm in the flume to see how the pressure differentials change.

Further an attempt has been made to validate the CFD results based on the varying protrusion/diameter data. There are 2 main reasons to do this:

1. If the testing data is fairly similar it can be proved that the flow regime is similar in the EFA to the model and therefore stable.

2. A more accurate representation can be used of the shear stress when discussing results. One must keep in mind that during testing only the pressure drop over the sample is measured, in other words it is possible to calculate the average shear stress over the sample and piece of the erosion flume. However, because the eroding sample is an obvious obstruction in the flow tube it is to be expected that there is a higher shear stress at the sample than the average shear stress. In the CFD model it is possible to get a shear stress result from the top of the sample itself and obtain the pressures from the points where in the EFA the polyflow points are installed to determine the average shear stress. It is then possible to compare the pressure drops from the model and actual pressure drops. If these are similar the "actual" shear stresses at the sample can be used when establishing the erosion curves of the respective clays.

And last but not least also the effect of time on the testing results is investigated. In literature concerning the use of the EFA only 1 millimeter is eroded of a clay sample at a given velocity and a cap is set on the time that can take (1 hour). However, it is definitely possible that this erosion rate may differ due to prolonged (or shorter) time frames of testing.

Now the outcomes of each type of test is discussed.

C.1. Pumping curve

The pumping curve has been determined in order to check if the expected pump performance as calculated in Appendix F is met. This has been determined by letting the pump run with a granite sample of 38 mm protruding 1 mm and measuring the results of the pitot tube. This way it is possible to correlate the speed to the frequency of the pump. Also the pressure drop over the polyflow points as well as the absolute pressure are measured. This data is also used in order to validate the CFD modelling. The results of determining the Pumping curve is given in figures C.1 C.2 and C.3.

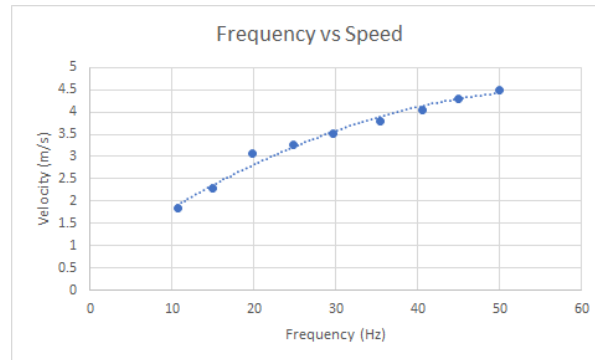


Figure C.1: Velocity in flow tube as a function of the pump operating frequency

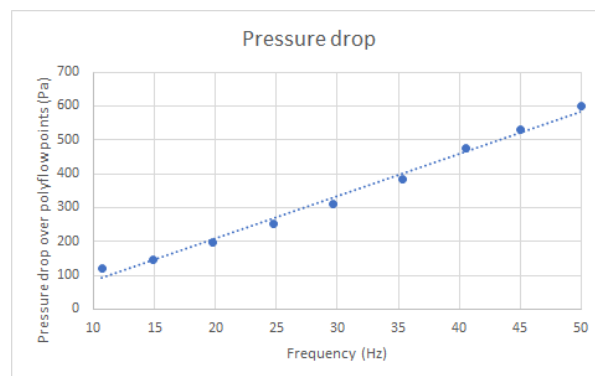


Figure C.2: Pressure drop over polyflow points

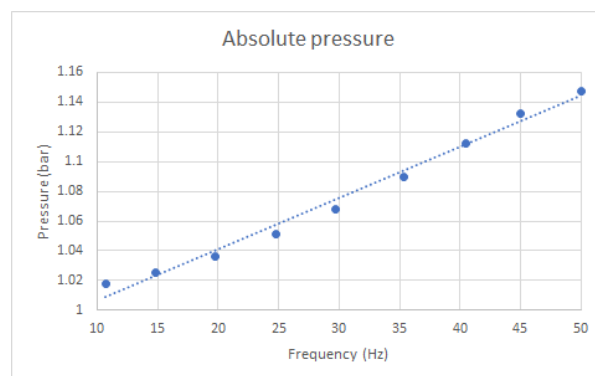


Figure C.3: Absolute pressure as a function of pump operating pressure

From figure C.1 there can be seen that a maximum velocity of 4.5 m/s can be reached, slightly above the estimated 4.4 m/s as stated in Appendix F meaning that the pump has enough capacity. This is especially the case when comparing what shear stresses occur during overflow of dikes. As stated in Appendix D shear stresses occur up to 40 kPa during overflow. However, in this test average shear stresses of:

$$\tau_{average;max} = \frac{\Delta P * (h * b)}{(2 * h + 2 * b) * L} = \frac{600 * (0.05 * 0.06)}{(2 * 0.05 + 2 * 0.06) * 0.15} = 54.9 Pa \quad (C.1)$$

Please also note that this is an average shear stress, the actual shear stress at this sample is because it is an obstruction in the flume. This means that the actual shear stress is even higher, meaning that the EFA is more than capable of working properly. The detailed testing forms are given in Appendix I

C.2. System accuracy

This section discusses system accuracy. This measurement system accuracy consists of 2 parts: the accuracy of the Rosemount itself, as well as the accuracy of the entire set-up. Concerning the first, this involves connecting the Rosemounts up to an ultra-sensitive measurement system subjecting the Rosemount to different pressures and measuring its response. By doing this one knows what the absolute error of the Rosemount is (and compensate for it), as well as the relative measurement error. This gives an idea how accurate the reading is.

The second part involves measuring how stable the system is; one has to realize that the Rosemount is connected with polyflow tubes to the EFA, possibly inducing extra errors. But it is also very reasonably possible that the combination of the pump, the frequency regulator and flow tube will result in not fully stable conditions. It is important to know how much the measurement error and unstable flow conditions could influence the results. This says then something about the quality of testing.

Rosemount accuracy

The Rosemount accuracy has been measured by very accurately using equipment subjecting the rosemount to various very accurately controlled pressures and very accurately measuring the responses. This way the accuracy of the system is known. The results are given in tables C.1, C.2 and C.3.

Abs rosemount		Diff rosemount		Pitot	
Bar input	Error (%)	Bar input	Error (%)	Bar input	Error (%)
0	-0.022	0	-1.596	0	-0.130
0.4	0.010	0.1	0.358	0.1	-0.046
0.8	0.003	0.2	0.106	0.2	-0.036
1.2	0.005	0.3	0.134	0.3	-0.018
1.6	-0.007	0.4	0.225	0.4	-0.002
2	-0.006	0.5	0.191	0.5	-0.011
2.4	-0.012	0.6	-0.321	0.6	-0.003
2.8	-0.017	0.7	-0.244	0.7	-0.013
3.2	-0.032	0.8	-0.208	0.8	-0.011
3.6	-0.031	0.9	-0.066	0.9	-0.016
4	-0.028	1	-0.097	1	-0.017

Table C.1: Response Absolute pres-Table C.2: Response Differential Table C.3: Response pitot rose-
 sure Rosemount pressure Rosemount mount

From this it can be seen that the pitot rosemount as well as the absolute pressure rosemount are extremely accurate. The differential pressure rosemount is a bit less so however, however, when carefully looking at the data it is mostly a systematic error occurring rather than a fluctuating error which can therefore be compensated. In this case it is deemed sufficient.

System accuracy

Further the system accuracy has been determined as has been described above. To determine this the same data has been used as the data to establish the pumping curve. To determine the accuracy a running average was calculated over a period of 11 seconds which can be described in an equation as follows:

$$difference = \frac{R_t}{\sum_{t=t-5}^{t+5} R_t} * 100 - 100 \tag{C.2}$$

To determine this accuracy the data was used which measured the Rosemount responses when a 1 mm sample of 38 mm diameter was placed in the tube. Only the data that was sampled when changing from 1 speed to a different speed was excluded (because there were no stable readings then).

Doing this yielded the running average plots for the velocity in the flow tube, the differential pressure and the absolute pressure as described in figures C.4, C.5 and C.6 .

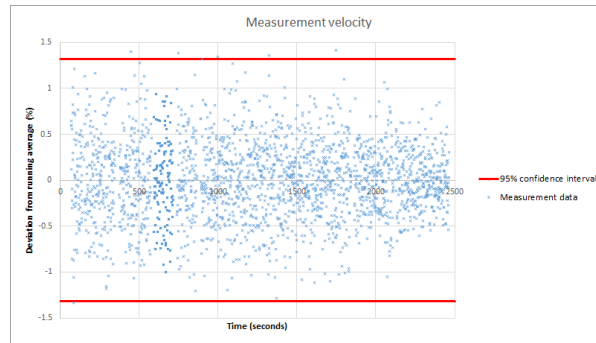


Figure C.4: Accuracy of velocity measurement

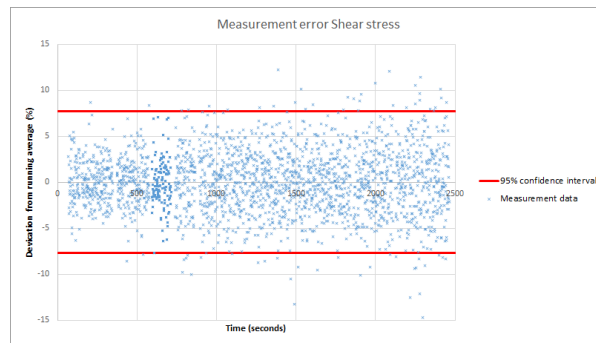


Figure C.5: Accuracy of shear stress measurement

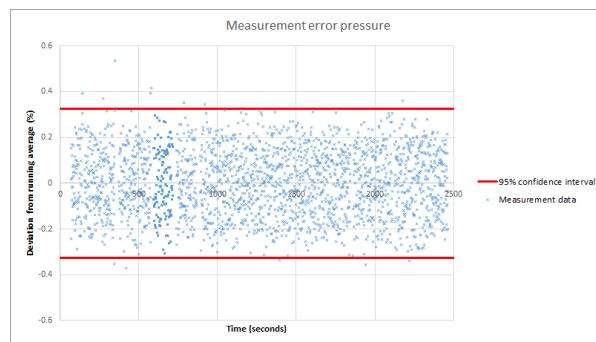


Figure C.6: Accuracy of pressure measurement

In the graph above one can see a point cloud of how much all different data points differ from the running average. From this a standard deviation can be calculated and a 95 % confidence interval can be calculated.

As can be seen in figure C.4 this confidence interval is 1.5% from either end of the running average. This means that all readings are fairly consistent and that the system can be considered accurate.

Considering the accuracy of the shear stress measurement in figure C.5 it can be seen it is less accurate. This is not surprising however, because this system is measuring a much lower pressure drop than the pitot tube and will therefore have a higher corresponding error. This error is plus or minus 6.5 % and is acceptable, considering the long-term averaging.

Finally, the pressure is measured very accurately and has a very narrow 95 % confidence range between -0.2 and 0.2 % of the mean measured pressure.

C.3. Differing protrusion

This section looks into the effects of differing protrusions into the erosion flume. This will likely cause a difference in measured pressure drop and it is important to see how sensitive the system is to such slight perturbations. This is important because then there is knowledge about how much the results can be trusted.

To measure the effect of a differing protrusion a granite sample has been used which protrudes 1, 2 and 4 mm in the flume and the measured shear stresses, speeds and absolute pressures are measured. These results are given in figures C.7, C.8 C.9.

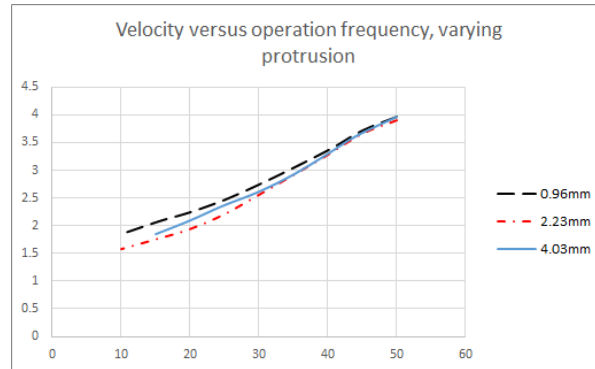


Figure C.7: Effect of protrusion on velocity

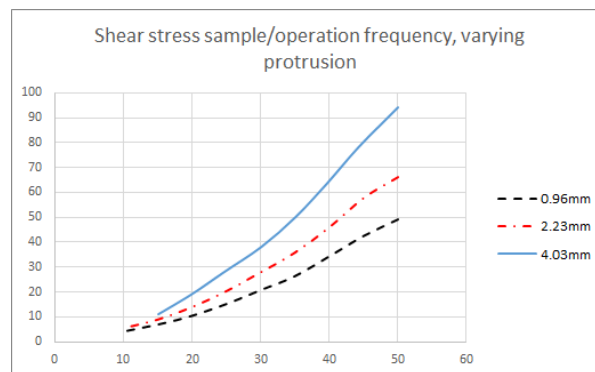


Figure C.8: Effect of protrusion on shear stress

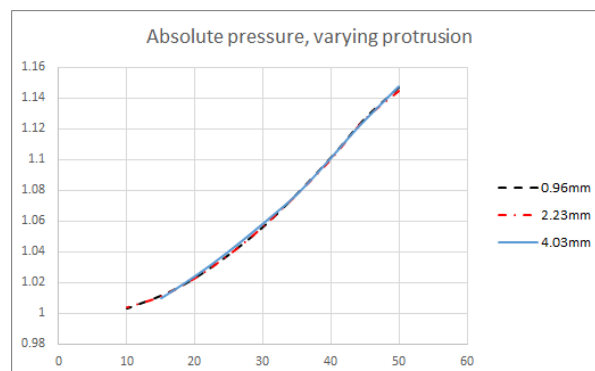


Figure C.9: Effect of protrusion on the absolute pressure

From these graphs it is clear that the protrusion has a very limited effect on the absolute pressure in the erosion flume and that the protrusion has a relatively limited effect on the speed in the erosion flume. This is of importance because it means that the EFA has been designed in a proper way, such that the pitot tube is in a very stable flow regime, and that the absolute pressure sensor as well. Finally, it is obvious that a

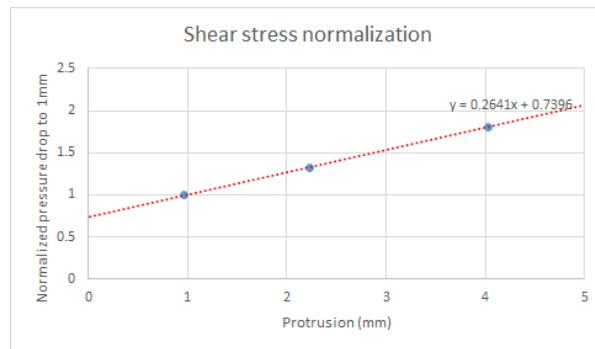


Figure C.10: Normalization with differing protrusions

varying protrusion has a significant effect on the average shear stress measured. This means that getting the protrusion as close as reasonably possible to 1.0 mm is very important.

Luckily however, it is possible to normalize these shear stresses taking the 0.96 mm as a baseline and it is observed that a very good fit is obtained. This fit is given below in figure C.10.

What can be taken away from this normalization curve is that it is very well possible to normalize this data, and that luckily this protrusion effect is fairly limited within range +/- 0.2 mm from 1 millimeter to a maximum of 5 % difference and can therefore be neglected.

However, when keeping in mind the proposed erosion curve in literature it is very undesirable to allow for larger differences in protrusion because the big difference in shear stress will result in a very different erosion rate. **Conclusion**

Based on the performed tests it can be stated that

C.4. Diameter effects

This section will look into the effects of differences in diameter of the soil sample which is being eroded. This has been done for similar reasons as the investigation looking into the effects of differing protrusions.

This has been done because during sample preparation it is very easily possible to have a slightly differing diameter (mainly larger diameter). In order to investigate this a granite sample of 38 mm was made, as well as one of 40 mm and finally also one of 42 mm. These samples were placed 1 mm in the EFA flume and the response of these "samples" were measured. These are then compared. This yielded the following results:

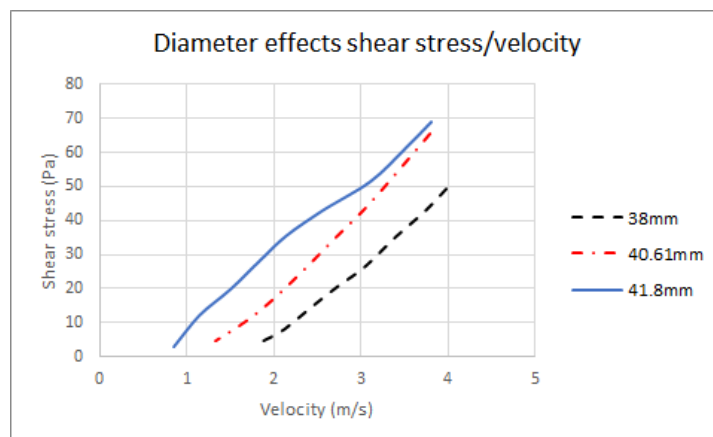


Figure C.11: Diameter effects on the shear stress/velocity relationship

From these graphs it can be seen that at the same pumping frequency the smaller diameter sample will endure a higher velocity in the flow tube and will sustain a lower average shear stress.

However, this is speaking about average shear stresses. There is no correction in these graphs however for the fact that the larger diameter samples have a higher surface area.

Taking into account the differing surface area the results are obtained presented in figures C.13 and C.14.

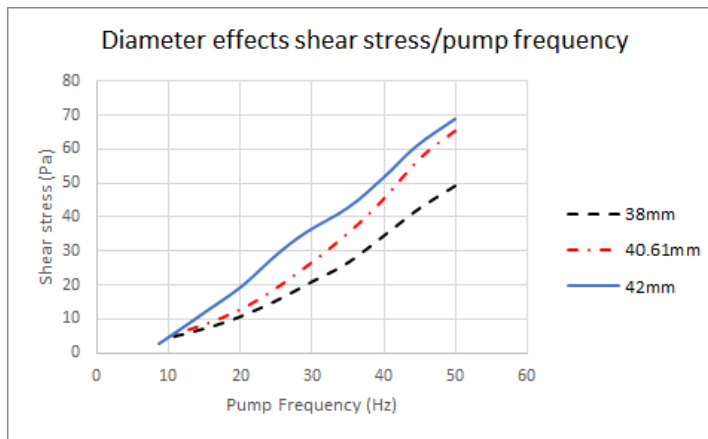


Figure C.12: Diameter effects on the shear stress/pump frequency relationship

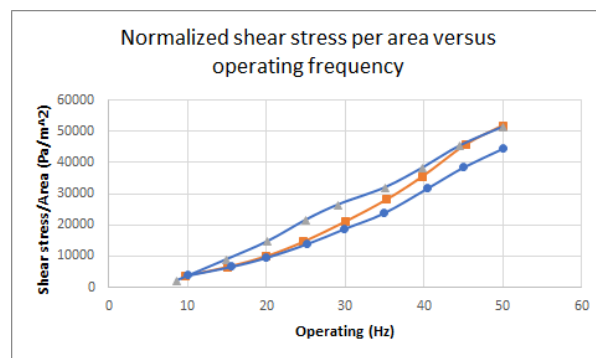


Figure C.13: Normalized shear stress versus operating frequency pump

Looking at these graphs it is obvious that when the shear stress is normalized for the area the shear stress is similar for a samples, regardless of their diameter.

Practically, this means that it is necessary to carefully measure the diameter of all samples before erosion testing starts and if there is a significant difference in the diameter of 38 mm a compensation must be made in the results. This means that when a comparison is made between shear stress and the erosion rate an adjustment must be made based on the area, as such:

$$\tau_{new} = \frac{\tau_{old}}{D^2} * 38^2 \tag{C.3}$$

Also, when correlating the erosion rate to the speed in the flow tube a correction must be made for the flow speed. This because a larger sample will have a similar normalized shear stress at a lower speed. This means that to correct a higher speed must be registered.

C.5. Time-effect testing

Scope Also tests have been performed to see what the effect is of differing the testing length. In the literature (Briaud (2001)) a maximum testing length of 1 hour is maintained, but it is certainly possible that the erosion of the samples does not occur in a perfectly linear fashion. This because during testing water will infiltrate the soil, saturating it and the making the soil weaker and easier to fail. Therefore, the time frame in which testing occurs is very important.

To test this effect the boom clay has been tested for 30 minutes, 1 hour, 2 hours and 4 hours and seen how much the difference in the calculated erosion rate is. There has been chosen for such long times because the boom clay will not always erode away within 1 hour, so it is important to see how much the erosion rate will change if the length of testing dramatically increases. If the erosion rate does not significantly change, it is still sufficient to use a time span of 1 hour.

Also the Kampen cat III clay has been tested, for 5, 10 minutes, 20 minutes and 30 minutes. These different time-frames have been chosen because the Kampen cat III clay is much less erosion resistant than the boom

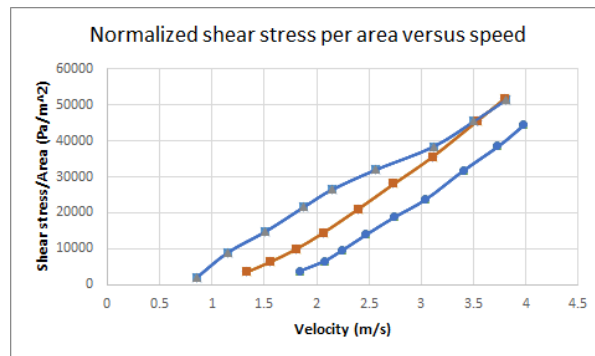


Figure C.14: Normalized shear stress versus velocity

clay. This test is performed slightly different than with the boom clay, the boom clay is so erosion resistant that it might not erode away in 1 hour, so it is important to know the erosion behavior develops over the time span of 1 hour. The category III clay does easily erode away within 1 hour. It is unknown however how the erosion of the sample will progress if after 1 millimeter is eroded away the erosion rate will change when subjecting the sample to a longer erosion period.

As discussed previously, it is suspected that the clay will erode away faster over time due to the infiltrating water. However, to properly put the results above in context it is good to know some kind of "infiltration failure limit". This can then properly explain why a certain time frame of testing can be justified.

To determine such a limit the sandcastle test is used as described in Appendix D. This test essentially involves putting a compacted soil sample in a bucket and timing how long it takes for the sample to fail due to the infiltrating water.

This overall leads to the following tests being performed in order to determine the time-effects:

- Sandcastle test on Boom clay
- Sandcastle tests on Kampen III clay
- Test Boom clay for 30 minutes
- Test Boom clay for 1 hour
- Test Boom clay for 2 hours
- Test Boom clay for 4 hours
- Test Boom clay for 6 hours
- Test Kampen III clay for 5 minutes
- Test Kampen III clay for 10 minutes
- Test Kampen III clay for 20 minutes
- Test Kampen III clay for 30 minutes

Now first the sandcastle test results will be discussed.

Sandcastle tests

To perform these tests compacted clay samples have been made in an identical fashion as for the tests performed with the EFA. These samples are then 50 mm tall and have a diameter of 38 mm. This then gives a good comparison to the samples put in the EFA. These samples are then put in a bucket and yielded the following results:

During testing the observation is made that the soil on the exterior is getting more and more wet and then slowly the exterior fails. It is also seen that the Kampen III clay fails in a much more brittle way, as also will be observed during testing. The Boom clay is failing in a much more gradual way, as only small flakes are falling off the sample over time. This is also an observation that will be seen during erosion testing in the

Clay type	Compaction Level	Water content (%)	time to failure (hours)
Kampen III	Proctor	Optimum	1
Kampen III	Modified Proctor	Optimum	3
Boom	Proctor	Optimum	24
Boom	Modified Proctor	Optimum	+/-500

EFA. Finally, it is also observed that the clays that have been compacted with a modified proctor have a much higher stand-up time compared to the same clay compacted at proctor density.

Later on the results of the sandcastle tests will be used when assessing the time-effect tests and when putting the results of all erosion tests into context.

Boom clay length testing

Time	Erosion rate (mm/hr)	Shear stress (Pa)	Velocity
30 minutes	0.55	67.5	4.27
1 hour	0.95	69	4.32
2 hours	1.62	71	4.39
4 hours	2.1	48.7	4.14

Kampen III clay length testing

Time (sec)	Erosion rate (mm/hour)	Shear stress (Pa)	Velocity (m/s)
30	103.2	63.4	4.28
60	110.7	70.5	4.34
120	150.8	61.6	4.36
240	300.2	72.4	4.24

C.6. Repeatability testing

Repeatability tests have been performed for quite a simple reason: to see how well reproducible the results of testing are and to see how large the confidence interval is of testing.

To do this 4 samples have been extracted from a proctor mold and tested to see how similar the results are. This has been conducted for both the Boom clay as well as the Kampen III clay. Both these clays have been compacted at proctor density at their respective optimum water content. Both clays have also been tested at their maximum velocity. There has been chosen to do this for both types of clay because there is the suspicion that the repeatability of the test will differ for the different clay types. It is suspected that Boom clay will have a higher repeatability than Kampen III clay because it has a less granular structure increasing its repeatability. This means that there are actually 2 types of repeatability: error in repeatability caused by the EFA and error in repeatability due to the soil. Therefore it is good to know how this repeatability will differ due to the varying combinations.

This means that the following tests will be performed:

Clay type	Compaction Level	Water content (%)	amount of tests
Kampen III	Proctor	Optimum	4
Boom	Proctor	Optimum	4

This gave the following results:

Clay type	Erosion rate (mm/hr)	Shear stress (Pa)	Velocity (m/s)
Kampen III	155	65	3.59
	126	120	3.51
	140	90	3.01
	143	95	3.76
Boom	27.4	48	4.22
	26.8	53.4	4.2
	26.7	44.1	4.19
	26.5	55	4.17

From these results it can be observed that the tests with the boom clay are fairly repeatable considering the erosion rate, shear stress and velocity that the tests take place. Considering the category III clay, the same holds, except that the ranges are considerably larger.

Conclusion

The tests are well repeatable, and therefore the results can be well trusted.

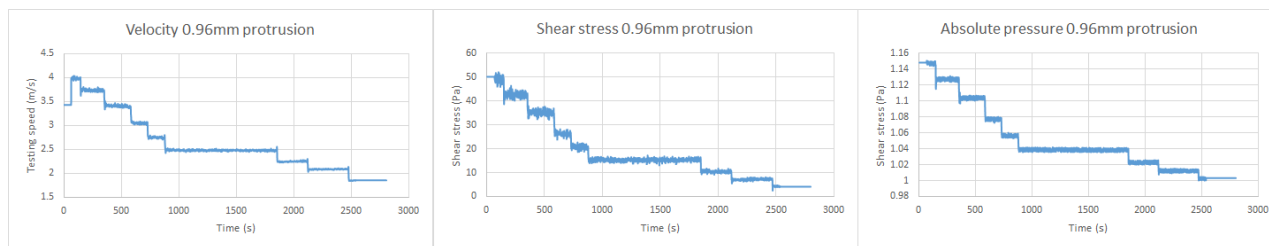


Figure C.15: Raw data for producing pumping curve

C.7. Validation of CFD modelling

This section is devoted in order to see if the results from the CFD modelling can be validated. As a small reminder, the CFD modelling was focused on the following aspects:

- Prove the (longitudinal)-stability of flow given the current design
- Prove that the soil sample is in a homogeneous (cross-sectional) flow regime
- Estimate the shear stress accurately
- Perform a sensitivity analysis (with respect to diameter and protrusion)

The stability of the flow, given the current design can be proved by observing the accuracy of the measurements over time as presented in figures C.4 and C.6, and in a slightly less manner as presented in C.5. This is even more obvious when looking at the raw data used to produce these figures, an overview of which is presented below in figure C.15.

It is clear from these graphs that the EFA has a stable flow regime between the pitot tube and at the level of the sample, due to the very stable readings of the raw data. Another indicator that the flow regime in longitudinal direction is fairly stable is that the results from the EFA are reproducible.

Further there needed to be proof that the soil sample is in homogeneous flow regime. From testing it can be observed that this is the case by seeing that the sample erodes equally in the cross-sectional direction.

Further the CFD modelling has been used to try and pre-estimate the shear stress accurately. This has been compared for the the data used to produce the pumping curve (of which the raw data has already been presented in figure C.15).

Unfortunately this fit is pretty poor, and despite numerous attempts to get a better fit (more dense mesh, inputting the smallest details etc.) it remains pretty poor which can be attributed to several flaws in the model that are impossible to incorporate:

- The "sample" in the CFD model does not erode, whereas during testing data this is the case.
- It is impossible to properly incorporate the hose connection from the pump to the tube. The losses associated with the hoses are significant however.

The first point of argument does not really hold towards comparing the data used in this comparison (which is the pumping curve data, in which a granite sample is used), but is important however. As the clay sample continues to further erode, the resulting shear stress will decrease significantly as has been seen in the tests with clay sample. This means that the calculation of the shear stress with the CFD model is only valid when the sample has not yet eroded.

The second point regards the impossibility to properly model the effects that the hoses have on the system. These hoses cause extra losses to the system due to:

- Extra length in the system, causing friction
- Height losses, because the pump is positioned lower than the hydraulic inlet in the model
- Bends in the hoses
- Losses due to contraction and widening

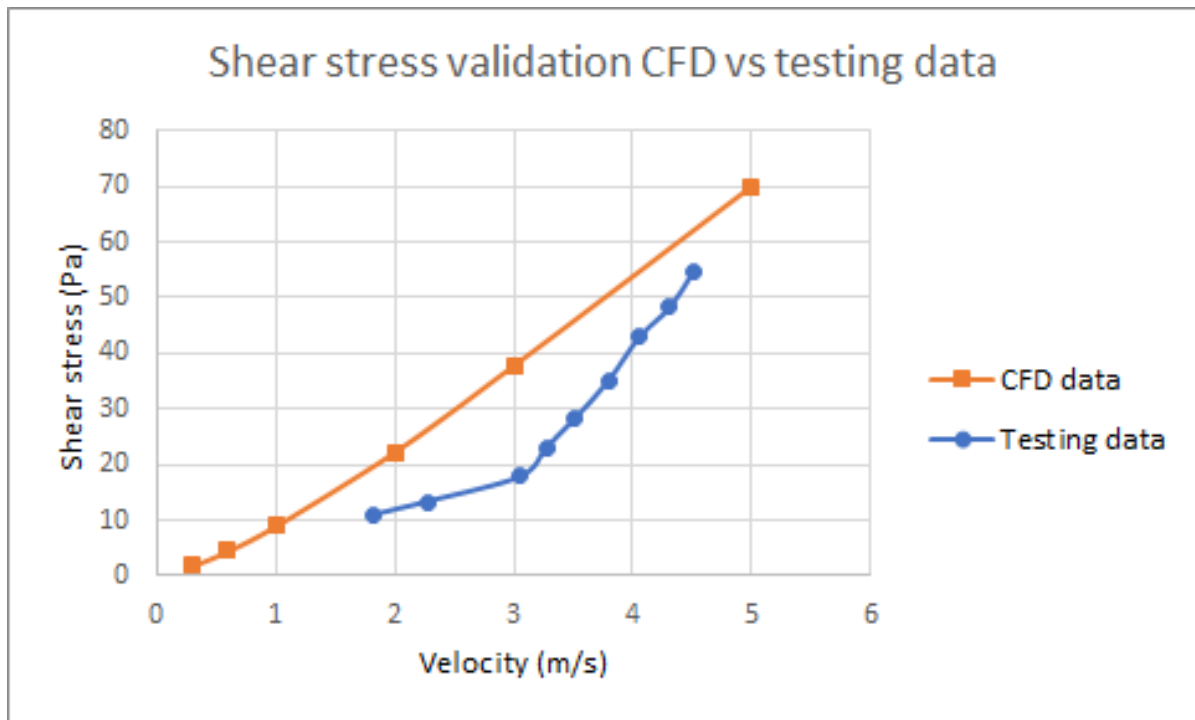


Figure C.16: Comparison of maximum shear stress development CFD and average shear stress test data

- The presence of valves causes headloss

These extra losses result in a significant headloss resulting in lower absolute pressures and lower shear stresses than modelled, as has also been observed during testing.

However, because these hoses is a flexible material it can not be properly modelled in the CFD model. This will continue to lead to an inherent difference between the model and the true laboratory results, despite enhanced mesh and enhanced modelling of the details.

Because of all the above no use will be made of the shear stress estimation of the CFD model in analyzing the samples. This will also mean that no use will be made of adjusting the shear stress in analysis based on the difference between the shear stress at the sample and the average shear stress in the CFD model will be performed.

Despite the above, it can be seen in the CFD model that there is an inherent difference between the shear stress at the sample and the average shear stress on the measuring trajectory, which has a linear correlation of approximately 3. This means that the shear stress at the sample is estimated to be 3 times larger than the average shear stress, as can be seen in figure C.19.

Finally, also the assumption of Briaud that the shear stress can be estimated by $\tau = \frac{1}{8} * \rho * f * v^2$ while estimating the roughness as $0.5 * D_{50}$ is tested using the data to establish the pumping curve. Using the moody's chart and the methodology prescribed by (Briaud (2001))

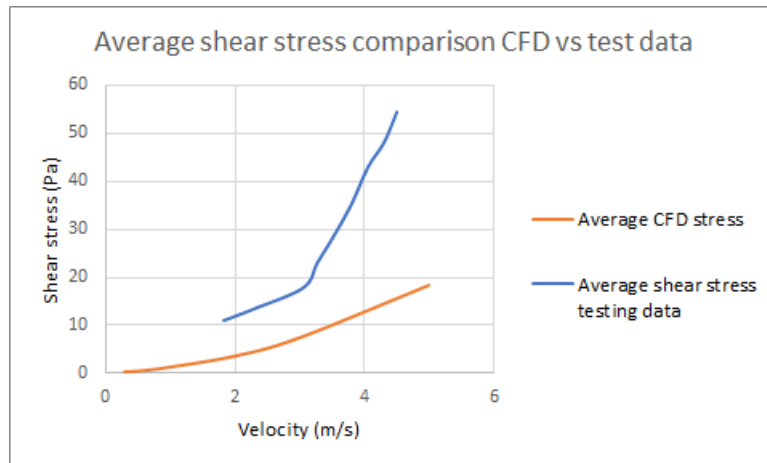


Figure C.17: Comparison of average shear stress development CFD and average shear stress test data

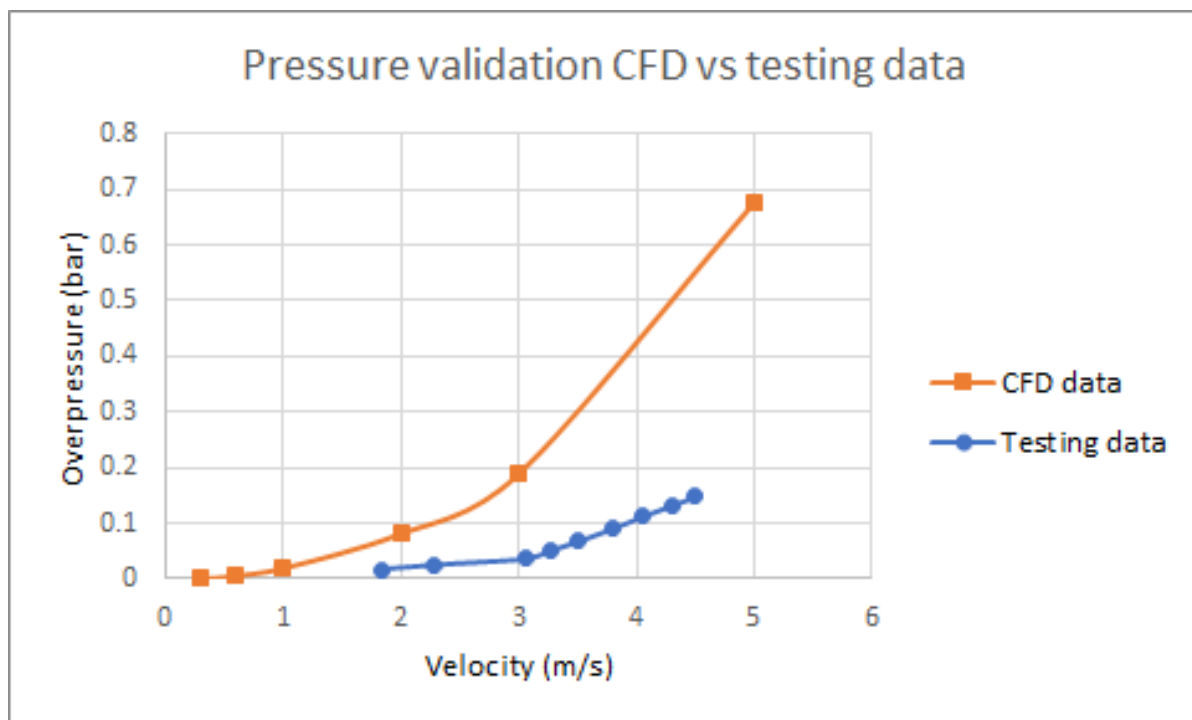


Figure C.18: Comparison of absolute pressure development between CFD and real data

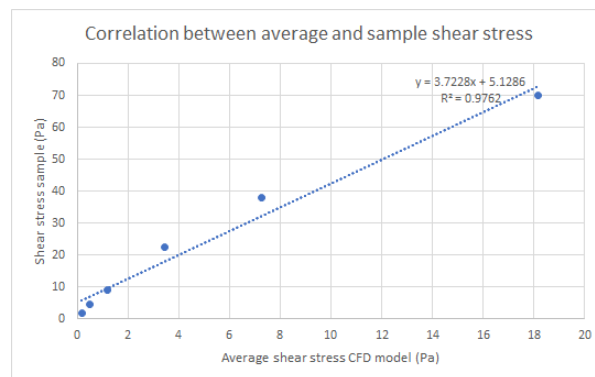


Figure C.19: Correlation between average shear stress EFA and shear stress at sample in CFD



Further Literature review

D.1. Proctor compaction procedure

In general there are 2 types of proctor tests: a standard proctor test which compacts the soil at an energy level of $0.6 \text{ MJ}/\text{m}^3$ and a modified proctor test which compacts at an energy level of $2.7 \text{ MJ}/\text{m}^3$ NEN (2010).

This means that the tests imply the following:

A normal proctor test implies a weight of 2.5 kg falling over a height of 1 foot (0.305 meter) creating 3 layers with 25 blows each leading to a sample of 100 mm diameter, 120 mm high.

A modified proctor test implies a weight of 4.5 kg falling over a height of 1 foot 6 inches (0.457 meter) creating 5 layers, with 25 blows each leading to a sample of 100 mm, 120 mm high. This all when using a normal proctor mould.

By densifying the soil in layers it is possible to get a relatively homogeneous compaction, with same strength and stiffness characteristics.

One point of attention is the following: when compacting the 3 layers the bottom most layer will obviously compact more due to the firm sub-grade of the mold. It must therefore be taken into account when testing the sample.

D.2. Building Practices Clay cover

D.2.1. General

In general the clay is brought on in layers of 40 centimeters which are then compacted by bulldozers, but also sometimes performed in layers of 20 centimeters. This is usually done by driving a bulldozer up against the slope of a dike. A minimum density of 97 % proctordensity is required by (adviescommissie voor de waterkeringen (1996)) which specifies the Dutch guidelines for levee construction. According to the same report, the water content of the clay should be between the liquid limit and plastic limit, being close towards the liquid limit. It further states that clays with a consistency index of approximately 0.6 can be well compacted.

This concerns the lower layers of the clay cover of a levee. For the uppermost part of a levee a more sandy clay should be used which is less compacted to ensure a good matrix for the future grass cover.

However, caution must be exercised according to (van Meurs and Kruse (2017)) using proctor density as a check if the clay layer has been compacted successfully. There are 2 main reasons for this:

1. In practice it is not as straightforward to determine the proctor curves and proctor density as it might seem.
2. It has been observed regularly that voids occur in the bottom of a compacted clay layer which are not stumbled upon when taking samples and checking them against the proctor density.

However, experience learns us that the proctor test has been also been used for clay in projects for decades in a successful manner. Therefore, the proctor test can and will be used in this research, but there must also be a good check on site if the bulldozers compact the soil in a good way.

The same type of considerations are made in the American guidelines for levee and dam construction (US Army Corps of Engineers (2000)) (US Army Corps of Engineers (2004)) (United States Federal Bureau of Reclamations (2015)).

It is however common practice that clay is compacted in layers of 6"/15 centimeter instead of 40 centimeters.

D.2.2. Dike revetment project visit

Compaction practice

A site visit was conducted to a Dutch dike revetment project, to see how in the field the clay compaction occurs.

The clay cover in the dike of this dike revetment project is compacted in 3 lifts of 30 centimeter, 30 centimeter and a final 25 centimeter respectively. The reason why the clay is compacted in relatively thin lifts is because the clay is relatively dry upon arrival and no wetting of the soil is done. To then get a good compaction the soil is compacted in smaller lifts, resulting in a higher energy per unit volume. The soil is not being wetted or dried due to the in-practicalities of (evenly) changing the water content in large boulders of clay and it being easier to compact in smaller layers. The compaction is done by using bulldozers first spreading out the compacted clay and then compacting the clay by driving the bulldozer uphill.

This resulted in a the following clay cover as presented in D.1.



Figure D.1: Observed clay cover

Left a cross-section of the clay cover with the cell-phone as a reference for length, right the same cross-section from another angle. Please note how cracked the most upper layers (however this is also due to use of less erosion resistant clay in the upper layers to facilitate vegetation growth) are and how moist the lower layers are. This is a good illustration of the changes in structure the clay undergoes due to meteorological conditions.

Quality control compaction

The quality control of the compaction at this project is done by taking 2 tests every 100 meter stretch of dike, of every single lift (meaning that in this project a total of 6 tests every 100 meters is performed). First of this sample the bulk density is determined, after which a proctor test is done on the sample. This establishes the proctor density (proctor bulk density, not dry density), which is then compared to the bulk density on site. The bulk density on site must then be at least 95 % of the proctor bulk density. This methodology is quite similar when comparing it to other Boskalis projects. There it is common however to not divide the dike up in segments of such strict length, but rather to other factors. One should think of things such as the clay batch that is being used, or the changes in alignment of the levee.

D.3. Flow through pipes

When water flows through pipes it does not flow uniformly over height or width, rather than uniformly, but is more a type of parabolic function as can be seen in figure D.2.

However, while the processes of water flow are generally well understood, it is only possible in a limited amount of cases to obtain an analytical solution White (2011). Unfortunately, there is no analytical solution available for flow in rectangular tubes, and an obvious way out is to use computational fluid dynamics modelling.

Then to estimate the shear stress that the soil experiences a look must be taken in how the speed profile of the soil is correlated to the shear stress.

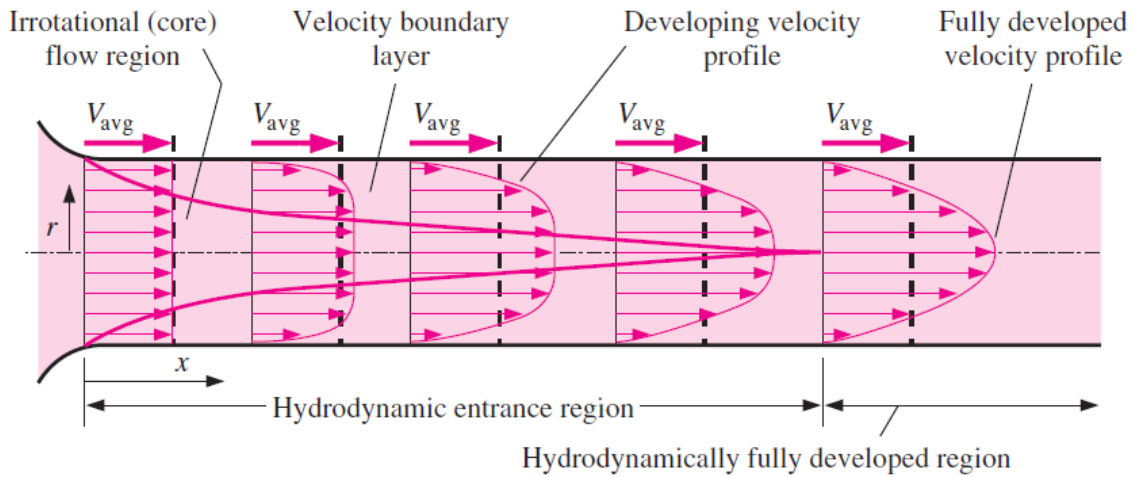


Figure D.2: Fluid flow in conduits

As can be seen in Battjes (2002) the shear stress and the speed profile are connected as is described in equation D.1.

$$\tau = \eta * \frac{du}{dr} \tag{D.1}$$

In this equation η is the dynamic viscosity of the fluid and $\frac{du}{dz}$ is the speed gradient in the direction of interest (e.g. over height).

An other option to estimate the shear stress is to correlate it to the pressure drop over distance in a conduit. Taking into account a balance of mass and volume this results in equation D.2.

$$\Delta P = - \frac{\tau * 2 * (a + b)}{a * b} \tag{D.2}$$

D.4. Hydraulic loads

To know how the soil in the laboratory must be investigated, it is vital to know how much loads can be expected in outdoor real situations. In T. Pullen et al. (2007) an overview is made of how severely the overflow discharges are deemed. This presents the following:

Overflow rate (l/s/m)	Severity
<0.1	Insignificant
1	Clay on crest and inner slopes could start eroding
10	Significant overtopping, erosion occurs
100	Clay must be protected by asphalt or concrete

Further, adviescommissie voor de waterkeringen (1996) states that dikes with a good (also bare clay) cover can sustain an overflow rate of 10 l/s/m with some damage, however without damaging the structural integrity of the dike as a whole. Therefore it states that an overflow rate of 10 l/s/m dike should not be desirable.

More detailed information on how to calculate the expected shear stresses on soils can be found in S. Hughes, J. Shaw and I. Howard (2012). In this study multiple small scale experiments have been conducted on a dike cross-section with surge overflow and surge overtopping. It suggested that a fit of the mean shear stress on the levee can be estimated as follows:

$$\tau_{mean} = 0.106 * \gamma_w * \left(\frac{q^2}{g}\right)^{(1/3)} \quad (D.3)$$

In this equation γ_w is the density of water and q the discharge per unit length.

It further states that a translation from a mean to a maximum shear stress can be found by multiplying the mean shear stress by 1.41. The difference between the maximum and mean shear stress occurs due to the following:

- Due to wave impact there is a local shear stress peak
- Due to spatial variation of the shear stress (increase of the shear stress as the water flows down the inner slope)

Taking into account the proposed overflow discharges in T. Pullen et al. (2007) this would result in the following shear stresses:

Overflow rate (l/s/m)	Average shear stress (Pa)	Maximum shear stress (Pa)
0.1	2.3	3.2
1	5.0	7.0
10	10.7	15.0
100	23.0	32.4

Overall this means that testing should occur in the region between 0 and (roughly) 40 Pa in order to properly simulate the erosion stresses that occur due to wave overtopping.

D.5. Additional erosion testing devices

When testing erosion many different devices are available other than the Erosion Centrifuge and the Erosion Function Apparatus. These devices will be mentioned in this section and briefly explained. Throughout this section extensive use has been made of the information provided by (Haghigi (2013)).

Generally speaking, most erosion testing devices can be placed in one of the following groups:

- Devices which test external erosion
- Devices which test internal erosion
- Devices which test erosion due to rain activity
- Devices which test jetting erosion

Finally, there are also a 2 other tests used to determine the erosion potential of a soil, not by means of a device, which will also be briefly touched upon.

Note that the erosion centrifuge and erosion function apparatus already have been discussed in the main report because these type of devices have been deemed to most closely represent the effects of erosion by wave overtopping of a levee by the author.

D.5.1. Devices which test internal erosion

The following devices are available which test internal erosion:

- The hole erosion test
- Flow Pump test
- Triaxial Erosion test

Hole Erosion test

The hole erosion test takes a sample with a given diameter and a 6 mm diameter hole in the middle and to which a hydraulic gradient is applied. Due to the flowing water through the hole erosion will take place, after which the mass loss is correlated to the hydraulic gradient applied to the sample. A schematic overview of the set-up can be found below in figure D.3. The advantage of this test is that it represents internal erosion quite well, however only very crude correlations can be made with the shear stress that the sample is experiencing. This means that testing results will always be in terms of hydraulic gradients.

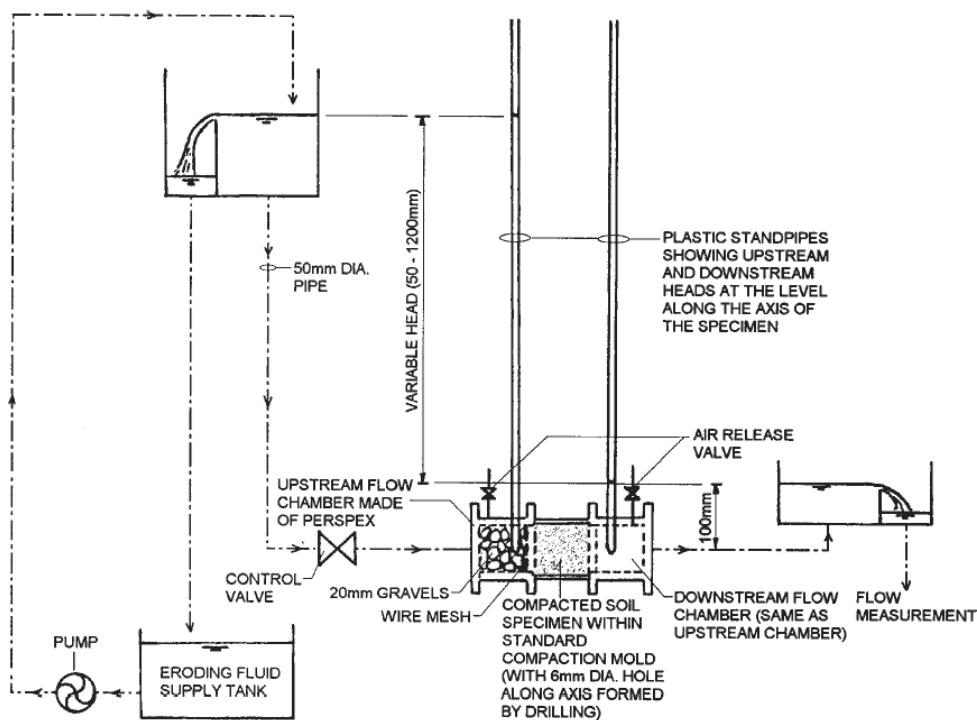


Figure D.3: Schematic overview Hole erosion test

Flow pump test

The flow pump test is quite similar to the hole erosion test. It also involves a sample which has been prepared (25 mm diameter with a 6 mm diameter opening in the center) but differs in a slight way. It does not apply a hydraulic gradient to the soil, however it forces a certain discharge through the opening in the middle of the sample. This way the erosion resistance is measured in terms of discharge, rather than hydraulic gradient. The main advantage of this test compared to the hole erosion test is that the set-up is generally speaking much easier than with the hole erosion test. A schematic overview of the set-up can be seen below in figure D.4.

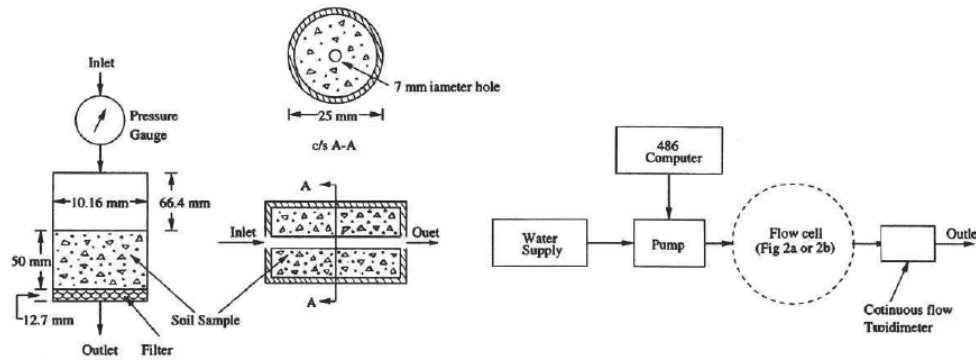


Figure D.4: Schematic overview Flow pump test

Triaxial erosion test

At the heart of a triaxial erosion test is a modified triaxial cell in which a sample is placed (with no openings) through which at a certain pressure water is injected in to sample at the top. This water then travels through the sample and causes a certain amount of erosion. The water and eroded soil then is caught at the bottom of the sample. This way erosion can be reproduced in a very analogous manner as in nature in a very controlled way (stress levels can be controlled and all). It is however a very complex set-up. An overview of this setup can be seen below in figure D.5.

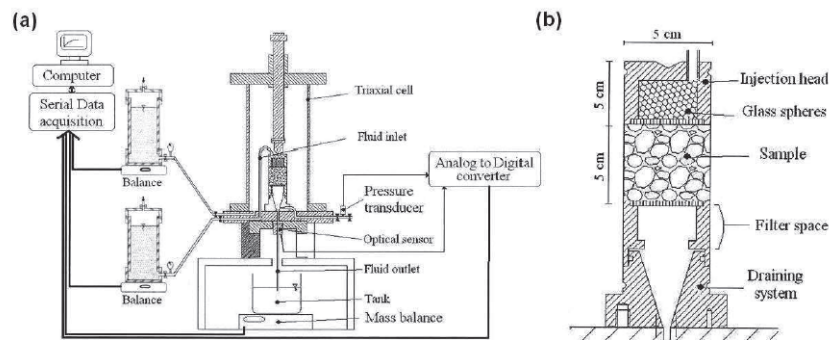


Figure D.5: Schematic overview Triaxial erosion test

D.5.2. Devices which test external erosion

The following devices have been found which test external erosion:

- Erosion Centrifuge
- Erosion Function Apparatus
- Hydraulic flume
- Ex/In-situ Erosion testing devices

Of these tests the erosion centrifuge and the erosion function apparatus have already been discussed in the main report and thus will not be done so again. The reason why the hydraulic flume and ex/in-situ erosion testing devices have not been considered will also be discussed in their respective parts.

Hydraulic Flume

The hydraulic flume was developed to simulate the erosion of a clay bed in a river for instance. In this flume plates of prepared clay are layed down after which the flume can be inclined if necessary. After this the water can pass through at the desired speed and the speed of erosion can be analyzed. An overview of the set-up can be seen in figure D.6. The main advantage of this set-up is that it can relatively easily be built and represents the erosion of clay in a waterway quite well. The reason why this set-up is not used in this research is the difficulty of accurately preparing samples in a controlled way which can then be placed on plates and lowered into the flume. This is quite a pity, because if inclined at a proper angle it could be a good representation of water flow over the crest of a levee.

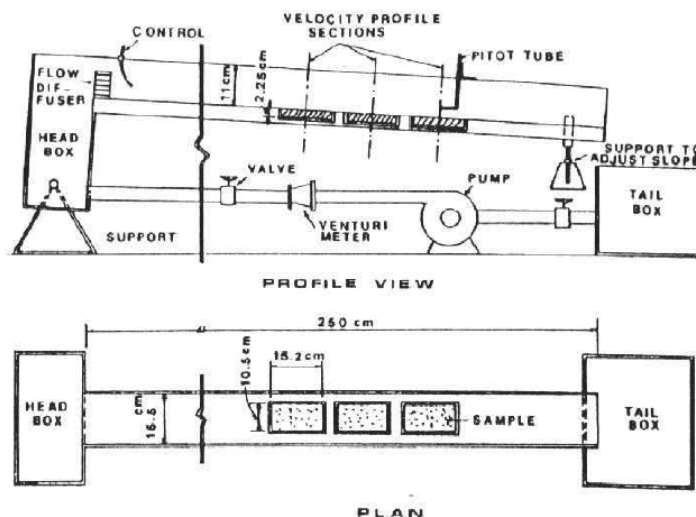


Figure D.6: Hydraulic flume erosion test

Ex/in-situ erosion testing devices

The ex and in-situ erosion testing devices are quite identical, however one is able to be used on a specific site, and the other must be used in the laboratory. The main idea is to place a container over a soil sample and let the water rotate around the soil. However, no research has been found in which this machinery has ever been built or used and these are only ideas. An overview of these machines are given in figures D.7 and D.8.

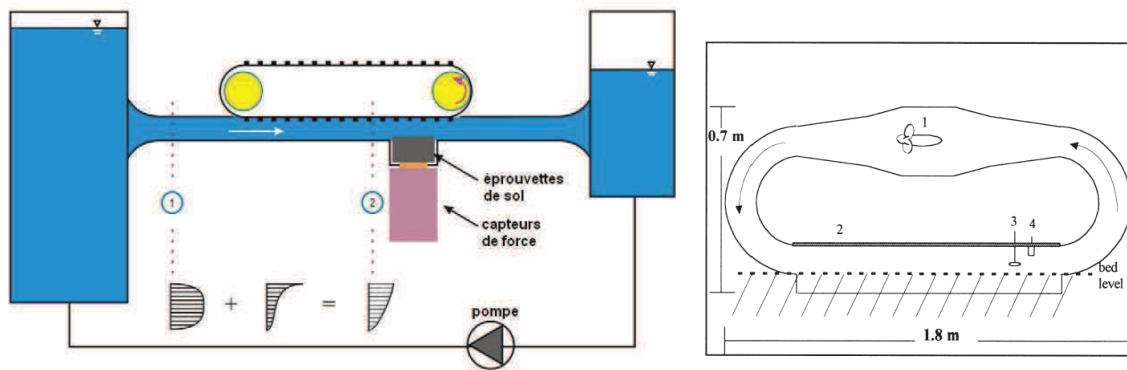


Figure D.7: Schematic set-up ex-situ erosion device

Figure D.8: Schematic set-up in-situ erosion device

D.5.3. Devices which test erosion due to rain activity

The following devices have been found to test erosion due to rain activity

- Pocket Erodrometer
- Pluvial Erosion Simulator

Pocket Erodrometer

This device has been developed by Briaud and test the effect of erosion due to rain spraying water with a mini-jet horizontally en let it fall on soil sample on the floor. By measuring the depth of the hole after 20 impacts an indication is obtained of the erodibility of the soil. The positive point is the simplicity of testing, however it is only indicative. An overview of the set-up is given in figure D.9.

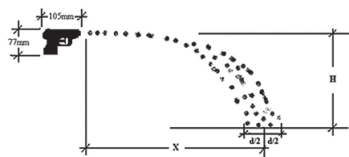


Figure D.9: Overview Pocket Erodrometer

Pluvial Erosion Simulator

The pluvial erosion simulator is in essence a box of clay which can be tilted to a wanted angle and than can be sprinkled from above. If necessary, an additional flow of water over the sample is possible. This way a much larger portion of a sample can be tested for its erosion capabilities. Another nice thing is that it is possible to let grass grow over the sample and test it, something which is only possible with a limited other amount of tests. A figure of the pluvial erosion simulator is given in figure D.10.

D.5.4. Devices which test erosion due to jetting

To test erosion due to jetting only one option is possible: the jet erosion test. However, it is also possible to have in-situ and laboratory versions, however these work exactly the same.

The jet erosion test works by pointing a nozzle towards a clay sample and measuring the pressure it takes to create a certain penetration in the sample within a given time. This is a reason why this type of testing is mainly used for dredging purposes. A figure of the set-up is given in figure D.11.

D.5.5. Test for erosion

Also several tests have been developed which should say something about the erosion resistance of soil. These tests are the following:

- Sandcastle test

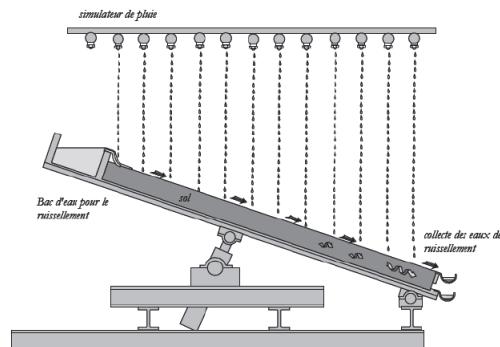


Figure D.10: Overview pluvial erosion simulator

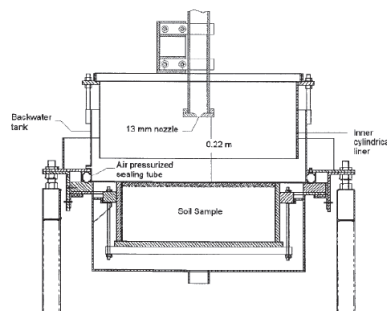


Figure D.11: Set-up Jet erosion test

- Double hydrometer test
- Crumb test

The scope of these tests will be briefly touched upon to give a complete overview of all methods known to characterize erosion.

Sandcastle test

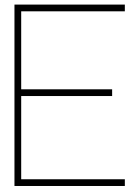
This test is actually quite a simple one: one takes a soil with the shape of a tapered cylinder and puts in a jar with 1 gallon of water. Then one waits until the soil sample collapses. The soil is then classified based on its stand-up time. The longer the stand-up time, the better the performance of the soil. It is a relatively easy test, but does not necessarily say something about the effect of flowing water on the sample.

Double Hydrometer test

The idea of a double hydrometer test is to conduct 2 hydrometer tests: 1 with soil with a dispersing agent, 1 without. Then these tests are conducted after which a sieving curve is made. From this test the difference in the amount of flocculation can be determined. As stated in chapter 2.5 this difference in structure has its impact on the erosion resistance of soil, and this effect can then be taken into account.

Crumb test

The crumb test is a test wherein a cube with an edgesize of 15 mm which is submerged in a jar of fluid of 250 mm. Then the size and turbidity of the erosion cloud is measured at regular intervals after which the soil is classified into 1 out of the 4 available classes, ranging from a non-dispersive to a very dispersive clay. The advantage of this test is that it is very easy to do, very cheap to do, and can be done with very little facilities. However, the test cannot be used with a soil with a PI above 8, the results are user-dependent, and it is a qualitative test in general.



Overview drawing EFA flow tube

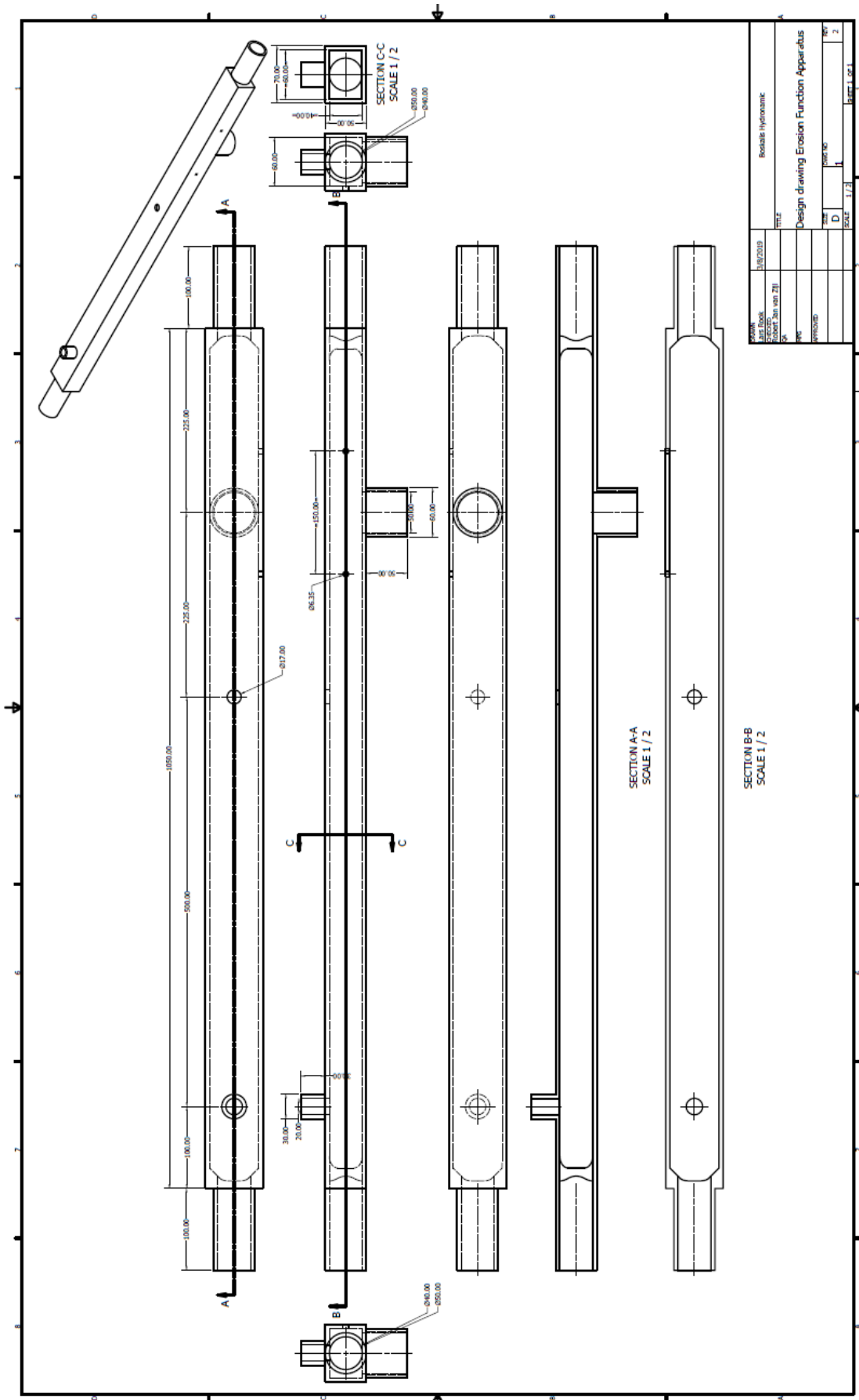


Figure E.1: Design drawing Erosion Function Apparatus flowtube

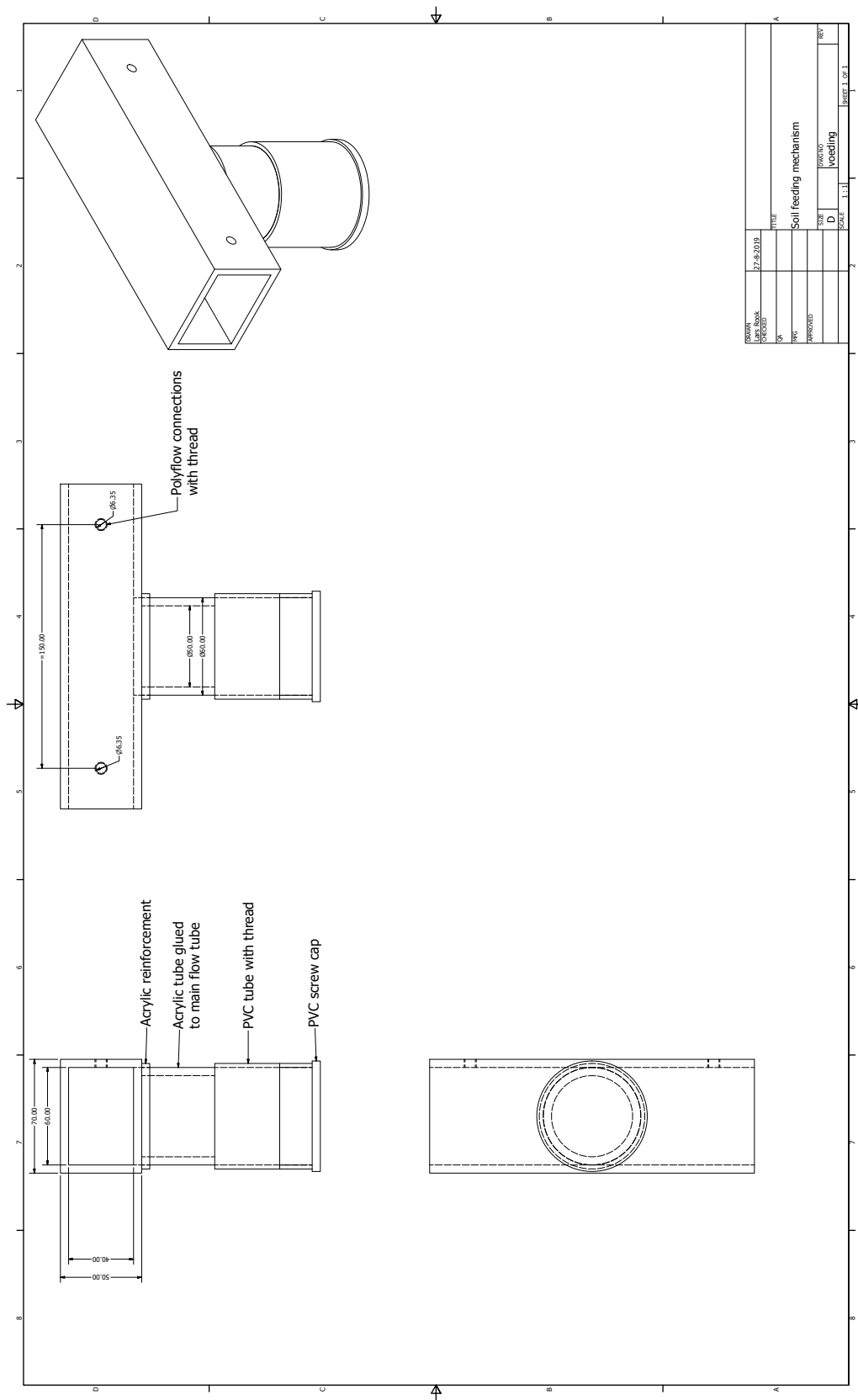


Figure E.2: Soil feeding mechanism EFA

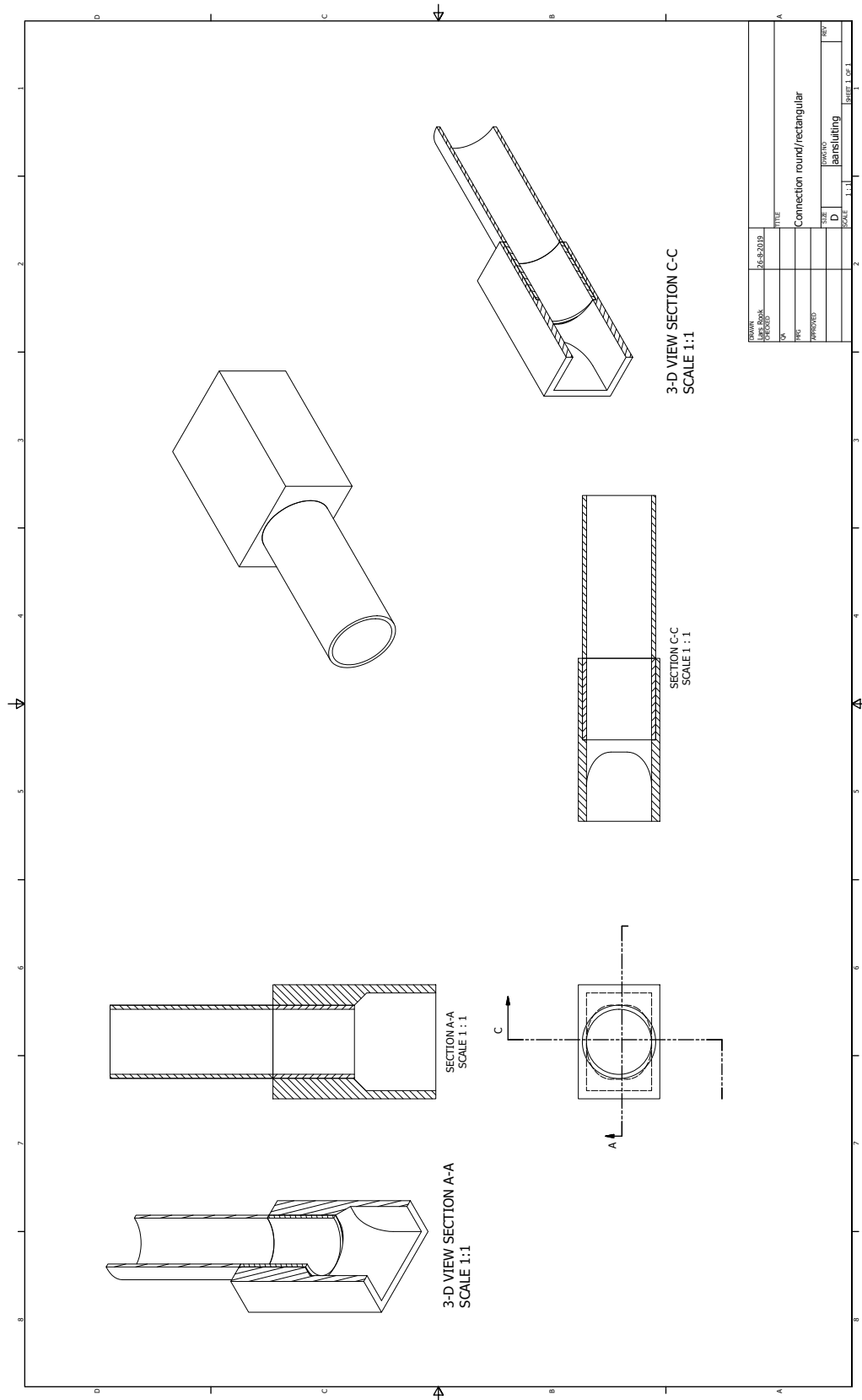


Figure E.3: Connection round tube to rectangular tube

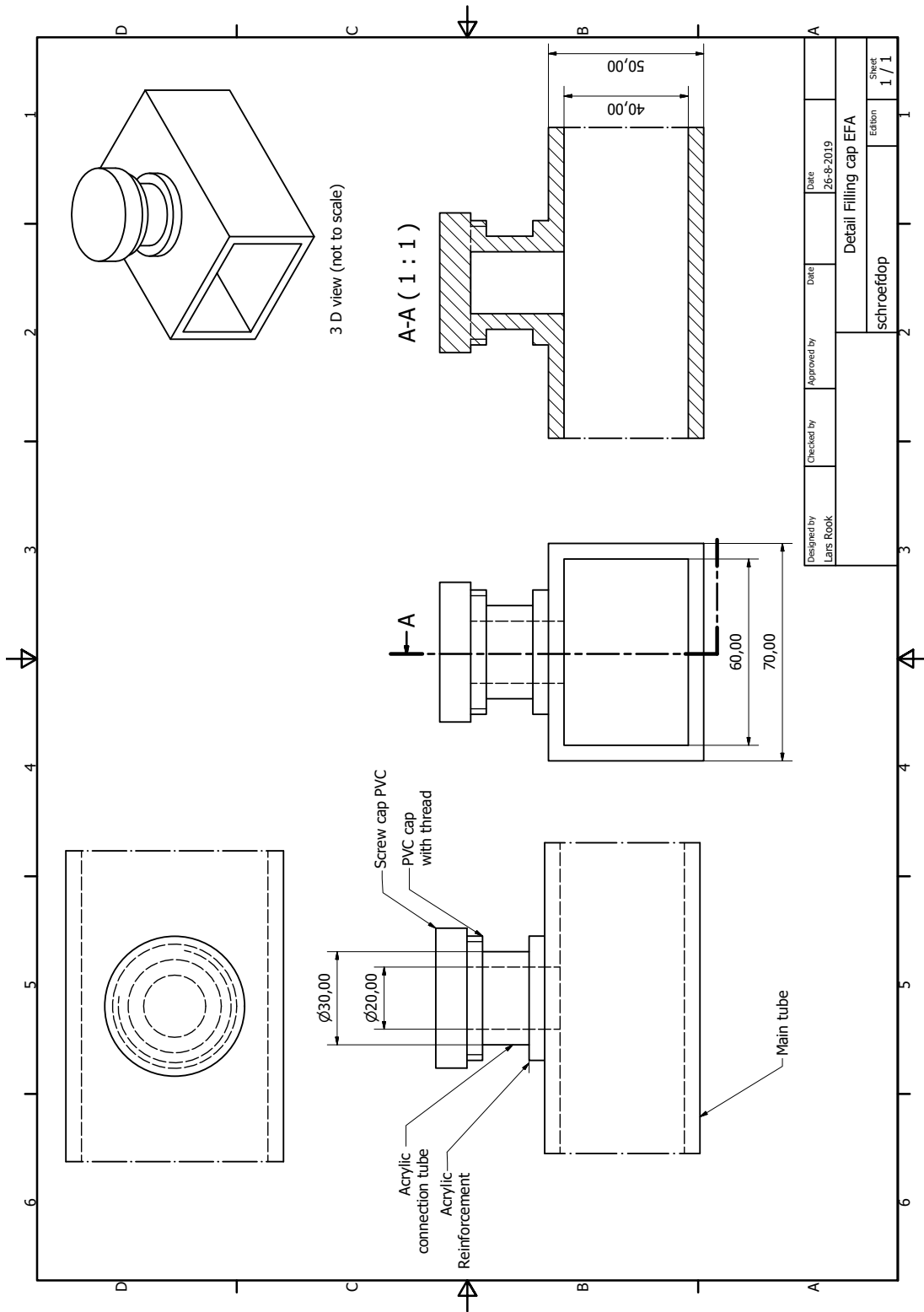


Figure E.4: Filling cap

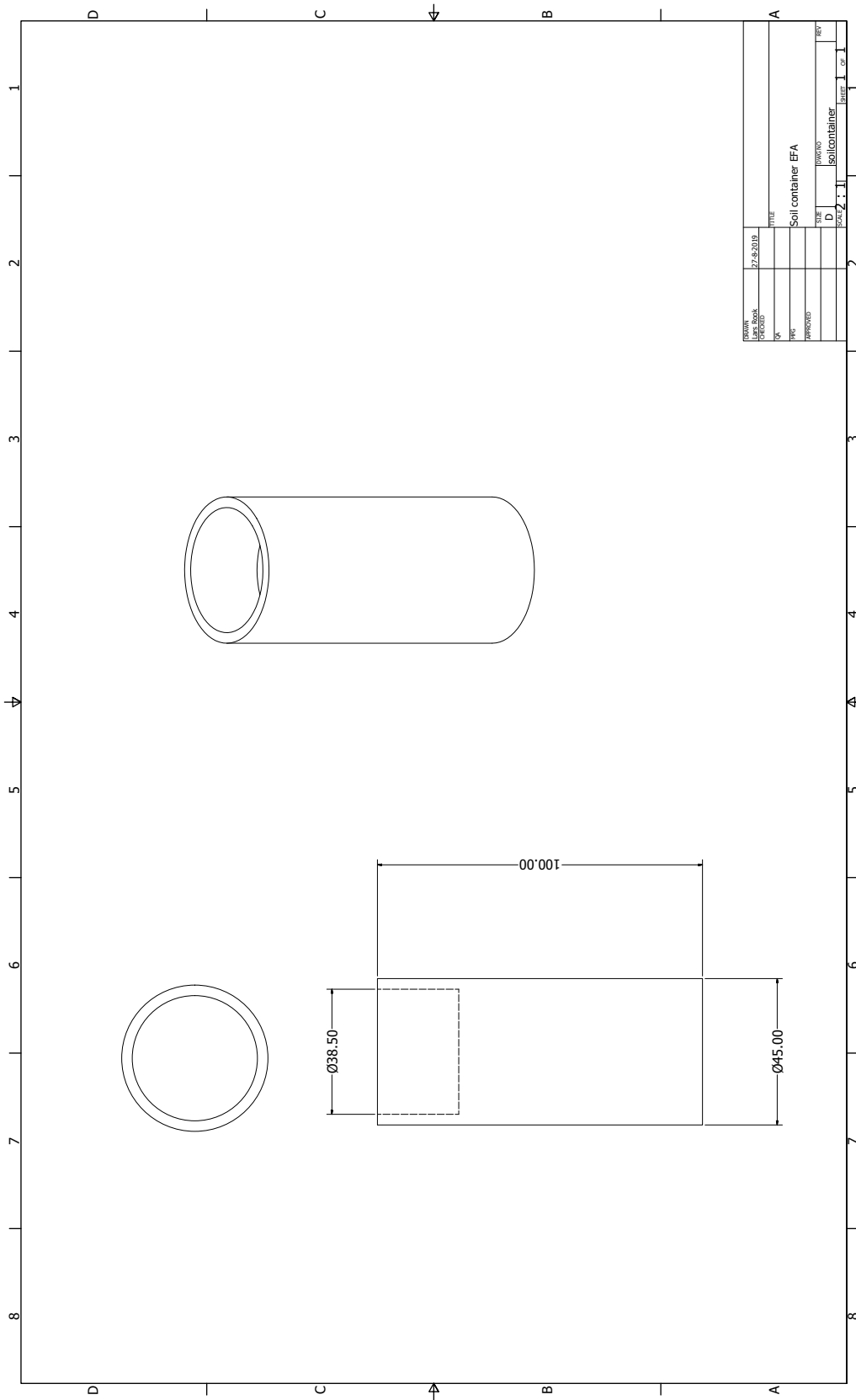
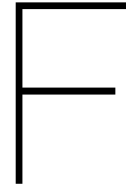


Figure E.6: Soil container



Calculation flow pump

The calculation of the flow of the pump has been done during design to see if the pump provides enough power and flow rate to get a proper speed in the flow tube. This is a preliminary calculation in order to distinguish between the performance of the different types of pumps. The calculation sheet can be found below in table F1.

		Extrema 500/13	Extream 400/12	DAB FEKA VS 1200 M-A	BEDU Zenit Mai series	BEDU DGX 200/2/65 A0CM/(T)50
Price	€	399	409	799	3100	3500
P	(kW)				0.74	1.5
L	(m)	4	4	4	4	4
h	(m)	0.05	0.05	0.05	0.05	0.05
w	(m)	0.06	0.06	0.06	0.06	0.06
k	(m)	10 ⁻⁶	10 ⁻⁶	10 ⁻⁶	10 ⁻⁶	10 ⁻⁶
D	(m)	0.055	0.055	0.055	0.055	0.055
lambda	(-)	0.014	0.014	0.014	0.014	0.014
p_drop	(kPa)	7.18	10.48	11.98	23.26	34.21
h_drop	(m)	0.72	1.05	1.2	2.3	3.4
Q	(m ³ /hr)	24	29	31	34	38
u	(m/s)	2.2	2.7	2.9	3.1	4.4

Table F1: Overview pumps

This calculation sheet has been made in co-operation with the Research and Development department in which reasonable values for the length and resistance parameters which has been done in a very early stage of the design of the EFA. The final result of the actual pumping performance is given in chapter C in which these first estimates are checked. During making this overview regular turbulent flow fluid mechanics theory has been used as reported in Battjes (2002).

The sheet then works as follows:

- Input height, width and length parameters of the flume
- input a roughness parameter k (estimated at $10^{-6}m$)
- Calculate equivalent diameter from height and width
- Calculate λ parameter, which is a characteristic length parameter

- Calculate pressure drop from λ , the equivalent diameter and the roughness parameter k . Convert this to meters head loss
- Looking up from the graph correlating the head loss to the flow rate which flow rate can be achieved
- Calculate the associated speed that is then possible in the flume



Testing method index testing

In this appendix the methods by which the results of the index testing have been found will be discussed. If a certain method is not that clear, or if there are multiple methods to determine a certain parameter a further elaboration will be made. All tests have been performed according to the guidelines set by (CROW (2010)).

Bulk density

The bulk density has been determined by hammering in a soil probe with a diameter of 10 centimeters and measuring the weight of the soil inside.

Clay content

The determination of the clay content is done with a so-called lutum test. A sample of soil is placed grounded to a very fine level after which it is done in a beaker. Then an overload of hydrogen-peroxide is added and let rest for 12 hours (in order to remove the organic matter in the soil). Then a precise amount of hydrogen-chloride is added to react with the lime (meaning that the lime content must be known upfront). A dispersion agent is then added to the soil to bring it into a suspension. Then after 4 hours 20 milliliter is taken out of the beaker at a certain depth (dependent on the temperature of the suspension). The mass of the solids in this suspension is then deemed to be the lutum content for the entire sample

Grain density

The grain density can be determined in different ways, but the method used in this study is using a pycnometer. This is a bottle with a very precise determined volume in which an amount of dried soil is put. This is then filled with water and put in a vacuum chamber as to maximize the possibility of water entering the clay minerals. This is then let to rest and weighed afterwards. After the content of the bottle is washed away, rinsed and filled again with water. If then the empty mass of the bottle, the mass of clay, the mass of the bottle filled with clay and water and the mass of the bottle filled with water is known the grain density can be calculated.

Lime content

To determine the lime content 20 gram dried soil is taken, grounded at put into demineralized water and 100 ml of dispersion agent. Then hydrogenchloride is added in steps (at Boskalis 10 ml, at a 10 % concentration) and waited until it does no longer reacts. When it no longer reacts one calculates back the concentration of Lime using basic chemistry.

Liquid limit

The liquid limit is determined either by the penetrometer or casagrande cup. In this study an automated Casagrande-cup is used. This method is so common that no further elaboration is made.

Determination % particles <63 μm

The determination of the percentage of particles smaller than 63 μm (or inversely the sand content) is done by wet sieving a portion of the material through a 63 micrometer sieve.

Organic content

The organic content is determined by taking 20 grams of oven-dried, ground soil and placing it in a beaker with demineralized water and dispersion agent. Then hydrogenperoxide is added in steps (10 ml at 10% concentration) until the reaction stops. Then the concentration of organic matter can be back calculated because the amount of added hydrogenperoxide is known.

Undrained shear strength

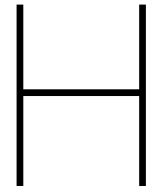
The undrained shear strength is determined by means of a pocket vane tester and a penetrometer. It is known that there are differences in results generated by the different means of testing and therefore the results will be averaged.

Salt concentration

The salt concentration is determined by taking exactly 10 grams of dried, oven-dried soil and dispersing it in 100 ml demineralized water. Then gradually silver nitrate is added to the solution ($AgNO_3$). This induces a reaction of the Silver ions with the chloride ions to the solid silver chloride which precipitates. During this reaction the electrical conductivity of the solution is continuously measured. During the start of this reaction the electrical conductivity remains roughly the same (the chloride ions are being replaced by nitrate). However, when all chloride ions have precipitated the silver nitrate is just being added without any reaction occurring. This will then increase the electrical conductivity significantly. If the the amount of added silver nitrate added is known the chloride concentration (and in a rough sense the salt concentration) is known.

Plastic limit

The plastic limit has been determined by rolling a small thread at a certain water content until it cracks. However, this is deemed universal knowledge and will not be discussed further.



Photo's end result EFA

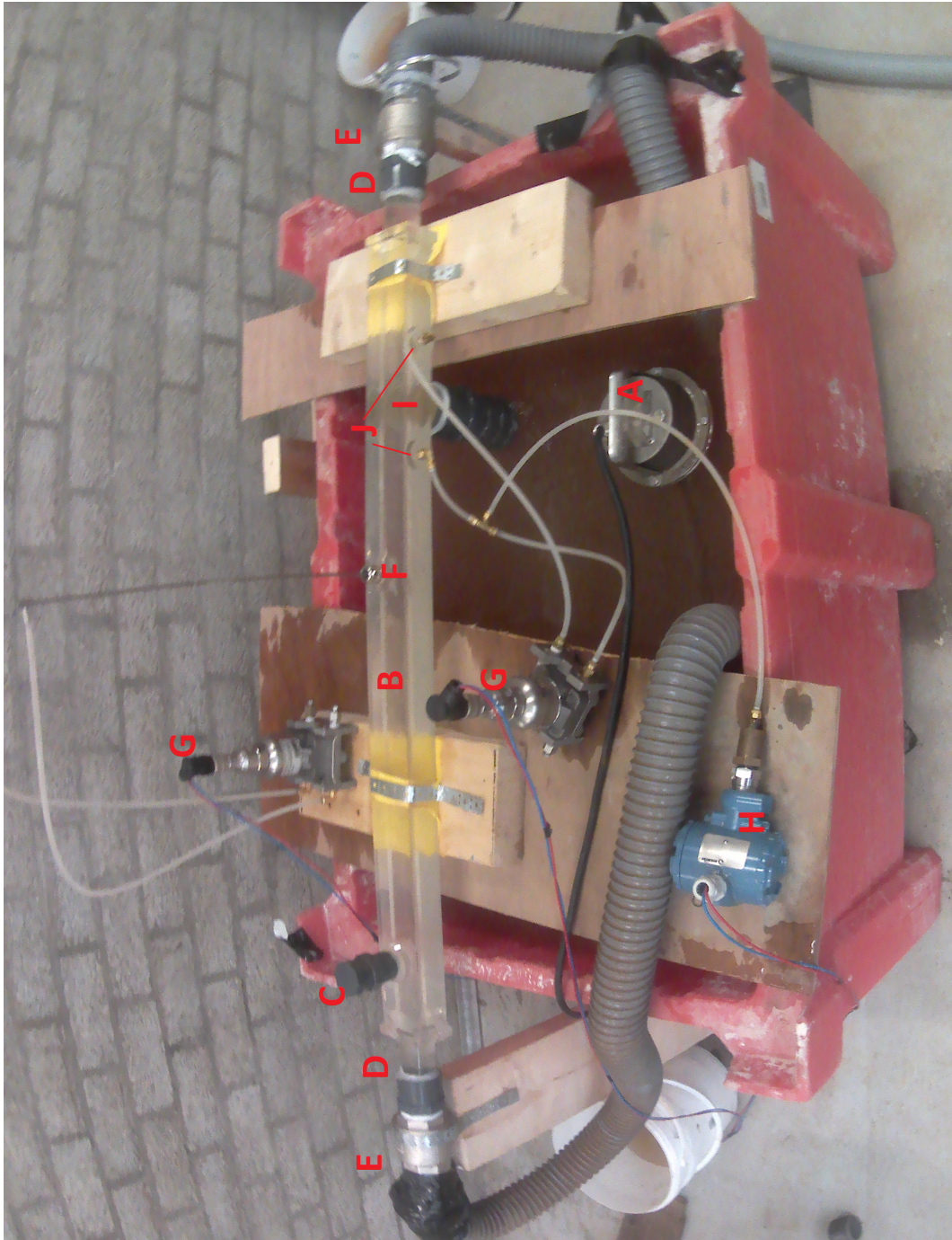


Figure H.1: Overview end result EFA

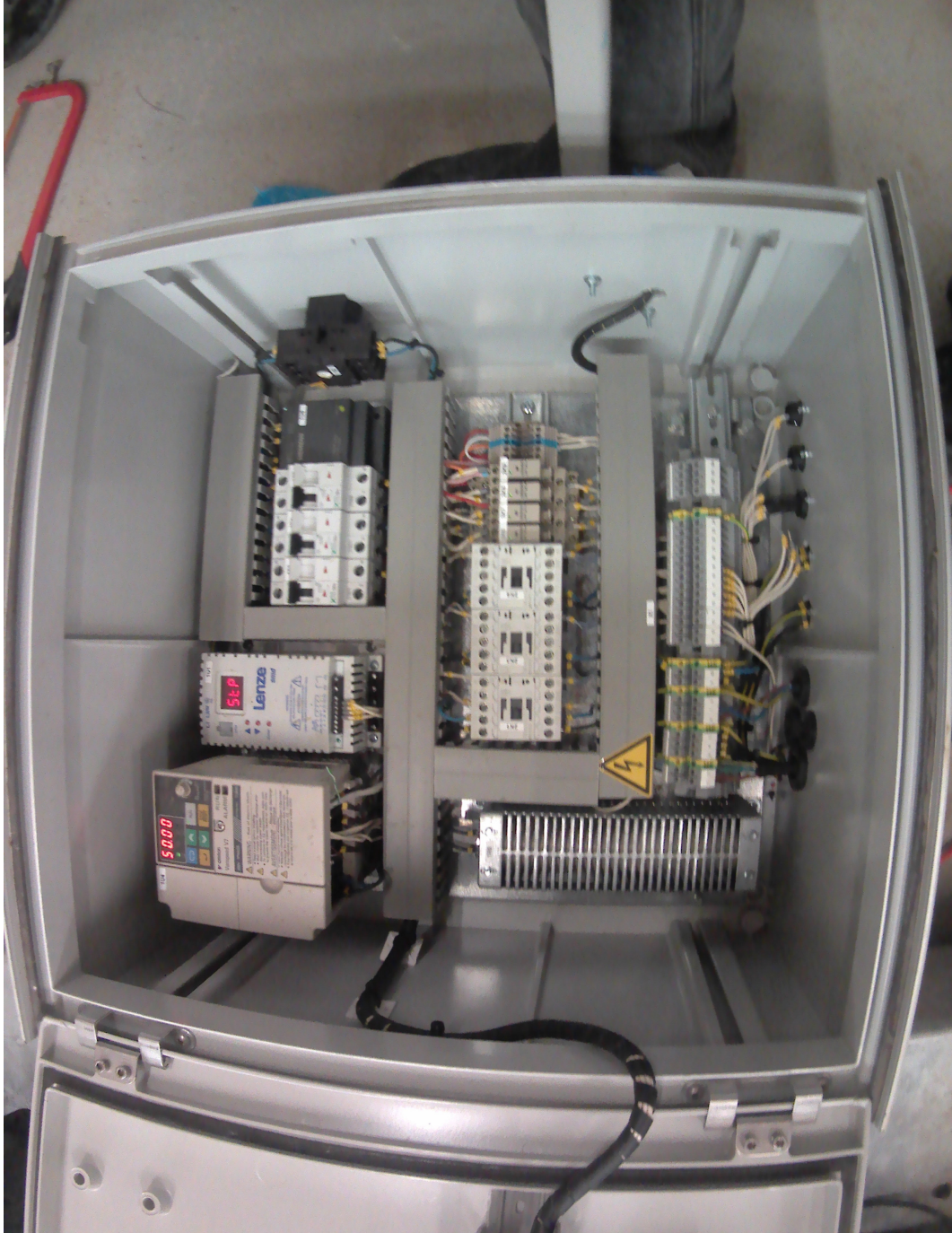


Figure H.2: Result Variable Frequency Drive



Figure H.3: Result Opto 22 data box

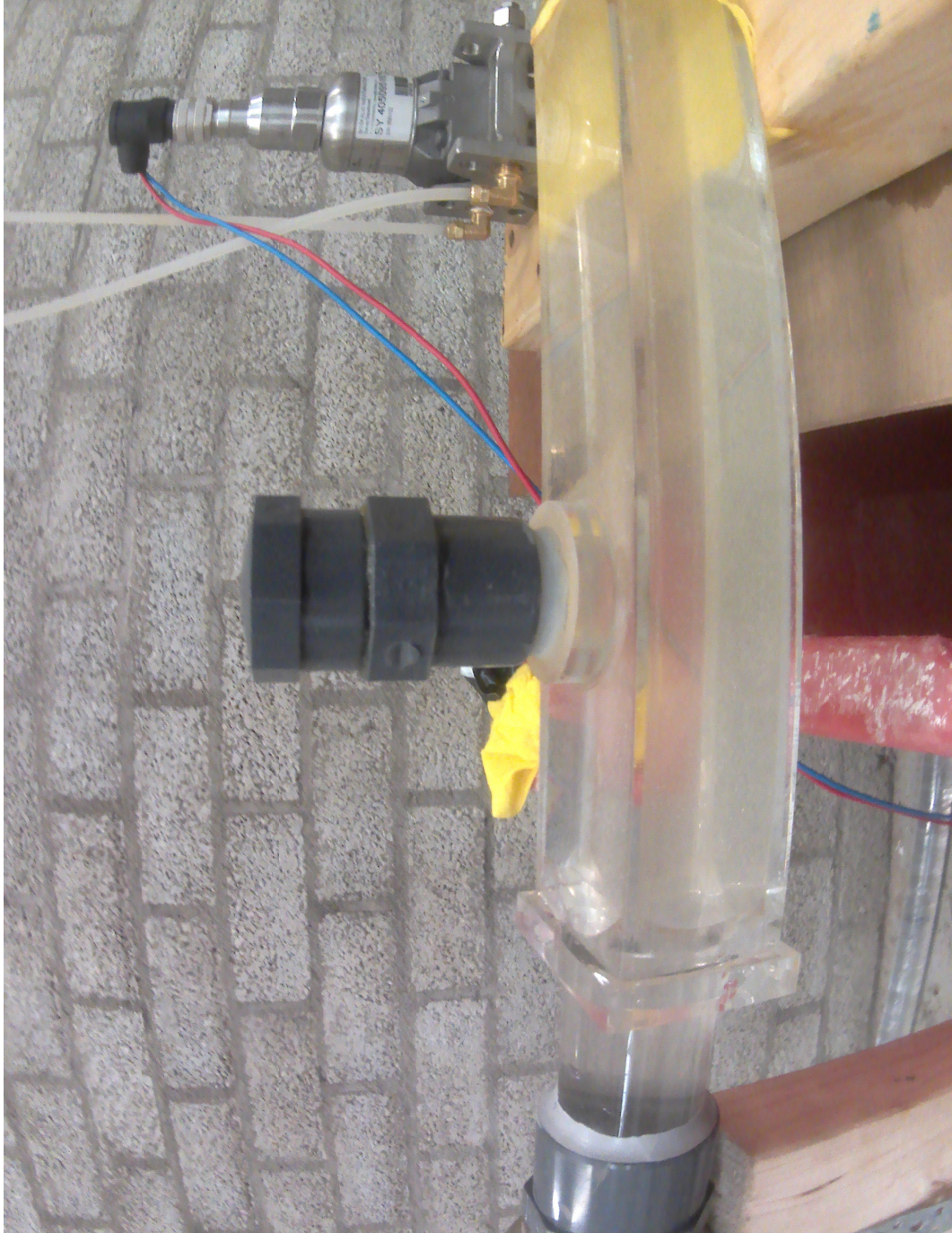


Figure H.4: Result filling cap



Figure H.5: Result connection round to rectangular tube



Figure H.6: Result transition pieces to gradually change flow

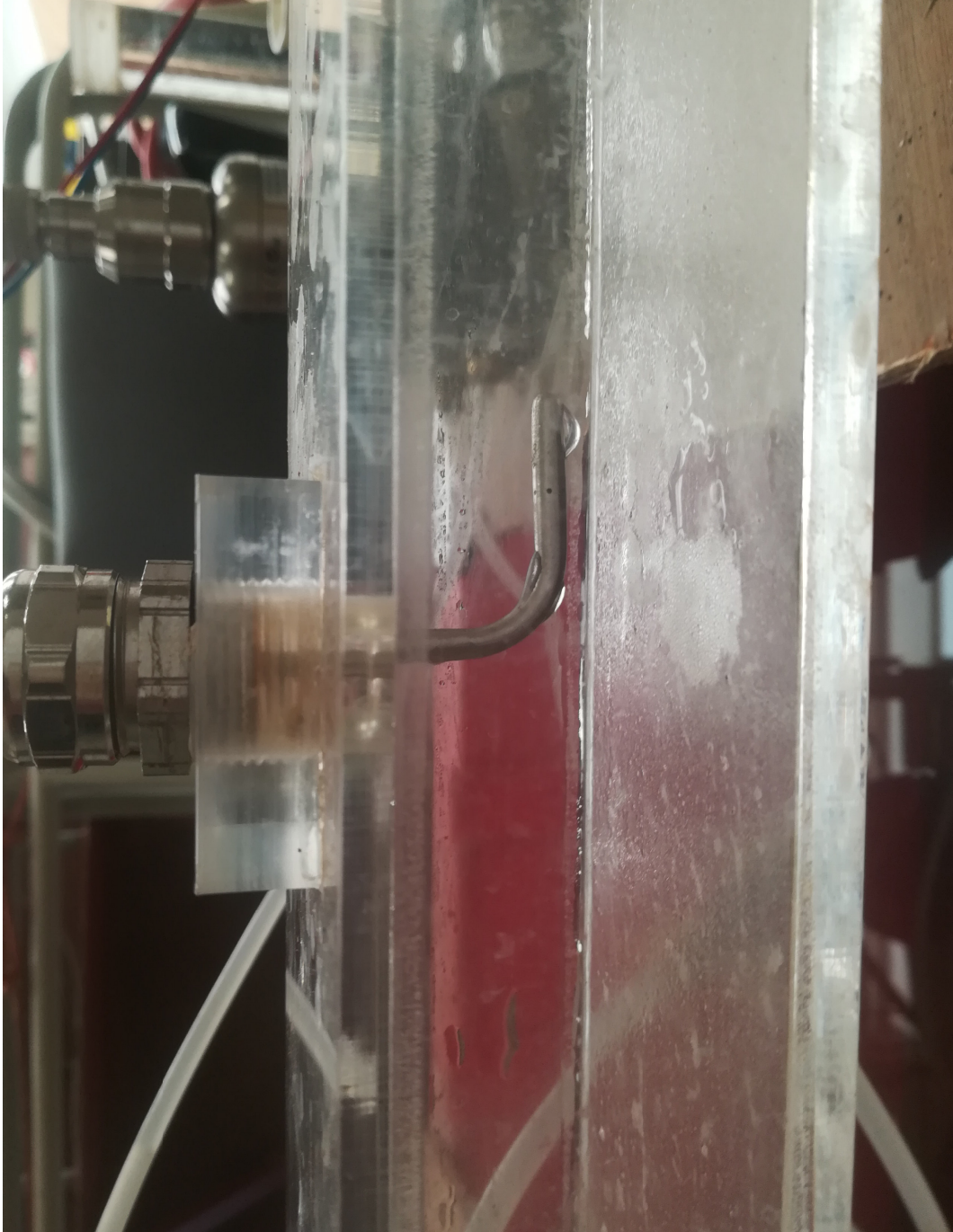


Figure H.7: Result connection pitot tube



Figure H.8: Result soil feeding mechanism and polyflow connectors



Figure H.9: Result soil container



Testing forms

This appendix lists the forms which were used to characterize the erosion tests. For completeness they are all posted here in order that the results can be looked into once more and there is complete transparency in how the results were obtained.

I.1. Proof of concept testing

In this section the proof of concept testing forms are displayed, and will concern the following topics:

- The pumping curve
- Repeatability testing
- Sensitivity analysis (i.e. effects of protrusion and diameter)
- Time-effects

As one might recall, in the main report there was also looked into the system accuracy and the validation of CFD modelling. However, this has been done by using the data that was generated by the above. More specifically, the system accuracy and the CFD modelling was investigated using the pumping curve data and the data of the sensitivity analysis.

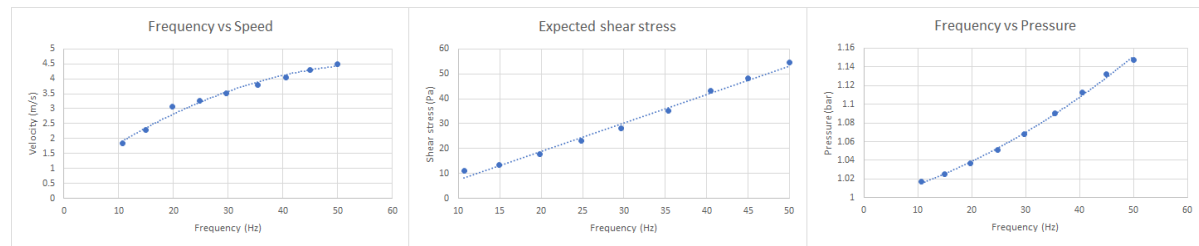


Figure I.1: Idealized pumping curve

I.1.1. Pumping curve testing

This subsection lists the testing form used to establish a pumping curve. A granite sample with a diameter of 38.01 mm was protruding 0.96 mm into the erosion flume. The sample was then tested at various pumping frequency decreasing from 50 hz to 45 hz to 40 hz back to 10 hz. This resulted in the following.

Pumping curve			
Goal: Establishing pumping curve			
Soil properties			
Diameter		38.01 mm	
Protrusion		0.96 mm	
Frequency (Hz)	Velocity (m/s)	Shear stress (Pa)	Absolute pressure (bar)
50	4.50	54.51	1.15
45	4.31	48.21	1.13
40.52	4.06	43.05	1.11
35.36	3.79	35.04	1.09
29.69	3.51	28.16	1.07
24.81	3.27	23.01	1.05
19.79	3.06	17.85	1.04
14.88	2.29	13.38	1.03
10.70	1.83	10.98	1.02

I.1.2. Repeatability testing

This subsection presents the results of the repeatability tests. All samples have been tested at the maximum velocity of the flume, because it is assumed that at a maximum velocity the differences in the repeatability of the results is minimal.

Repeatability test Kampen III clay							
Goal: prove the repeatability of testing Kampen III clay							
Soil properties							
$\rho_d(Mg/m^3)$				1.836			
$w(\%)$				0.126			
$\rho_b(Mg/m^3)$				2.067			
#1		#2		#3		#4	
diameter (mm)	38.6	diameter (mm)	42.09	diameter (mm)	40.4	diameter (mm)	36.29
protrusion (mm)	1.23	protrusion (mm)	1.34	protrusion (mm)	1.67	protrusion (mm)	0.89
shear stress (Pa)	65	shear stress (Pa)	120	shear stress (Pa)	90	shear stress (Pa)	95
velocity (m/s)	3.59	velocity (m/s)	3.51	velocity (m/s)	3.01	velocity (m/s)	3.76
erosion rate (mm/hour)	155	erosion rate (mm/hour)	126	erosion rate (mm/hour)	140	erosion rate (mm/hour)	143

Repeatability test Boom clay (Proctor density, optimum water content)							
Goal: prove the repeatability of testing Kampen III clay							
Soil properties							
$\rho_d(Mg/m^3)$				1.429			
$w(\%)$				0.301			
$\rho_b(Mg/m^3)$				1.859			
#1		#2		#3		#4	
diameter (mm)	42.59	diameter (mm)	38.5	diameter (mm)	39.49	diameter (mm)	40.22
protrusion (mm)	1.24	protrusion (mm)	1.66	protrusion (mm)	1.32	protrusion (mm)	1.07
shear stress (Pa)	48	shear stress (Pa)	53.4	shear stress (Pa)	44.1	shear stress (Pa)	55
velocity (m/s)	4.22	velocity (m/s)	4.2	velocity (m/s)	4.19	velocity (m/s)	4.17
erosion rate (mm/hour)	27.4	erosion rate (mm/hour)	26.8	erosion rate (mm/hour)	26.7	erosion rate (mm/hour)	26.5

I.1.3. Sensitivity testing

This subsection lists the testing forms used to establish results concerning sensitivity testing. More specifically, what the impact is of varying protrusion and diameter. The results of these tests have been discussed in chapter C.

Varying protrusion

Varying protrusion								
Sample type			Granite sample 38 mm, varying protrusion					
Goal: establishing different pumping curves for the same granite sample, with different protrusions								
Protrusion # 1			Protrusion # 2			Protrusion # 3		
Diameter (mm)	38.01		Diameter (mm)	38.01		Diameter (mm)	38.01	
Initial protrusion (mm)	0.96		Initial protrusion (mm)	2.23		Initial protrusion (mm)	4.03	
Testing frequency	Shear stress	Flow velocity	Testing frequency	Shear stress	Flow velocity	Testing frequency	Shear stress	Flow velocity
50.0	49.12	3.98	50.0	66.16	3.90	50.0	94.28	3.96
45.06	42.60081	3.73037	44.97	57.72514	3.655797	44.18	78.12317	3.619163
40.5	35.2038	3.400104	39.98	45.99348	3.27689	39.73	63.96812	3.275587
34.89	26.28673	3.040457	34.92	35.74997	2.907696	35.08	50.23054	2.926979
29.96	20.81574	2.741794	29.32	26.95148	2.51149	30.07	38.15929	2.61933
25.16	15.42301	2.472453	24.96	20.34659	2.209205	24.63	28.0151	2.35501
19.97	10.53085	2.238675	19.99	13.99129	1.944419	20.03	19.31885	2.101169
15.52	7.347267	2.076883	15.09	9.060066	1.762983	15.07	11.06278	1.856236
10.05	4.253664	1.843384	10.07	5.56474	1.586983	N.A	N.A	N.A

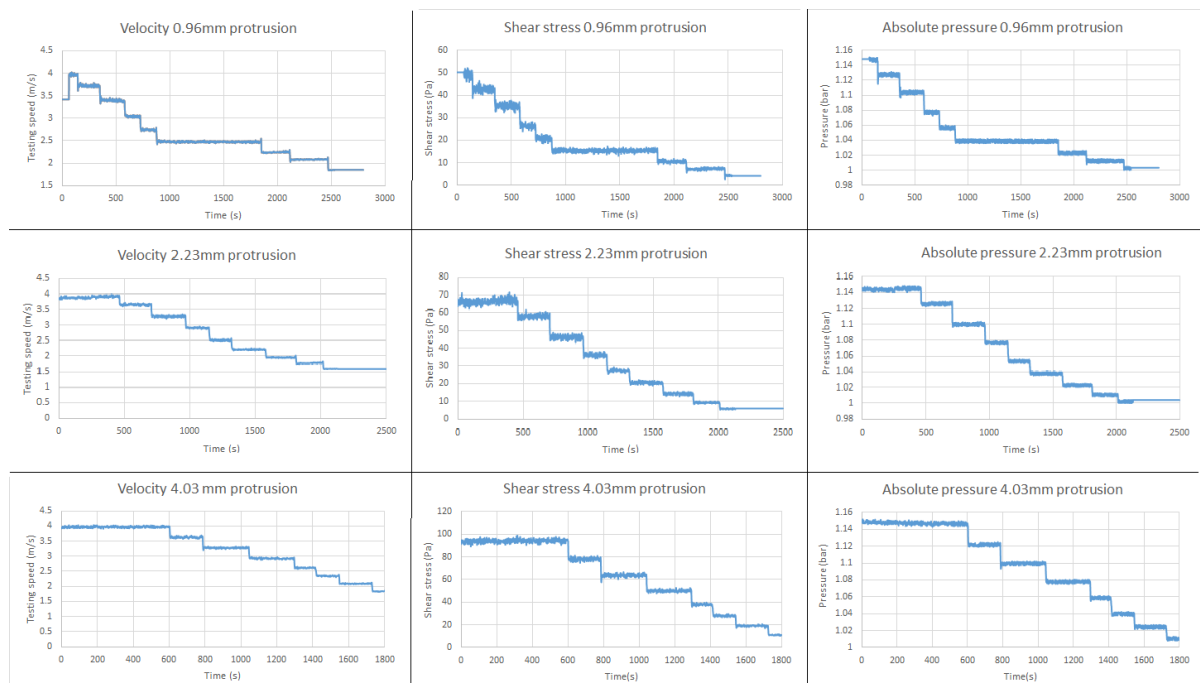


Figure I.2: Output graphs from protrusion differences

Varying diameter

Varying diameter								
Sample type			Granite sample varying diameter, +/- 1mm protrusion					
Goal: establishing different pumping curves for granite samples with different diameter, with the same protrusion								
Diameter # 1			Diameter # 2			Diameter # 3		
Diameter (mm)	38.01		Diameter (mm)	40.61		Diameter (mm)	41.80	
Initial protrusion (mm)	0.96		Initial protrusion (mm)	1.03		Initial protrusion (mm)	1.01	
Testing frequency	Shear stress	Flow velocity	Testing frequency	Shear stress	Flow velocity	Testing frequency	Shear stress	Flow velocity
50.0	49.12	3.98	50	65.64399	3.794277	50	69.1627	3.808087
45.06	42.60081	3.73037	45.28	57.91103	3.536403	44.59	61.16167	3.502547
40.5	35.2038	3.400104	39.88	45.15961	3.104932	39.89	51.69422	3.114826
34.89	26.28673	3.040457	35.27	35.6978	2.734495	35.07	43.08469	2.566354
29.96	20.81574	2.741794	30.07	26.79542	2.39356	29.1	35.63189	2.14813
25.16	15.42301	2.472453	24.63	18.45847	2.058651	25.06	29.16591	1.87932
19.97	10.53085	2.238675	20.03	12.70192	1.798135	20.17	19.85177	1.507915
15.52	7.347267	2.076883	15.07	8.278042	1.554751	14.97	12.08747	1.1497
10.05	4.253664	1.843384	9.72	4.725424	1.333711	8.59	2.835015	0.857914

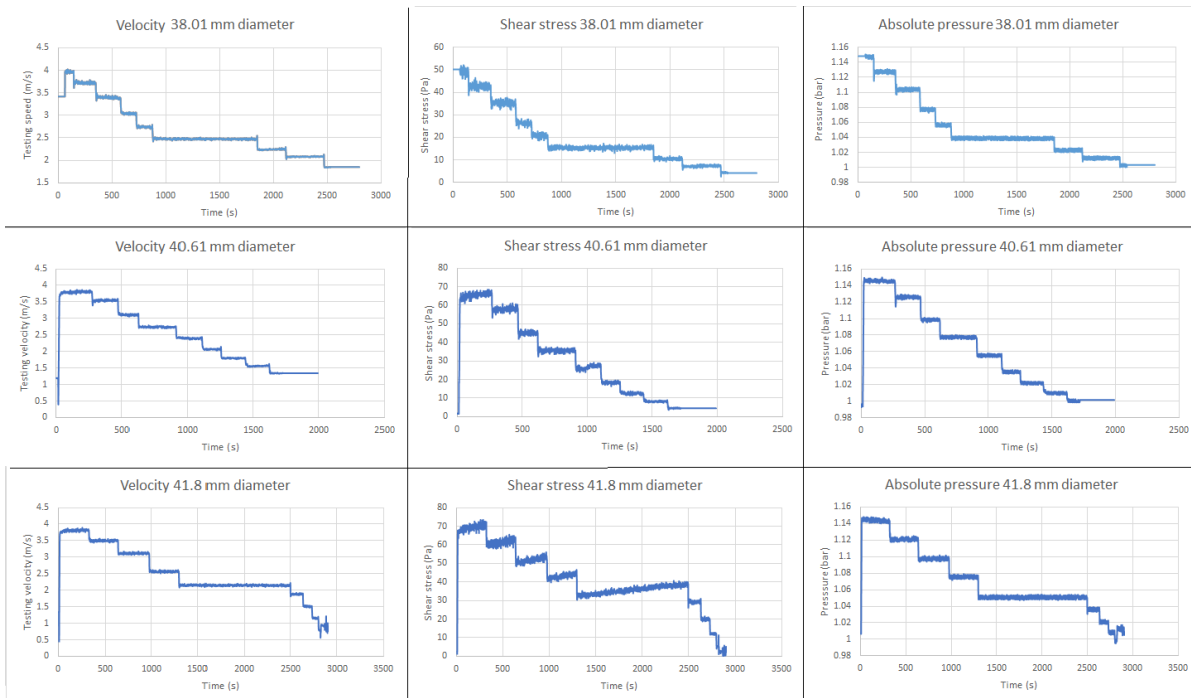


Figure I.3: Output graphs from diameter differences

I.1.4. Time-influence testing

This subsection gives the

I.2. Erosion testing

This section lists all the results from all erosion tests.

I.2.1. Testing Kampen III proctor

Erosion test							
Bag identification				ψ			
Sample description				Kampen III, proctor density, drier than optimum			
Soil properties							
$\rho_d(Mg/m^3)$				1.821			
$w(\%)$				0.128			
$\rho_b(Mg/m^3)$				2.05			
Test #1		Test #2		Test #3		Test #4	
Diameter (mm)	40.14	Diameter (mm)	41.09	Diameter (mm)	n.a.	Diameter (mm)	n.a.
Initial Protrusion (mm)	1.8	Initial Protrusion (mm)	1.2	Initial Protrusion (mm)	n.a.	Initial Protrusion (mm)	n.a.
Testing speed (m/s)	3.24	Testing speed (m/s)	4.19	Testing speed (m/s)	n.a.	Testing speed (m/s)	n.a.
Shear stress (Pa)	5.63	Shear stress (Pa)	41.47	Shear stress (Pa)	n.a.	Shear stress (Pa)	n.a.
Erosion rate (mm/hour)	29.75	Erosion rate (mm/hour)	66.47	Erosion rate (mm/hour)	n.a.	Erosion rate (mm/hour)	n.a.
Erosion curve results							
$\tau_{auc}(Pa)$		1.2		$S_i(mm/hr/Pa)$		15.3225	
$\epsilon_{3.2Pa}(mm/hr)$	19.38	$\epsilon_{7.0Pa}(mm/hr)$	33.77	$\epsilon_{15Pa}(mm/hr)$	47.78	$\epsilon_{32.4Pa}(mm/hr)$	61.94

Erosion test							
Bag identification				χ			
Sample description				Kampen III, proctor density, optimum water content			
Soil properties							
$\rho_d(Mg/m^3)$				1.843			
$w(\%)$				0.132			
$\rho_b(Mg/m^3)$				2.09			
Test #1		Test #2		Test #3		Test #4	
Diameter (mm)	40.4	Diameter (mm)	39.64	Diameter (mm)	n.a.	Diameter (mm)	n.a.
Initial Protrusion (mm)	2.15	Initial Protrusion (mm)	1.78	Initial Protrusion (mm)	n.a.	Initial Protrusion (mm)	n.a.
Testing speed (m/s)	3.61	Testing speed (m/s)	4.22	Testing speed (m/s)	n.a.	Testing speed (m/s)	n.a.
Shear stress (Pa)	19.32	Shear stress (Pa)	37.64	Shear stress (Pa)	n.a.	Shear stress (Pa)	n.a.
Erosion rate (mm/hour)	3.50	Erosion rate (mm/hour)	97.87	Erosion rate (mm/hour)	n.a.	Erosion rate (mm/hour)	n.a.
Erosion curve results							
$\tau_c(Pa)$		18.8		$S_i(mm/hr/Pa)$		7.52	
$\epsilon_{3.2Pa}$	0	$\epsilon_{7.0Pa}$	0	$\epsilon_{15.0Pa}$	0	$\epsilon_{32.4Pa}$	0

Erosion test							
Bag identification				τ			
Sample description				Kampen III, proctor density, optimum water content			
Soil properties							
$\rho_d(Mg/m^3)$				1.845			
$w(\%)$				0.141			
$\rho_b(Mg/m^3)$				2.11			
Test #1		Test #2		Test #3		Test #4	
Diameter (mm)		Diameter (mm)		Diameter (mm)	n.a.	Diameter (mm)	n.a.
Initial Protrusion (mm)	1.24	Initial Protrusion (mm)	1.67	Initial Protrusion (mm)	1.56	Initial Protrusion (mm)	n.a.
Testing speed (m/s)	3.24	Testing speed (m/s)	3.90	Testing speed (m/s)	4.47	Testing speed (m/s)	n.a.
Shear stress (Pa)	12.91	Shear stress (Pa)	38.87	Shear stress (Pa)	51.55	Shear stress (Pa)	n.a.
Erosion rate (mm/hour)	12.82	Erosion rate (mm/hour)	18.045	Erosion rate (mm/hour)	75.53	Erosion rate (mm/hour)	n.a.
Erosion curve results							
$\tau_c(Pa)$		10.4		$S_i(mm/hr/Pa)$		3.26	
$\epsilon_{3.2Pa}$	0	$\epsilon_{7.0Pa}$	0	$\epsilon_{15.0Pa}$	12.48	$\epsilon_{32.4Pa}$	38.56

Erosion test							
Bag identification		ρ					
Sample description		Kampen III, proctor density, slightly above optimum water content					
Soil properties							
$\rho_d(Mg/m^3)$		1.802					
$w(\%)$		0.158					
$\rho_b(Mg/m^3)$		2.09					
Test #1		Test #2		Test #3		Test #4	
Diameter (mm)		Diameter (mm)		Diameter (mm)	n.a.	Diameter (mm)	n.a.
Initial Protrusion (mm)	1.36	Initial Protrusion (mm)	1.39	Initial Protrusion (mm)	1.42	Initial Protrusion (mm)	n.a.
Testing speed (m/s)	3.52	Testing speed (m/s)	4.26	Testing speed (m/s)	4.53	Testing speed (m/s)	n.a.
Shear stress (Pa)	11.62	Shear stress (Pa)	49.32	Shear stress (Pa)	59.70	Shear stress (Pa)	n.a.
Erosion rate (mm/hour)	10.1	Erosion rate (mm/hour)	450	Erosion rate (mm/hour)	516	Erosion rate (mm/hour)	n.a.
Erosion curve results							
$\tau_c(Pa)$		11.2		$S_i(mm/hr/Pa)$		27.43	
$\epsilon_{3.2Pa}$	0	$\epsilon_{7.0Pa}$	0	$\epsilon_{15.0Pa}$	88.19	$\epsilon_{32.4Pa}$	324.79

Erosion test							
Bag identification		π					
Sample description		Kampen III, proctor density, above optimum water content					
Soil properties							
$\rho_d(Mg/m^3)$		1.775					
$w(\%)$		0.167					
$\rho_b(Mg/m^3)$		2.07					
Test #1		Test #2		Test #3		Test #4	
Diameter (mm)		Diameter (mm)		Diameter (mm)	n.a.	Diameter (mm)	n.a.
Initial Protrusion (mm)	1.12	Initial Protrusion (mm)	1.17	Initial Protrusion (mm)	1.29	Initial Protrusion (mm)	n.a.
Testing speed (m/s)	3.24	Testing speed (m/s)	3.89	Testing speed (m/s)	4.16	Testing speed (m/s)	n.a.
Shear stress (Pa)	10.41	Shear stress (Pa)	29.31	Shear stress (Pa)	43.63	Shear stress (Pa)	n.a.
Erosion rate (mm/hour)	9.25	Erosion rate (mm/hour)	275	Erosion rate (mm/hour)	289.53	Erosion rate (mm/hour)	n.a.
Erosion curve results							
$\tau_c(Pa)$		8.9		$S_i(mm/hr/Pa)$		20.32	
$\epsilon_{3.2Pa}$	0	$\epsilon_{7.0Pa}$	0	$\epsilon_{15.0Pa}$	92.36	$\epsilon_{32.4Pa}$	231.03

I.2.2. Testing Kampen III modified proctor

Erosion test							
Bag identification				μ			
Sample description				Kampen III, proctor density, far above optimum water content			
Soil properties							
$\rho_d(Mg/m^3)$				1.716			
$w(\%)$				0.190			
$\rho_b(Mg/m^3)$				2.04			
Test #1		Test #2		Test #3		Test #4	
Diameter (mm)		Diameter (mm)		Diameter (mm)	n.a.	Diameter (mm)	n.a.
Initial Protrusion (mm)	1.06	Initial Protrusion (mm)	1.08	Initial Protrusion (mm)	1.21	Initial Protrusion (mm)	n.a.
Testing speed (m/s)	3.24	Testing speed (m/s)	3.66	Testing speed (m/s)	3.98	Testing speed (m/s)	n.a.
Shear stress (Pa)	17.00	Shear stress (Pa)	24.73	Shear stress (Pa)	44.31	Shear stress (Pa)	n.a.
Erosion rate (mm/hour)	105	Erosion rate (mm/hour)	118.85	Erosion rate (mm/hour)	138.075	Erosion rate (mm/hour)	n.a.
Erosion curve results							
$\tau_c(Pa)$		0.8		$S_i(mm/hr/Pa)$		42.99	
$\epsilon_{3.2Pa}$	47.92	$\epsilon_{7.0Pa}$	74.84	$\epsilon_{15.0Pa}$	101.06	$\epsilon_{32.4Pa}$	127.54

Erosion test							
Bag identification				ν			
Sample description				Kampen III, Modified proctor density, below optimum water content			
Soil properties							
$\rho_d(Mg/m^3)$				1.966			
$w(\%)$				0.094			
$\rho_b(Mg/m^3)$				2.15			
Test #1		Test #2		Test #3		Test #4	
Diameter (mm)		Diameter (mm)		Diameter (mm)		Diameter (mm)	n.a.
Initial Protrusion (mm)	1.16	Initial Protrusion (mm)	1.11	Initial Protrusion (mm)	1.08	Initial Protrusion (mm)	n.a.
Testing speed (m/s)	3.59	Testing speed (m/s)	4.16	Testing speed (m/s)	4.47	Testing speed (m/s)	n.a.
Shear stress (Pa)	25.87	Shear stress (Pa)	50.25	Shear stress (Pa)	67.24	Shear stress (Pa)	n.a.
Erosion rate (mm/hour)	8.95	Erosion rate (mm/hour)	11.58	Erosion rate (mm/hour)	11.11	Erosion rate (mm/hour)	n.a.
Erosion curve results							
$\tau_c(Pa)$		0.7		$S_i(mm/hr/Pa)$		3.64	
$\epsilon_{3.2Pa}$	3.84	$\epsilon_{7.0Pa}$	5.83	$\epsilon_{15.0Pa}$	7.78	$\epsilon_{32.4Pa}$	9.74

I.2.3. Testing Kampen II lighter proctor

Erosion test							
Bag identification				ω			
Sample description				Kampen III, Modified proctor density, optimum water content			
Soil properties							
$\rho_d (Mg/m^3)$				1.984			
$w(\%)$				0.117			
$\rho_b (Mg/m^3)$				2.216			
Test #1		Test #2		Test #3		Test #4	
Diameter (mm)		Diameter (mm)		Diameter (mm)		Diameter (mm)	n.a.
Initial Protrusion (mm)	1.37	Initial Protrusion (mm)	1.63	Initial Protrusion (mm)	1.21	Initial Protrusion (mm)	n.a.
Testing speed (m/s)	3.60	Testing speed (m/s)	4.14	Testing speed (m/s)	4.47	Testing speed (m/s)	n.a.
Shear stress (Pa)	25.87	Shear stress (Pa)	37.79	Shear stress (Pa)	67.24	Shear stress (Pa)	n.a.
Erosion rate (mm/hour)	13.9	Erosion rate (mm/hour)	20.13	Erosion rate (mm/hour)	21.93	Erosion rate (mm/hour)	n.a.
Erosion curve results							
$\tau_c (Pa)$		4.2		$S_i (mm/hr/Pa)$		1.96	
$\epsilon_{3.2Pa}$	0	$\epsilon_{7.0Pa}$	4.09	$\epsilon_{15.0Pa}$	10.37	$\epsilon_{32.4Pa}$	16.71

Erosion test							
Bag identification				ϕ			
Sample description				Kampen III, Modified proctor density, above optimum water content			
Soil properties							
$\rho_d (Mg/m^3)$				1.921			
$w(\%)$				0.138			
$\rho_b (Mg/m^3)$				2.19			
Test #1		Test #2		Test #3		Test #4	
Diameter (mm)		Diameter (mm)		Diameter (mm)		Diameter (mm)	n.a.
Initial Protrusion (mm)	1.03	Initial Protrusion (mm)	1.25	Initial Protrusion (mm)	1.16	Initial Protrusion (mm)	n.a.
Testing speed (m/s)	3.28	Testing speed (m/s)	3.96	Testing speed (m/s)	4.36	Testing speed (m/s)	n.a.
Shear stress (Pa)	8.09	Shear stress (Pa)	39.15	Shear stress (Pa)	60.01	Shear stress (Pa)	n.a.
Erosion rate (mm/hour)	12.14	Erosion rate (mm/hour)	27.18	Erosion rate (mm/hour)	47.35	Erosion rate (mm/hour)	n.a.
Erosion curve results							
$\tau_c (Pa)$		4.0		$S_i (mm/hr/Pa)$		3.84	
$\epsilon_{3.2Pa}$	0	$\epsilon_{7.0Pa}$	8.29	$\epsilon_{15.0Pa}$	20.02	$\epsilon_{32.4Pa}$	31.87

I.2.4. Testing Kampen II proctor

N.B. During test Pitot tube was faulty and therefore no speed measurements were made.

Erosion test							
Bag identification				β			
Sample description				Kampen II, Sub-proctor density, below optimum water content			
Soil properties							
$\rho_d (Mg/m^3)$				1.619			
$w(\%)$				0.162			
$\rho_b (Mg/m^3)$				1.881			
Test #1		Test #2		Test #3		Test #4	
Diameter (mm)		Diameter (mm)		Diameter (mm)		Diameter (mm)	
Initial Protrusion (mm)		Initial Protrusion (mm)		Initial Protrusion (mm)		Initial Protrusion (mm)	
Testing speed (m/s)		Testing speed (m/s)		Testing speed (m/s)		Testing speed (m/s)	
Shear stress (Pa)		Shear stress (Pa)		Shear stress (Pa)		Shear stress (Pa)	
Erosion rate (mm/hour)		Erosion rate (mm/hour)		Erosion rate (mm/hour)		Erosion rate (mm/hour)	
Erosion curve results							
$\tau_c (Pa)$				9.0			
$\epsilon_{3.2Pa}$				0			
$\tau_c (Pa)$				$S_i (mm/hr/Pa)$			
$\epsilon_{7.0Pa}$				0			
$\epsilon_{15.0Pa}$				30.48			
$\epsilon_{32.4Pa}$				76.65			

Erosion test							
Bag identification				γ			
Sample description				Kampen II, Sub-proctor density, just below optimum water content			
Soil properties							
$\rho_d (Mg/m^3)$				1.640			
$w(\%)$				0.188			
$\rho_b (Mg/m^3)$				1.948			
Test #1		Test #2		Test #3		Test #4	
Diameter (mm)		Diameter (mm)		Diameter (mm)		Diameter (mm)	
Initial Protrusion (mm)		Initial Protrusion (mm)		Initial Protrusion (mm)		Initial Protrusion (mm)	
Testing speed (m/s)		Testing speed (m/s)		Testing speed (m/s)		Testing speed (m/s)	
Shear stress (Pa)		Shear stress (Pa)		Shear stress (Pa)		Shear stress (Pa)	
Erosion rate (mm/hour)		Erosion rate (mm/hour)		Erosion rate (mm/hour)		Erosion rate (mm/hour)	
Erosion curve results							
$\tau_c (Pa)$				19.8			
$\epsilon_{3.2Pa}$				0			
$\tau_c (Pa)$				$S_i (mm/hr/Pa)$			
$\epsilon_{7.0Pa}$				0			
$\epsilon_{15.0Pa}$				0			
$\epsilon_{32.4Pa}$				11.42			

1.2.5. Testing Kampen II modified proctor

Erosion test							
Bag identification				η			
Sample description				Kampen II, Sub-proctor density, just above optimum water content			
Soil properties							
$\rho_d (Mg/m^3)$				1.636			
$w(\%)$				0.216			
$\rho_b (Mg/m^3)$				1.99			
Test #1		Test #2		Test #3		Test #4	
Diameter (mm)		Diameter (mm)		Diameter (mm)		Diameter (mm)	n.a.
Initial Protrusion (mm)	1.08	Initial Protrusion (mm)	0.91	Initial Protrusion (mm)	1.12	Initial Protrusion (mm)	n.a.
Testing speed (m/s)	3.61	Testing speed (m/s)	4.19	Testing speed (m/s)	4.47	Testing speed (m/s)	n.a.
Shear stress (Pa)	26.27	Shear stress (Pa)	55.44	Shear stress (Pa)	72.57	Shear stress (Pa)	n.a.
Erosion rate (mm/hour)	9.44	Erosion rate (mm/hour)	13.6	Erosion rate (mm/hour)	59.47	Erosion rate (mm/hour)	n.a.
Erosion curve results							
$\tau_c (Pa)$		23.7		$S_i (mm/hr/Pa)$		1.68	
$\epsilon_{3.2Pa}$	0	$\epsilon_{7.0Pa}$	0	$\epsilon_{15.0Pa}$	0	$\epsilon_{32.4Pa}$	12.44

Erosion test							
Bag identification				θ			
Sample description				Kampen II, Sub-proctor density, above optimum water content			
Soil properties							
$\rho_d (Mg/m^3)$				1.597			
$w(\%)$				0.242			
$\rho_b (Mg/m^3)$				1.98			
Test #1		Test #2		Test #3		Test #4	
Diameter (mm)		Diameter (mm)		Diameter (mm)		Diameter (mm)	n.a.
Initial Protrusion (mm)	1.01	Initial Protrusion (mm)	0.98	Initial Protrusion (mm)	1.12	Initial Protrusion (mm)	n.a.
Testing speed (m/s)	3.26	Testing speed (m/s)	3.93	Testing speed (m/s)	4.36	Testing speed (m/s)	n.a.
Shear stress (Pa)	19.86	Shear stress (Pa)	33.75	Shear stress (Pa)	69.20	Shear stress (Pa)	n.a.
Erosion rate (mm/hour)	0	Erosion rate (mm/hour)	15.38	Erosion rate (mm/hour)	83.20	Erosion rate (mm/hour)	n.a.
Erosion curve results							
$\tau_c (Pa)$		28.6		$S_i (mm/hr/Pa)$		3.30	
$\epsilon_{3.2Pa}$	0	$\epsilon_{7.0Pa}$	0	$\epsilon_{15.0Pa}$	0	$\epsilon_{32.4Pa}$	11.51

I.2.6. Testing Boom clay lighter proctor

Erosion test							
Bag identification				v			
Sample description				Kampen II, Sub-proctor density, far above optimum water content			
Soil properties							
$\rho_d (Mg/m^3)$				1.536			
$w(\%)$				0.269			
$\rho_b (Mg/m^3)$				1.95			
Test #1		Test #2		Test #3		Test #4	
Diameter (mm)		Diameter (mm)		Diameter (mm)		Diameter (mm)	n.a.
Initial Protrusion (mm)	1.09	Initial Protrusion (mm)	1.21	Initial Protrusion (mm)	1.33	Initial Protrusion (mm)	n.a.
Testing speed (m/s)	3.59	Testing speed (m/s)	4.16	Testing speed (m/s)	4.47	Testing speed (m/s)	n.a.
Shear stress (Pa)	25.87	Shear stress (Pa)	50.25	Shear stress (Pa)	67.24	Shear stress (Pa)	n.a.
Erosion rate (mm/hour)	8.95	Erosion rate (mm/hour)	11.58	Erosion rate (mm/hour)	11.11	Erosion rate (mm/hour)	n.a.
Erosion curve results							
$\tau_c (Pa)$		0.7		$S_i (mm/hr/Pa)$		3.64	
$\epsilon_{3.2Pa}$	3.84	$\epsilon_{7.0Pa}$	5.83	$\epsilon_{15.0Pa}$	7.78	$\epsilon_{32.4Pa}$	9.74

Erosion test							
Bag identification				κ			
Sample description				Kampen II, Proctor density, far below optimum water content			
Soil properties							
$\rho_d (Mg/m^3)$				1.633			
$w(\%)$				0.162			
$\rho_b (Mg/m^3)$				1.897			
Test #1		Test #2		Test #3		Test #4	
Diameter (mm)		Diameter (mm)		Diameter (mm)		Diameter (mm)	n.a.
Initial Protrusion (mm)	1.21	Initial Protrusion (mm)	1.07	Initial Protrusion (mm)	1.11	Initial Protrusion (mm)	n.a.
Testing Speed (m/s)	3.24	Testing Speed (m/s)	3.95	Testing Speed (m/s)	3.34	Testing Speed (m/s)	n.a.
Shear stress (Pa)	4.96	Shear stress (Pa)	36.46	Shear stress (Pa)	60.56	Shear stress (Pa)	n.a.
Erosion rate (mm/hour)	45.68	Erosion rate (mm/hour)	190.42	Erosion rate (mm/hour)	198	Erosion rate (mm/hour)	n.a.
Erosion curve results							
$\tau_c (Pa)$		2.3		$S_i (mm/hr/Pa)$		27.90	
$\tau_{3.2Pa}$	20.42	$\tau_{7.0Pa}$	70.64	$\tau_{15.0Pa}$	119.54	$\tau_{32.4Pa}$	168.95

1.2.7. Testing Boom clay proctor

Erosion test							
Bag identification				t			
Sample description				Kampen II, Proctor density, optimum water content			
Soil properties							
ρ_d (Mg/m ³)				1.708			
w(%)				0.176			
ρ_b (Mg/m ³)				2.009			
Test #1		Test #2		Test #3		Test #4	
Diameter (mm)		Diameter (mm)		Diameter (mm)		Diameter (mm)	n.a.
Initial Protrusion (mm)	1.02	Initial Protrusion (mm)	0.93	Initial Protrusion (mm)	1.05	Initial Protrusion (mm)	n.a.
Testing Speed (m/s)	3.21	Testing Speed (m/s)	3.89	Testing Speed (m/s)	4.33	Testing Speed (m/s)	n.a.
Shear stress (Pa)	6.72	Shear stress (Pa)	29.88	Shear stress (Pa)	60.95	Shear stress (Pa)	n.a.
Erosion rate (mm/hour)	2.34	Erosion rate (mm/hour)	10.17	Erosion rate (mm/hour)	10.925	Erosion rate (mm/hour)	n.a.
Erosion curve results							
τ_c (Pa)		3.4		S_f (mm/hr/Pa)		1.21	
$\tau_{3.2Pa}$	0	$\tau_{7.0Pa}$	2.90	$\tau_{15.0Pa}$	6.03	$\tau_{32.4Pa}$	9.20

Erosion test							
Bag identification							
Sample description				Kampen II, Proctor density, just above optimum water content			
Soil properties							
ρ_d (Mg/m ³)				1.800			
w(%)				0.182			
ρ_b (Mg/m ³)				2.127			
Test #1		Test #2		Test #3		Test #4	
Diameter (mm)		Diameter (mm)		Diameter (mm)		Diameter (mm)	n.a.
Initial Protrusion (mm)	1.13	Initial Protrusion (mm)	1.24	Initial Protrusion (mm)	n.a.	Initial Protrusion (mm)	n.a.
Testing Speed (m/s)	3.61	Testing Speed (m/s)	4.22	Testing Speed (m/s)	n.a.	Testing Speed (m/s)	n.a.
Shear stress (Pa)	19.315	Shear stress (Pa)	37.64	Shear stress (Pa)	n.a.	Shear stress (Pa)	n.a.
Erosion rate (mm/hour)	3.50	Erosion rate (mm/hour)	97.87	Erosion rate (mm/hour)	n.a.	Erosion rate (mm/hour)	n.a.
Erosion curve results							
τ_c (Pa)		18.8		S_f (mm/hr/Pa)		7.52	
$\tau_{3.2Pa}$	0	$\tau_{7.0Pa}$	0	$\tau_{15.0Pa}$	0	$\tau_{32.4Pa}$	76.70

I.2.8. Testing Boom clay modified proctor

Erosion test							
Bag identification				c			
Sample description				Kampen II, Proctor density, above water content			
Soil properties							
ρ_d (Mg/m ³)				1.678			
w (%)				0.194			
ρ_b (Mg/m ³)				2.003			
Test #1		Test #2		Test #3		Test #4	
Diameter (mm)		Diameter (mm)		Diameter (mm)		Diameter (mm)	n.a.
Initial Protrusion (mm)	0.83	Initial Protrusion (mm)	1.12	Initial Protrusion (mm)	1.06	Initial Protrusion (mm)	n.a.
Testing Speed (m/s)	N.A.	Testing Speed (m/s)	N.A.	Testing Speed (m/s)	N.a.	Testing Speed (m/s)	n.a.
Shear stress (Pa)	37.29	Shear stress (Pa)	57.85	Shear stress (Pa)	70.67	Shear stress (Pa)	n.a.
Erosion rate (mm/hour)	58.66	Erosion rate (mm/hour)	64	Erosion rate (mm/hour)	390.6	Erosion rate (mm/hour)	n.a.
Erosion curve results							
τ_c (Pa)		36.1		S_i (mm/hr/Pa)		12.08	
$\tau_{3.2Pa}$	0	$\tau_{7.0Pa}$	0	$\tau_{15.0Pa}$	0	$\tau_{32.4Pa}$	0

Erosion test							
Bag identification				d			
Sample description				Kampen II, Proctor density, above water content			
Soil properties							
ρ_d (Mg/m ³)				1.619			
w (%)				0.242			
ρ_b (Mg/m ³)				2.011			
Test #1		Test #2		Test #3		Test #4	
Diameter (mm)		Diameter (mm)		Diameter (mm)		Diameter (mm)	n.a.
Initial Protrusion (mm)	1.14	Initial Protrusion (mm)	0.93	Initial Protrusion (mm)	1.22	Initial Protrusion (mm)	n.a.
Testing Speed (m/s)	3.26	Testing Speed (m/s)	3.57	Testing Speed (m/s)	4.15	Testing Speed (m/s)	n.a.
Shear stress (Pa)	6.72	Shear stress (Pa)	16.58	Shear stress (Pa)	60.95	Shear stress (Pa)	n.a.
Erosion rate (mm/hour)	0	Erosion rate (mm/hour)	10.84	Erosion rate (mm/hour)	61.66	Erosion rate (mm/hour)	n.a.
Erosion curve results							
τ_c (Pa)		12.6		S_i (mm/hr/Pa)		3.10	
$\tau_{3.2Pa}$	0	$\tau_{7.0Pa}$	0	$\tau_{15.0Pa}$	6.92	$\tau_{32.4Pa}$	36.99

Erosion test							
Bag identification							
Sample description				Kampen II, Proctor density, far above water content			
Soil properties							
ρ_d (Mg/m ³)				1.579			
w (%)				0.255			
ρ_b (Mg/m ³)				1.982			
Test #1		Test #2		Test #3		Test #4	
Diameter (mm)		Diameter (mm)		Diameter (mm)		Diameter (mm)	n.a.
Initial Protrusion (mm)	1.12	Initial Protrusion (mm)	1.35	Initial Protrusion (mm)	0.76	Initial Protrusion (mm)	n.a.
Testing Speed (m/s)	n.a.	Testing Speed (m/s)	n.a.	Testing Speed (m/s)	n.a.	Testing Speed (m/s)	n.a.
Shear stress (Pa)	11.53	Shear stress (Pa)	19.76	Shear stress (Pa)	44.01	Shear stress (Pa)	n.a.
Erosion rate (mm/hour)	254.7	Erosion rate (mm/hour)	350.6	Erosion rate (mm/hour)	444	Erosion rate (mm/hour)	n.a.
Erosion curve results							
τ_c (Pa)		1.75		S_i (mm/hr/Pa)		79.65	
$\tau_{3.2Pa}$	83.82	$\tau_{7.0Pa}$	192.91	$\tau_{15.0Pa}$	299.12	$\tau_{32.4Pa}$	406.45

Erosion test							
Bag identification				e			
Sample description				Kampen II, Modified Proctor density, far below optimum water content			
Soil properties							
ρ_d (Mg/m ³)				1.905			
w (%)				0.116			
ρ_b (Mg/m ³)				2.125			
Test #1		Test #2		Test #3		Test #4	
Diameter (mm)		Diameter (mm)		Diameter (mm)		Diameter (mm)	n.a.
Initial Protrusion (mm)	1.12	Initial Protrusion (mm)	1.08	Initial Protrusion (mm)	1.07	Initial Protrusion (mm)	n.a.
Testing Speed (m/s)	n.a.	Testing Speed (m/s)	n.a.	Testing Speed (m/s)	n.a.	Testing Speed (m/s)	n.a.
Shear stress (Pa)	14.24	Shear stress (Pa)	40.23	Shear stress (Pa)	49.19	Shear stress (Pa)	n.a.
Erosion rate (mm/hour)	51.25	Erosion rate (mm/hour)	103.7	Erosion rate (mm/hour)	118.85	Erosion rate (mm/hour)	n.a.
Erosion curve results							
τ_c (Pa)		5.47		S_i (mm/hr/Pa)		9.73	
$\tau_{3.2Pa}$	0	$\tau_{7.0Pa}$	13.05	$\tau_{15.0Pa}$	53.61	$\tau_{32.4Pa}$	94.60

Erosion test							
Bag identification		σ					
Sample description		Kampen II, Modified Proctor density, below optimum water content					
Soil properties							
ρ_d (Mg/m ³)		1.924					
w (%)		0.138					
ρ_b (Mg/m ³)		2.190					
Test #1		Test #2		Test #3		Test #4	
Diameter (mm)		Diameter (mm)		Diameter (mm)		Diameter (mm)	n.a.
Initial Protrusion (mm)	1.02	Initial Protrusion (mm)	1.03	Initial Protrusion (mm)	1.05	Initial Protrusion (mm)	n.a.
Testing Speed (m/s)	3.82	Testing Speed (m/s)	4.16	Testing Speed (m/s)	4.47	Testing Speed (m/s)	n.a.
Shear stress (Pa)	22.48	Shear stress (Pa)	40.24	Shear stress (Pa)	86.10	Shear stress (Pa)	n.a.
Erosion rate (mm/hour)	0	Erosion rate (mm/hour)	1.82	Erosion rate (mm/hour)	6.96	Erosion rate (mm/hour)	n.a.
Erosion curve results							
τ_c (Pa)		30.8		S_i (mm/hr/Pa)		0.22	
$\tau_{3.2Pa}$	0	$\tau_{7.0Pa}$	0	$\tau_{15.0Pa}$	0	$\tau_{32.4Pa}$	0.35

Erosion test							
Bag identification		ν					
Sample description		Kampen II, Modified Proctor density, below optimum water content					
Soil properties							
ρ_d (Mg/m ³)		1.871					
w (%)		0.152					
ρ_b (Mg/m ³)							
Test #1		Test #2		Test #3		Test #4	
Diameter (mm)		Diameter (mm)		Diameter (mm)		Diameter (mm)	n.a.
Initial Protrusion (mm)	0.96	Initial Protrusion (mm)	1.02	Initial Protrusion (mm)	1.05	Initial Protrusion (mm)	n.a.
Testing Speed (m/s)	3.59	Testing Speed (m/s)	4.16	Testing Speed (m/s)	4.47	Testing Speed (m/s)	n.a.
Shear stress (Pa)	25.87	Shear stress (Pa)	50.25	Shear stress (Pa)	67.24	Shear stress (Pa)	n.a.
Erosion rate (mm/hour)	8.95	Erosion rate (mm/hour)	11.10	Erosion rate (mm/hour)	11.57	Erosion rate (mm/hour)	n.a.
Erosion curve results							
τ_c (Pa)		0.7		S_i (mm/hr/Pa)		3.64	
$\tau_{3.2Pa}$	3.84	$\tau_{7.0Pa}$	5.83	$\tau_{15.0Pa}$	7.78	$\tau_{32.4Pa}$	9.74

Erosion test							
Bag identification							
Sample description		Kampen II, Sub-proctor density, way above optimum water content					
Soil properties							
ρ_d (Mg/m ³)		1.821					
w (%)		0.173					
ρ_b (Mg/m ³)		2.136					
Test #1		Test #2		Test #3		Test #4	
Diameter (mm)		Diameter (mm)		Diameter (mm)	n.a.	Diameter (mm)	n.a.
Initial Protrusion (mm)	1.23	Initial Protrusion (mm)	1.31	Initial Protrusion (mm)	n.a.	Initial Protrusion (mm)	n.a.
Testing speed (m/s)	3.24	Testing speed (m/s)	4.14	Testing speed (m/s)	n.a.	Testing speed (m/s)	n.a.
Shear stress (Pa)	15.47	Shear stress (Pa)	47.80	Shear stress (Pa)	n.a.	Shear stress (Pa)	n.a.
Erosion rate (mm/hour)	24.18	Erosion rate (mm/hour)	31.10	Erosion rate (mm/hour)	n.a.	Erosion rate (mm/hour)	n.a.
Erosion curve results							
τ_c (Pa)		0.3		S_i (mm/hr/Pa)		20.41	
$\epsilon_{3.2Pa}$	14.53	$\epsilon_{7.0Pa}$	19.32	$\epsilon_{15.0Pa}$	23.99	$\epsilon_{32.4Pa}$	28.71

Erosion test							
Bag identification		B					
Sample description		Boom clay, sub-proctor density, below optimum water content					
Soil properties							
ρ_d (Mg/m ³)		1.374					
w (%)		0.296					
ρ_b (Mg/m ³)		1.781					
Test #1		Test #2		Test #3		Test #4	
Diameter (mm)		Diameter (mm)		Diameter (mm)		Diameter (mm)	n.a.
Initial Protrusion (mm)	0.87	Initial Protrusion (mm)	1.23	Initial Protrusion (mm)	1.14	Initial Protrusion (mm)	n.a.
Testing speed (m/s)	3.62	Testing speed (m/s)	4.17	Testing speed (m/s)	5.05	Testing speed (m/s)	n.a.
Shear stress (Pa)	26.11	Shear stress (Pa)	51.55	Shear stress (Pa)	55.65	Shear stress (Pa)	n.a.
Erosion rate (mm/hour)	24.68	Erosion rate (mm/hour)	106.2	Erosion rate (mm/hour)	125.68	Erosion rate (mm/hour)	n.a.
Erosion curve results							
τ_c (Pa)		21.7		S_i (mm/hr/Pa)		5.907	
$\epsilon_{3.2Pa}$	0	$\epsilon_{7.0Pa}$	0	$\epsilon_{15.0Pa}$	0	$\epsilon_{32.4Pa}$	51.76

Erosion test							
Bag identification				C			
Sample description				Boom clay, sub-proctor density, optimum water content			
Soil properties							
$\rho_d(Mg/m^3)$				1.383			
$w(\%)$				0.323			
$\rho_b(Mg/m^3)$				1.829			
Test #1		Test #2		Test #3		Test #4	
Diameter (mm)		Diameter (mm)		Diameter (mm)		Diameter (mm)	n.a.
Initial Protrusion (mm)	1.21	Initial Protrusion (mm)	1.43	Initial Protrusion (mm)	0.97	Initial Protrusion (mm)	n.a.
Testing speed (m/s)	3.99	Testing speed (m/s)	4.20	Testing speed (m/s)	4.40	Testing speed (m/s)	n.a.
Shear stress (Pa)	27.02	Shear stress (Pa)	51.55	Shear stress (Pa)	63.95	Shear stress (Pa)	n.a.
Erosion rate (mm/hour)	0	Erosion rate (mm/hour)	9.64	Erosion rate (mm/hour)	15.26	Erosion rate (mm/hour)	n.a.
Erosion curve results							
$\tau_c(Pa)$		35.7		$S_i(mm/hr/Pa)$		0.731	
$\epsilon_{3.2Pa}$	0	$\epsilon_{7.0Pa}$	0	$\epsilon_{15.0Pa}$	0	$\epsilon_{32.4Pa}$	0

Erosion test							
Bag identification				D			
Sample description				Boom clay, sub-proctor density, above optimum water content			
Soil properties							
$\rho_d(Mg/m^3)$				1.310			
$w(\%)$				0.373			
$\rho_b(Mg/m^3)$				1.799			
Test #1		Test #2		Test #3		Test #4	
Diameter (mm)		Diameter (mm)		Diameter (mm)		Diameter (mm)	n.a.
Initial Protrusion (mm)		Initial Protrusion (mm)		Initial Protrusion (mm)		Initial Protrusion (mm)	n.a.
Testing speed (m/s)	3.59	Testing speed (m/s)	4.17	Testing speed (m/s)	4.47	Testing speed (m/s)	n.a.
Shear stress (Pa)	21.29	Shear stress (Pa)	62.30	Shear stress (Pa)	110.72	Shear stress (Pa)	n.a.
Erosion rate (mm/hour)	16.87	Erosion rate (mm/hour)	14.86	Erosion rate (mm/hour)	67.32	Erosion rate (mm/hour)	n.a.
Erosion curve results							
$\tau_c(Pa)$		15.2		$S_i(mm/hr/Pa)$		1.74	
$\epsilon_{3.2Pa}$	0	$\epsilon_{7.0Pa}$	0	$\epsilon_{15.0Pa}$	0	$\epsilon_{32.4Pa}$	20.11

Erosion test							
Bag identification				I			
Sample description				Boom clay, proctor density, far below optimum water content			
Soil properties							
$\rho_d(Mg/m^3)$				1.347			
$w(\%)$				0.252			
$\rho_b(Mg/m^3)$				1.686			
Test #1		Test #2		Test #3		Test #4	
Diameter (mm)		Diameter (mm)		Diameter (mm)		Diameter (mm)	n.a.
Initial Protrusion (mm)		Initial Protrusion (mm)		Initial Protrusion (mm)		Initial Protrusion (mm)	n.a.
Testing speed (m/s)	3.60	Testing speed (m/s)	4.17	Testing speed (m/s)	4.47	Testing speed (m/s)	n.a.
Shear stress (Pa)	26.44	Shear stress (Pa)	43.70	Shear stress (Pa)	85.44	Shear stress (Pa)	n.a.
Erosion rate (mm/hour)	45.09	Erosion rate (mm/hour)	60.0	Erosion rate (mm/hour)	62.6	Erosion rate (mm/hour)	n.a.
Erosion curve results							
$\tau_c(Pa)$		1		$S_i(mm/hr/Pa)$		14.39	
$\epsilon_{3.2Pa}$	17.63	$\epsilon_{7.0Pa}$	28.85	$\epsilon_{15.0Pa}$	39.77	$\epsilon_{32.4Pa}$	50.81

Erosion test							
Bag identification				J			
Sample description				Boom clay, proctor density, below optimum water content			
Soil properties							
$\rho_d(Mg/m^3)$				1.369			
$w(\%)$				0.261			
$\rho_b(Mg/m^3)$				1.726			
Test #1		Test #2		Test #3		Test #4	
Diameter (mm)		Diameter (mm)		Diameter (mm)		Diameter (mm)	n.a.
Initial Protrusion (mm)		Initial Protrusion (mm)		Initial Protrusion (mm)		Initial Protrusion (mm)	n.a.
Testing speed (m/s)	3.60	Testing speed (m/s)	4.14	Testing speed (m/s)	4.47	Testing speed (m/s)	n.a.
Shear stress (Pa)	14.42	Shear stress (Pa)	46.06	Shear stress (Pa)	93.61	Shear stress (Pa)	n.a.
Erosion rate (mm/hour)	0	Erosion rate (mm/hour)	16.91	Erosion rate (mm/hour)	43.85	Erosion rate (mm/hour)	n.a.
Erosion curve results							
$\tau_c(Pa)$		17		$S_i(mm/hr/Pa)$		1.327	
$\epsilon_{3.2Pa}$	0	$\epsilon_{7.0Pa}$	0	$\epsilon_{15.0Pa}$	0	$\epsilon_{32.4Pa}$	15.72

Erosion test							
Bag identification				L			
Sample description				Boom clay, proctor density, optimum water content			
Soil properties							
$\rho_d (Mg/m^3)$				1.446			
$w(\%)$				0.299			
$\rho_b (Mg/m^3)$				1.878			
Test #1		Test #2		Test #3		Test #4	
Diameter (mm)		Diameter (mm)		Diameter (mm)		Diameter (mm)	
Initial Protrusion (mm)		Initial Protrusion (mm)		Initial Protrusion (mm)		Initial Protrusion (mm)	
Testing speed (m/s)	3.70	Testing speed (m/s)	4.17	Testing speed (m/s)	4.34	Testing speed (m/s)	4.47
Shear stress (Pa)	30.76	Shear stress (Pa)	62.61	Shear stress (Pa)	79.19	Shear stress (Pa)	90.59
Erosion rate (mm/hour)	0	Erosion rate (mm/hour)	0	Erosion rate (mm/hour)	0	Erosion rate (mm/hour)	7.56
Erosion curve results							
$\tau_c (Pa)$		79.2		$S_i (mm/hr/Pa)$		0.663	
$\epsilon_{3.2Pa}$	0	$\epsilon_{7.0Pa}$	0	$\epsilon_{15.0Pa}$	0	$\epsilon_{32.4Pa}$	0

Erosion test							
Bag identification				M			
Sample description				Boom clay, proctor density, slightly above optimum water content			
Soil properties							
$\rho_d (Mg/m^3)$				1.403			
$w(\%)$				0.316			
$\rho_b (Mg/m^3)$				1.846			
Test #1		Test #2		Test #3		Test #4	
Diameter (mm)		Diameter (mm)		Diameter (mm)	n.a.	Diameter (mm)	n.a.
Initial Protrusion (mm)		Initial Protrusion (mm)		Initial Protrusion (mm)	n.a.	Initial Protrusion (mm)	n.a.
Testing speed (m/s)	4.17	Testing speed (m/s)	4.47	Testing speed (m/s)	n.a.	Testing speed (m/s)	n.a.
Shear stress (Pa)	62.42	Shear stress (Pa)	89.45	Shear stress (Pa)	n.a.	Shear stress (Pa)	n.a.
Erosion rate (mm/hour)	0.24	Erosion rate (mm/hour)	0.3125	Erosion rate (mm/hour)	n.a.	Erosion rate (mm/hour)	n.a.
Erosion curve results							
$\tau_c (Pa)$		19		$S_i (mm/hr/Pa)$		0.01	
$\epsilon_{3.2Pa}$	0	$\epsilon_{7.0Pa}$	0	$\epsilon_{15.0Pa}$	0	$\epsilon_{32.4Pa}$	0.108

J

Working protocol

In this appendix the working protocol is explained of the compaction of the clay (and extraction of the sample from the proctor mold) and the working protocol of the EFA testing. This has been documented carefully in order to maximize repeatability of testing. The reporting of how to obtain the index testing results has been done in Appendix G.

J.1. Protocol soil compaction and extraction

The soil has been prepared as described in the flowchart as presented in figure J.1. A more detailed explanation of why these steps have been taken is explained below this figure.

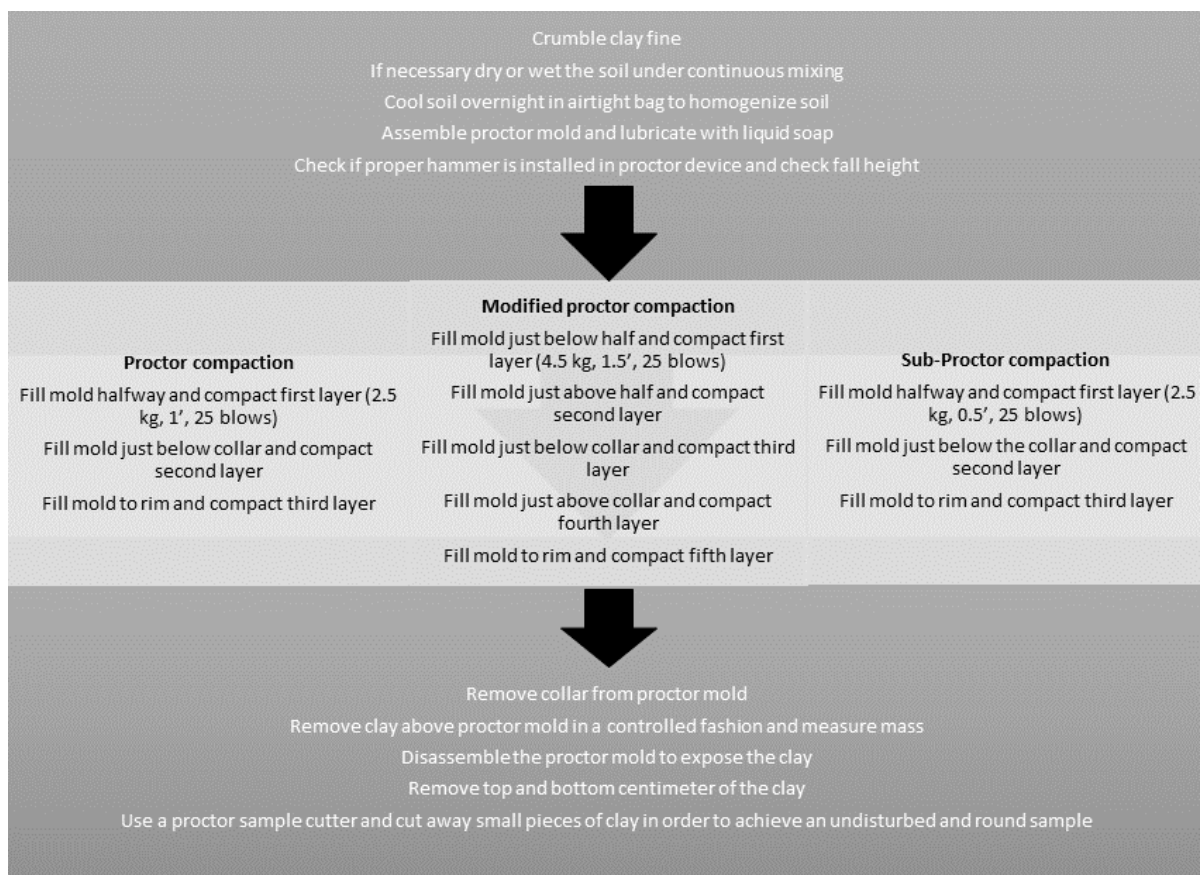


Figure J.1: Flowchart soil compaction and extraction

First, the soil is crumbled as fine as is reasonably possible, because a finer soil will result in a better compaction and a more reproducible result which can clearly be observed when cutting the sample, all clay chunks are then visible. Also the testing will then result in a more granular failure, whilst the clay itself might not have such a nature. Finally, if there are clearly discernible chunks, this has a very large influence on the sample, which is rather small.

Then if necessary the soil is wetted or dried if necessary to obtain a certain point on the proctor curve. If the soil needs to be dried that is done by spreading the crumbled soil in a large pan and expose it to the air (but no direct sunlight). The soil is then also mixed every half hour in order to dry the soil evenly. Then overnight the soil is put in a watertight bag and put in the refrigerator. This causes in a homogenization of the moisture content in the soil. If necessary this process is then repeated the following day. If the soil is to be wetted this is done in steps of roughly 2 % water content increase. This is then added to the clay which is put in a bucket and vigorously mixed initially and then mixed every half hour after that. Finally the soil is also set to chill overnight in the refrigerator in order to homogenize the soil.

The preparation of the clay being complete it is time to compact the soil. To this end the proctor mold is assembled and the inside of the mold and collar are lubricated with liquid soap as to prevent when the collar is removed off the mold the sample is torn apart. Or that when the 2 halves of the mold are taken apart the sample is torn apart.

The sample is then compacted as described in the procedure in J.1. With the normal proctor this is not a really big deal because the compaction procedure is fully automated with a proctoring hammer machine. For the Modified proctor however the proctor-hammer must be replaced as well as the drop-wheel. This must then be checked if it properly functions before operation starts. And when done replaced afterwards. Finally, for the "sub-Proctor" compaction a different tactic needed to be applied. This because it is not possible to do this with the Proctor machine. However, to still be able to reach a compaction level below proctor density it was decided to take a hand proctor device and block its dropping height in half by point welding a steel tube in the proctor hammer. It was chosen not to limit the number of blows rather than the drop height, because it was assumed that limiting number of blows would cause a compaction which is not evenly distributed thorough the sample. Limiting the drop height is at the very least something that limits the drop energy evenly through the sample.

When the sample has been compacted the collar is removed from the mold and the excess soil above the mold is removed. This is done very gradually and not in one go in order to preserve the structure of the soil and not alter the density of the soil. The mass of the sample can now be measured and from this the density can be accurately calculated. Also some clay is oven dried to determine the water content (and know the dry density, not only the bulk density).

Then finally the sample is trimmed with a triaxial soil trimmer. This is also done very gradually, cutting away only small pieces of clay at a time in order to preserve the structure and density of the soil.

This sample is then wrapped in plastic foil, put in an airtight bag and sealed with a tie-wrap and stored in a cooled environment.

Having discussed the working protocol of the sample preparation, it is now time to continue to the testing operation.

J.2. Testing protocol EFA

The testing protocol of the EFA has been summarized in figure J.2 below. After this a this step plan has been described in detail.

First the soil sample is put the soil container, and is trimmed to only put as limited as necessary length of the sample in the flume as to maximize the number of speed steps which can be performed. Then the mass of the soil container plus sample is measured, as well as the protrusion of the soil sample above the soil container with a very accurate caliper. It is then the idea to get the soil container collar parallel with the erosion flume, which require the later described double check.

Then the preparations can take place by filling up the erosion flume to prevent that the sample does not flush away with the first gust of water. Also all air is vented from the polyflow tubes in order to get good consistent results. Further, the camera is already set-up and video recording has started. Also a start will be made with the data acquisition to get a fair base-reading. Finally the pump frequency will be set up in order get a quick start up.

Now the true testing can start up. To do this the valves are opened and the pumped started. During testing one has to regularly check the progression of testing until the millimeter of soil has failed or significant

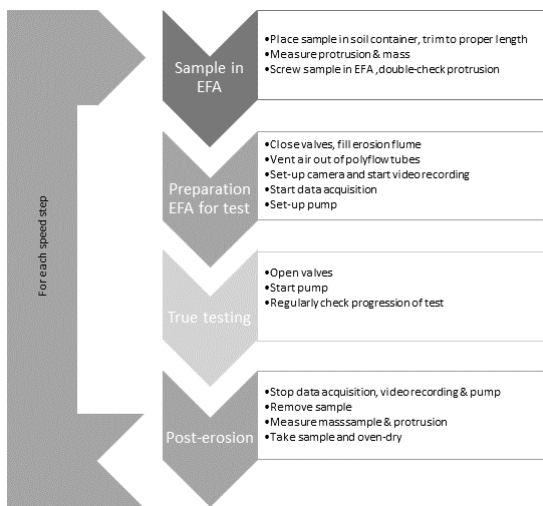


Figure J.2: Testing protocol EFA

chunks of soil have failed resulting in a non conclusive test.

When the test is then (finally) over the data acquisition is stopped, as well as video recording and the pump. The sample is then removed and the mass registered. Also the protrusion differences in the soil sample afterwards are recorded (which are regularly very different) Finally, also a part of the sample is oven dried